

DRY EYE THERAPY USING CANNABINOID LIGANDS

Inaugural Dissertation

zur

Erlangung des Doktorgrades
philosophiae doctor (PhD) in Health Sciences
der Medizinischen Fakultät
der Universität zu Köln

vorgelegt von

Bao Ngoc Tran

aus **Hanoi, Vietnam**

Hundt Druck GmbH
Cologne, Germany

2023

Betreuerin / Betreuer:

Prof. Dr. Philipp Steven

Gutachterin / Gutachter:

Prof. Dr. Helmar Lehmann

Prof. Dr. Uwe Fuhr

Datum der Mündlichen Prüfung:

12-01-2023

Table of contents

Table of contents.....	1
Abstract	4
Zusammenfassung.....	6
1 Introduction	8
1.1 Dry eye disease	8
1.1.1 Dry eye disease (DED) definition.....	8
1.1.2 Morbidity of dry eye	9
1.1.3 Epidemiology	10
1.1.4 DED treatment and management	10
1.2 The ocular surface system.....	11
1.2.1 Ocular surface tissues	11
1.2.2 Lacrimal functional units (or the ocular surface system).....	12
1.2.3 Nociception and corneal nerve.....	12
1.3 DED core pathomechanisms (inflammation, neurosensory abnormalities, and wound healing).....	13
1.3.1 Brief overview of the inflammatory pathway	13
1.3.2 Neurosensory abnormalities and dry-eye disease	15
1.3.3 Epithelial wound-healing in DED.....	17
1.4 The endocannabinoid system.....	18
1.4.1 Definition	18
1.4.2 Cannabinoid receptors (CBRs)	18
1.4.3 Endogenous cannabinoids and enzymes	18
1.4.4 Exogenous cannabinoids:.....	19
1.4.5 Cannabinoid receptor (CBR) function	20
1.5 Cannabinoid receptor (CBR) expression at the ocular surface	21
1.5.1 Previous studies about CBR expression at the ocular surface	21
1.5.2 DED model to study the role of the ECS	23
1.6 Cannabinoids and eye drop formulation.....	24
1.6.1 General information about cannabinoid eyedrop formulation.....	24
1.6.2 The ocular surface as a barrier for drug-delivery.....	24
1.6.3 Further requirements for cannabinoid eye drops	25
1.6.4 Recent drug formulations for THC and other cannabinoids	25
1.7 Aim of study and project overview	28
2 Material	29
2.1 Animals.....	29

2.2	Pharmaceutical active ingredients (cannabinoids)	29
2.3	Media, buffer, and solutions	30
2.4	Antibodies	31
2.5	KITs and commercial probes	31
2.6	Devices	32
2.7	General consumables	32
2.8	Software(s) and data analysis	33
3	Methods	34
3.1	In-vivo DED-induced mouse model and effect of cannabinoids	34
3.1.1	Experimental DED mouse model:	34
3.1.2	DED phenotype evaluation	35
3.1.3	Cannabinoid receptor ligands treatment:	36
3.1.4	Gene expression analysis by RT-qPCR	37
3.1.5	In-situ hybridization	38
3.1.6	Corneal nerve immunohistochemistry	38
3.1.7	Immunostaining CD4 ⁺ and CD8 ⁺ T-cell infiltration into conjunctiva	39
3.2	<i>In-vitro</i> wound healing model	40
3.2.1	Animals and tissue preparation:	40
3.2.2	Cannabinoid ligand treatment:	40
3.2.3	Imaging and data analysis:	40
3.3	Drug formulation study	41
3.3.1	Excipient selection study	41
3.3.2	Eyedrop permeability study with radio-labeled substances	42
3.3.3	Other pharmaceutical quality criteria.....	43
3.4	Statistics and data analysis	44
4	Results	45
4.1	Expression of cannabinoid receptors on naïve mice and DED-induced mice	45
4.1.1	Expression of cannabinoid on naïve mice.....	45
4.1.2	Desiccating stress (DS) model and DED phenotype readouts	47
4.1.3	Desiccating stress model and cannabinoid receptor (CBRs) expression	48
4.2	Effect of CBR ligands on DED pathogenesis	50
4.2.1	Phenotype readouts	50
4.2.2	Corneal-nerve morphology immunostaining	52
4.2.3	Inflammation cytokines following DED induction and cannabinoid treatment	55
4.2.4	The infiltration of CD4 ⁺ and CD8 ⁺ T-cell into the conjunctiva	56
4.2.5	CBRs expression following cannabinoid treatment.....	57
4.3	Effect of CBR ligands on corneal epithelial wound	59
4.3.1	Wound healing model	59

4.3.2	The biphasic effect of THC on the re-epithelialization process.....	59
4.3.3	The effect of antagonists on the re-epithelialization process.....	61
4.4	Drug formulation study.....	64
4.4.1	Excipient selection.....	64
4.4.2	Effect of sterile filtration and short-term stability.....	67
4.4.3	Other pharmaceutical criteria (particle size, pH, and osmolarity).....	69
4.4.4	Radio-labeled mannitol permeability for carriers.....	70
5	DISCUSSION.....	72
5.1	ECS and DED pathology:.....	72
5.1.1	CBR expression and DED pathogenesis.....	72
5.1.2	Cannabinoids in fluorescein score and inflammation.....	73
5.1.3	Cannabinoids in pain and disturbed mechanical sensitivity and corneal nerve morphology in DED.....	74
5.1.4	Cannabinoids in the re-epithelialization process:.....	75
5.2	Cannabinoid formulation study.....	76
5.2.1	Drug formulation selection.....	76
5.2.2	Permeability.....	77
5.2.3	Remarks and perspectives about proposed formulations.....	78
5.3	Legal discussion.....	79
5.4	Perspective.....	79
	Reference.....	80
	LIST OF FIGURES.....	89
	LIST OF TABLES.....	91
	Acknowledgments.....	92
	Bao tran's curriculum vitae.....	94
	Erklärung.....	95

Abstract

Dry eye disease (DED) has a high prevalence (up to 50% in some communities) with increasing incidence. Notably, patients have such high morbidity and burden that they desperately need effective treatment. However, as a "multifactorial disease," DED consists of various complex disorders, all of which interact to form a vicious circle and obscure the etiology. Even though physicians and patients have different therapeutic options, the common disadvantages in current treatments are (i) a lack of compliance due to an overload of products, (ii) the occurrence of side effects of different drugs, and (iii) limited efficiency in some particular cases. As a result, DED requires a novel therapy capable of simultaneously addressing multiple targets in DED pathogenesis.

To find suitable targets and candidates for DED, the endocannabinoid system (ECS) and its receptors (CBRs) present at the ocular surface are a promising choice, as ECS functions are involved in a plethora of physical processes. Experimental evidence showed that using CBRs ligands can modulate anti-inflammatory, neurosensory, and wound-healing processes, which are potential to control and prevent DED pathogenesis and the vicious circle. Therefore, this study was carried out to determine whether CBR ligand eye drops can provide a multiple-target therapy for DED. The project hereby consisted of three parts, addressing consecutive objectives:

Firstly, this study confirms the involvement of CBRs (in particular, CB1R and CB2R) in DED pathomechanism based on an experimental DED mouse model (desiccating stress model). CB1R and CB2R were detected by RT-qPCR and in-situ hybridization techniques in the cornea, conjunctiva, and lacrimal glands. During DED-induction, CB1R and CB2R expressions were increasing, concurrent with significant DED phenotypes (low tear production, high score of cornea epitheliopathy, and reduced cornea sensitivity). Furthermore, different CBRs ligands were topically applied to DED-induced mice. CBRs therapy suppressed the increasing trend of CBR expression, which coincided with improved phenotype readouts. Tetrahydrocannabinol (THC) is a promising candidate for anti-inflammatory effects, together with protecting nerve morphology and maintaining corneal sensitivity.

Secondly, an in-vitro wound-healing model was developed to characterize the influence of CBR on the re-epithelialization process. Interestingly, while CB1R was found to have a significant effect, selective CB2R ligand did not influence the re-epithelialization. In detail, activating CB1R improved the wound-healing rate while selectively inhibiting CB1R delayed the wound-healing process. Furthermore, tetrahydrocannabinol (THC), a non-selective agonist, showed a biphasic

effect: high concentration (from 1 to 10 μM) delayed wound healing, while low concentration (from 0.01 to 0.5 μM) increased the rate. This finding supports the functional role of CBRs in DED pathogenesis and management.

Thirdly, we proposed two eyedrop formulations for THC, in which THC was formulated in the form of micelle in water at the nanoscale (around 10nm). All ingredients are already used in pharmaceuticals and bio-products, so the formulations are expected to be safe and well-tolerated. Additionally, the formulation steps are feasible with low technical complexity, showing promise for commercial scaling-up. The finally proposed formulation contains 0.5% THC, adequate to provide a significant effect, as shown in the *in-vivo* model in the first part. Also, the obtained results confirmed stability when stored at room temperature or refrigerator (4-8°C), facilitating its use by patients.

In summary, this study confirmed the potentiality of CBR and CBR ligands, notably THC, as a multiple-target therapy for dry eye patients.

Zusammenfassung

Das Trockene Auge ist eine häufige Erkrankung (bis zu 50 Prozent in einigen Populationen) mit zunehmender Inzidenz. Die Krankheit beeinträchtigt die Lebensqualität des Patienten stark und erfordert eine wirksame Behandlung. Das trockene Auge ist eine „multifaktorielle Erkrankung“ und besteht aus verschiedenen komplexen Störungen, die alle miteinander interagieren, um einen Teufelskreis aus sich verstärkenden Pathologien zu bilden und die Ätiologie zu verschleiern. Obwohl viele verschiedene Behandlungsmöglichkeiten zur Verfügung stehen, bestehen Nachteile in aktuellen Behandlungsformen: (i) eine mangelnde Compliance aufgrund einer Anwendung von Multimedikationen, (ii) das Auftreten von Nebenwirkungen verschiedener Medikamente und (iii) die begrenzte Effizienz der Wirkstoffe. Daher besteht ein dringender Bedarf, neue therapeutische Ansätze zu finden, die in der Lage sind, die vielfältigen pathologischen Mechanismen des Trockenen Auges zu kontrollieren.

Als neuer therapeutischer Ansatzpunkte für die Behandlung des Trockenen Auges kommt das Endocannabinoid-System (ECS) und seine Rezeptoren (CBRs) in den Geweben der Augenoberfläche in Frage, da ECS-Funktionen mit einer Vielzahl von physikalischen Prozessen verbunden sind. Experimentelle Beweise zeigten, dass die Verwendung von CBRs-Liganden entzündungshemmende, neurosensorische und wundheilende Prozesse modulieren kann, die ebenfalls zentrale Pathomechanismen des Trockenen Auges sind. In dieser Studie wird daher die Hauptfrage beantworten, ob CBRs und CBR-Liganden-Augentropfen eine Multiple-Target-Therapie für DED darstellen können. Um diese Fragen zu beantworten, gibt es drei Untersuchungsteile:

Erstens bestätigte die Studie die Beziehung zwischen Cannabinoidrezeptoren (CB1R und CB2R) und der Pathogenese des Trockenen Auges unter Verwendung eines experimentellen Modells der Trockenen Auges bei Mäusen (Austrocknungsstressmodell). Im Einzelnen wurden CB1R und CB2R an Hornhaut, Bindehaut und Tränendrüsen nachgewiesen. Weiterhin wurden in diesem Modell Augentropfen mit unterschiedlichen CBRs-Liganden getestet. Die Ergebnisse zeigten, dass die Behandlung mit CBR-Liganden die CBR-Expression reduziert und eine Verbesserungen des Krankheitsstatus, einschließlich reduzierter Schäden und entzündungshemmender Wirkung auf die Hornhaut vermittelt. Neben der entzündungshemmenden Wirkung wird insbesondere die durch THC geschützte Morphologie des Hornhautnervs dargestellt, wodurch die Empfindlichkeit der Hornhaut aufrechterhalten und die Infiltration von CD4+-T-Zellen reduziert wird.

Zweitens wurde ein In-vitro-Wundheilungsmodell entwickelt, um die Auswirkungen von CBR auf die Reepithelisierung zu beschreiben. Interessanterweise wurde festgestellt, dass CB1R eine signifikante Wirkung hat, während selektive CB2R-Liganden die Reepithelisierung nicht beeinflussten. Insbesondere die Aktivierung von CB1R verbessert die Wundheilungsraten, während die selektive Hemmung von CB1R die Wundheilung verlangsamt. Darüber hinaus zeigte Tetrahydrocannabinol (THC), ein nicht-selektiver Agonist, eine zweiphasige Wirkung: Hohe Konzentrationen (von 1 bis 10 μM) verzögerten die Wundheilung, während niedrige Konzentrationen (von 0,01 bis 0,5 μM) die Wundheilung beschleunigten. Dieser Befund unterstützt nachdrücklich die funktionelle Rolle von CBRs bei der Pathogenese und Behandlung von DED.

Drittens schlugen wir zwei Augentropfenformulierungen für THC vor; wo THC als Mizellen in Nanogröße (etwa 10 nm) in Wasser hergestellt wird. Alle Inhaltsstoffe sind in Pharmazeutika und Probiotika üblich, daher wird erwartet, dass die Formulierungen sicher sind und von den Patienten gut vertragen werden. Darüber hinaus können die Formulierungsschritte als Krankenhauszubereitungen verwendet werden und sind vielversprechend für eine kommerzielle Maßstabsvergrößerung. Diese Formulierung enthält eine THC-Konzentration von 0,5 %, was ausreicht, um eine signifikante Wirkung zu erzielen, wie im ersten Teil des In-vivo-Modells gezeigt wurde. Darüber hinaus bestätigen die erhaltenen Ergebnisse die Stabilität bei Lagerung bei Raumtemperatur oder im Kühlschrank (4-8 °C), was die Anwendung am Patienten erleichtert.

Zusammenfassend bestätigte diese Studie das Potenzial von CBR-Liganden und CBRs als Multi-Targeting-Therapie für Patienten mit Trockenem Auge.

1 Introduction

1.1 Dry eye disease

1.1.1 Dry eye disease (DED) definition

With the aim to define and understand the Dry eye disease (DED), the two Dry eye workshop (final report were finalized in 2007 and 2017, respectively) were hosted by the Tear Film & Ocular Surface Society (TFOS). Based on DEWS II report executive summary released in 2017 (1), DED was defined as follows:

“Dry eye is a multifactorial disease of the ocular surface characterized by a loss of homeostasis of the tear film and accompanied by ocular symptoms, in which tear film instability and hyperosmolarity, ocular surface inflammation and damage, and neurosensory abnormalities play etiological roles.”

As a "multifactorial disease", DED includes a high number of complex physical disorders, making it difficult to trace the original causes of pathology. Furthermore, these multiple pathogenic factors interact to form a self-sustaining vicious circle of DED, exacerbating disease conditions (Figure 1, adapted from DEW II (2,3). In the vicious circle, DED is described with tear film instability and hyperosmolarity. Then the vicious circle is activated by three core mechanisms of DED: inflammation, neurosensory abnormalities, and wound healing. DED patients have such a high morbidity and burden that they are desperate for effective treatment. Because of the complexity of DED, physicians and patients need different therapeutic options to control different aspects of the disease. However, the common disadvantages in current treatments are (i) a lack of compliance with an overload of products, (ii) the occurrence of side effects of different drugs, and (iii) limited efficiency. As a result, DED requires a novel therapy capable of simultaneously addressing multiple targets in the DED pathomechanisms.

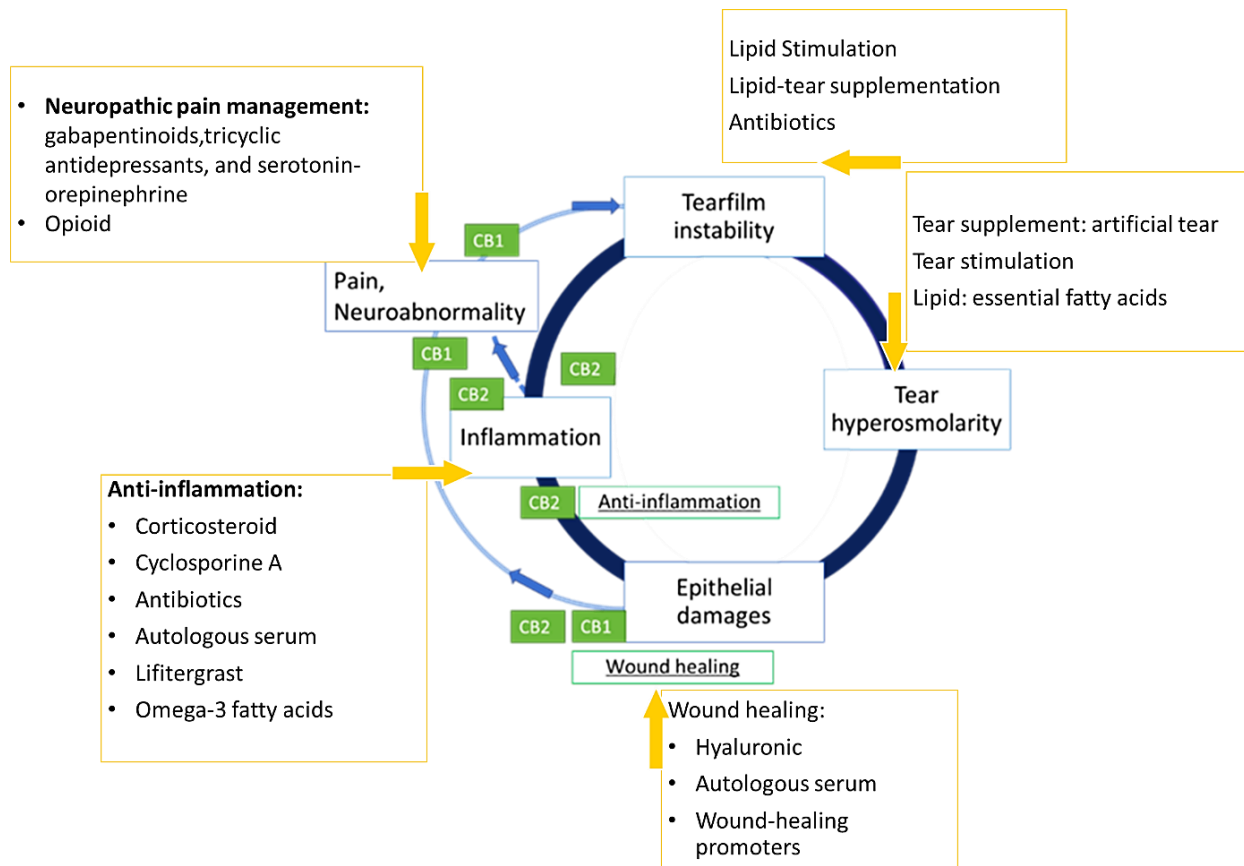


Figure 1: DED vicious circle, adapted from DEW II (2,3): Tear film instability and tear hyperosmolarity initiate inflammation, neuro-sensory abnormalities, and directly damage ocular surface epithelia. The vicious cycle happens when tear hyperosmolarity causes these three pathogenic processes to cascade and exacerbates hyperosmolarity. Combining different therapy approaches (yellow arrows) is required for DED patients. Cannabinoid receptors (CB1R and CB2R, green) are hypothesized to impact these 3 pathways as a potential DED therapy.

1.1.2 Morbidity of dry eye

Dry eye symptoms are reported as the most common reason for visiting medical eye care (4–6). DED has a significant socioeconomic burden, including medication, doctor visit costs, and difficulties in daily social and physical functioning (4–6). In a meta-analysis study to compare DED-diagnosed patients with non-DED individuals via questionnaires and logistic regression analysis, daily activities like driving, reading, computer use, writing, and watching television are three times more difficult for DED patients (4,6,7). DED severity grading scheme was also established (from 1 to 4) based on signs and symptoms (8). The higher severity DED patients (class 4) endured neuropathic disease and chronic pain, impaired visual function, and high-frequency discomfort in daily activities, potentially leading to depression and anxiety (6,9). In summary, due to the morbidity of their conditions, DED patients are in immediate need of effective therapies.

1.1.3 Epidemiology

DED was reported as a high-prevalence disease, though the prevalence range was expanding from 5% to 50% in different populations worldwide (6,10). DED signs and symptoms are abnormalities that indicate the presence and status of potential DED. According to the DEWS II report (6), DED signs are more prevalent and variable than symptoms. Whereas a symptom is a patient's subjective experience (for example, pain or scratchy sensation in the eye, blurred or fluctuating vision), a sign is an objective that can be observed by clinicians (for example, cornea epitheliopathy, lower tear production volumes, loss of goblet cells) (1,8,11).

There are consistent epidemiological factors considered DED risk factors, such as age, gender, and race. In general, women have a higher prevalence of DED than men; DED prevalence increases with age (6,10). Additionally, risk factors such as deficiency or autoimmunology diseases (Meibomian gland deficiency, Sjogren's syndrome), environmental factors, and medicinal use also increase the prevalence of the disease (6).

1.1.4 DED treatment and management

DED management is to restore the homeostasis of the ocular surface and tear film (2,12). As a "multifactorial disease", DED management demands different therapies to handle multiple symptoms and underlying pathologies to maintain the homeostasis of the ocular surface (Figure 1). Dry eye workshop 2017 (DEW 2017) mentioned a 4-stage approach for DED management & treatment (12). If a patient does not respond to one level of treatment or is experiencing severer symptoms, the next level of treatment is suggested.

At stage 1 of DED management, topical application of aqueous or lipid-based tear supplements (no pharmaceutical-active compound) is first-line indicated (12,13). Stages 2 and 3 (moderate to severe conditions) require prescription medicines for pathogenic therapies such as topical antibiotics for anterior blepharitis, topical corticosteroid, and non-glucocorticoid immunomodulatory drugs (such as cyclosporine A) for inflammation. In stage 3, combining medicines using thermo-mechanical medical devices, therapeutic contact lenses, and autologous serum eye drops are listed as available options. If other therapeutic options fail, surgical intervention will even be considered (Grade 4) to restore the ocular surface functions, such as tarsorrhaphy, surgical treatment for conjunctivochalasis, lid corrections, and gland transplantation (12,13). However, surgical

complications and inadequate data about efficiency in some techniques make this approach the last resort for patients (12).

Despite the abundance of therapeutic options available to doctors and patients, there is still a high frequency of unsuccessful treatment (14). While several therapies and procedures have limited efficacy (such as artificial eyedrops or environmental improvement), an overload of different therapies and side effects caused patients to be less compliant.

1.2 The ocular surface system

The term “Ocular Surface System” represents an elaboration of the “Lacrimal Functional Unit” (LFU), the content of which had been previously described by Stern et al. (15,16) and was mentioned in the first Dry eye workshop (DEW I 2007, Definition and classification) (8). As DED is mentioned as a disorder(s) of the LFU, abnormalities in any components of the LFU contribute to the disease (8). Details about LFU and the ocular surface tissues are presented in the following sub-sections (8).

1.2.1 Ocular surface tissues

The “ocular surface” is the eye’s outermost layer, which serves as the interface between the environment and the eye (8,17). The ocular surface comprises anatomical layers from the liquid tear film with oil, aqueous, and mucin layers covering continuous epithelium layers from the cornea to the conjunctiva. Moreover, the functions of the ocular surface are supported by relating and adnexal tissues in a complex integration (8,17). The term “ocular surface” can be described by the following (18):

- The term "ocular surface " refers to its primary function. The components mentioned above form and maintain a smooth and wet cornea surface and a functional tear film, a major refractive surface for visual function (15,18). Also, this important function is supported by the continuity of the epithelia, nerves, endocrine, vascular, and immune systems.
- The ocular surface epithelia are all continuous. The corneal and conjunctival epithelia are continuous and connect to the meibomian gland, nasolacrimal system, and accessory lacrimal glands (18).
- Epithelia in the different regions produces different components to form the tear film, a liquid layer that covers the cornea and conjunctiva (15,18):
 - In cornea and conjunctiva: hydrophilic mucins

- In lacrimal and accessory lacrimal glands: Lacrimal fluid forms the aqueous layer of the tear film, provides adequate tear amount and protective proteins
- In the meibomian gland: Meibum, an oily substance that forms a superficial lipid layer of the tear film

The adnexal tissues and structures, including nervous, endocrine, circulatory, and immune systems, support the continuous epithelial and eyelid blink functions. The nasolacrimal epithelial system maintains a delicate balance between secretion and outflow, which adsorbs tear components.

1.2.2 Lacrimal functional units (or the ocular surface system)

According to Stern et al. (15,16), the LFU was defined as an integrated system containing lacrimal glands, cornea, conjunctiva, meibomian glands, and lids (15,16). The LFU functions were maintained and controlled by the sensory or motor nerves, blood vessels, and lymphatic vessels (8,15). The primary role of LFU is to control the secretion of tears' aqueous, lipid, and mucin components in response to environmental stimuli, defined as a “negative feedback loop” (15). The delicate stability of tear film can be influenced and exaggerated by daily activities and environments with low humidity, windy conditions, or infection caused by bacteria or viruses (13). When tear film instability occurs, LFU is a first and rapid response system to provide tear (or required tear components) to repair and prevent environmental stresses (13).

DED is identified by the condition of tear hyperosmolarity, in which LFU cannot maintain the tears' homeostasis. Tear hyperosmolarity and changes in the tear film cause desiccation and epithelial damage, which initiate the subsequent cascade in the vicious circle.

1.2.3 Nociception and corneal nerve

Nociception is a process of the sensory nervous system to encode noxious stimuli; via this, the body receives a painful stimulus, converts it to a molecular biological signal, and initiates a defense response (19,20). As mentioned in 1.2.2, the LFU functions were supported by sensory and motor nerves (8,15). Similar to the “negative feedback loop” of the LFU, the nociception path is to transduce information from peripheral neurons (nociceptors) to more-central neural systems to evoke both sensations and responses to restore the ocular surface homeostasis conditions (19,20).

Corneal nerves:

Corneal sensory nerves originate from the ophthalmic division of the trigeminal ganglion (TG) (20,21). The cornea contains the highest density of nerves in the surface epithelium. In the stroma,

corneal nerves form a plexus, branches of which reach extensively to the outermost layers of the epithelial surface (20,21). Functionally, corneal sensory nerves belong to (i) polymodal nociceptor neurons, (ii) pure mechano- nociceptor neurons, and (iii) cold thermoreceptor neurons, which respond to different environment stresses:

- Polymodal nociceptors: normally inactive; this group contains multiple-function neurons responding to multiple chemical, mechanical, and thermal stimuli.
- Pure mechano-nociceptors: normally inactive; this group responds only to mechanical forces.
- Cold thermoreceptors: At normal temperature (34-35°C), cold thermoreceptor exhibits spontaneous firing of nerve impulses. Reducing environment temperature induces cold thermoreceptors to amplify or decrease the basal firing frequency.

Environmental stresses such as chemical, mechanical, or temperature activate corneal sensory nerves, which evoke responses to maintain tear production, and blinking behavior.

1.3 DED core pathomechanisms (inflammation, neurosensory abnormalities, and wound healing)

1.3.1 Brief overview of the inflammatory pathway

Inflammation is a critical mechanism in the pathogenesis of DED (13,16). In response to tear hyperosmolarity, corneal epithelial cells produce matrix metalloproteinases (MMPs) and other mediators (22,23). In detail, *in vitro* and *in vivo* models showed that tear hyperosmolarity induces the production of stress-associated protein kinases or pro-inflammatory molecules (22,23), which are similar to the ocular surface of DED patients such as interleukins (IL-1, IL-6), tumor necrosis factor (TNF), and matrix metalloproteinases (especially, MMP-9) (24). These inflammatory mediators could start inflammatory cascades on the ocular surface, leading to dysfunctions in LFU and stimulating the adaptive immune response (16,25).

Early-response immune cells such as macrophages and neutrophils are recruited and activated. Consecutively, resident antigen-presenting cells (APC) (dendritic cells, natural killer, Langerhans, T lymphocytes) are activated, causing apoptosis of ocular surface cells and further initiating an adaptive immune response (1). CD4⁺ T-cells, particularly IL-17-secreting Th-17 cells, infiltrate the ocular surface and release additional pro-inflammatory mediators (61). IL-17-producing T cells are identified as key effectors in inducing autoimmunity and sustained inflammation in DED (62).

When the inflammation is already activated, the immunopathogenesis is driven by Th-1, Th-7, and dendritic cells, which trigger adaptive immunity and disease progression and exacerbation. In case inflammation interference prevents LFU from responding to environmental stresses, multiple ocular surface dysfunctions will occur, leading to DED later (15,16,25).

In chronic DED, the adaptive immune response has already been activated. In detail, components of chronic DED are thin and unstable tear film, loss and death of superficial epithelium, reduced production of anti-inflammatory factors by the goblet cells, and the infiltration of pathogenic T cells to the cornea or conjunctiva. In response to stresses, inflammation will “flare up” at a higher rate and be sustained over a longer time (25,26).

As shown, inflammation plays an important role in the vicious circle (Figure 1). Apoptosis is induced due to a direct interaction of inflammatory mediators with surface receptors (extrinsic pathway)(24). Also, inflammation can interfere with the neurosensory processes, blocking potentially reversible neurosecretory, circulating antibodies, and muscarinic M3 receptors (13). The consequences are loss of tear film integrity and functions, alterations of tear aqueous, mucin, and lipid components. This reduces the ocular surface's ability to respond to environmental stimuli (15).

Targeting inflammation as a DED therapy:

Many DED therapies have anti-inflammatory properties. Generally, the strategy for DED early stage is to provide an adequately wet condition and maintain tear volumes. Examples of these medicines are artificial tears, punctual occlusion, and secretagogues (2,12). Those products lower tear film osmolarity and provide a viscous layer to prevent ocular surface friction by blinking and other mechanical interactions (12). Hence, these products have indirect anti-inflammatory activities.

If these indirect anti-inflammatories fail to work, corticosteroids and cyclosporine are indicated. These substances suppress T-cells and the apoptosis of epithelial cells (12,27). Corticosteroids, tetracyclines, and TNF-antagonists reduce matrix metalloproteinase activity on the ocular surface. Doxycycline targets corneal epithelia to produce less IL-1 and MMP. These substances interrupt the inflammation cascades and consequently stop the DED exacerbating process (12). Lifitegrast was approved by FDA for DED because it inhibits T-cell activities involving recruitment, activation, and proinflammatory mediator releasing (28). In addition to corticosteroids, Lifitegrast,

cyclosporine, and tacrolimus are immunomodulatory therapies for long-term inflammation in DED.

The autologous serum is a therapy of interest due to its similar biochemical properties to human tears (29,30). In addition to similar physiological and chemical properties, the autologous serum can provide nutrients, fibronectin, and essential growth factors (29,30). Applying autologous serum has therapeutic effects on DED conditions, such as wound-healing, neuro-regenerating, and anti-inflammatory effects (29,30). In particular inflammation pathway, autologous serum can suppress keratocyte apoptosis and migration of fibroblasts, myofibroblasts, and inflammatory cells, which consequently reduces cytokine release (29,30). However, serum application has several limitations, such as national laws (as blood samples) and difficulties in production (12).

1.3.2 Neurosensory abnormalities and dry-eye disease

The term "neurosensory abnormalities" has been added to the latest definition of DEW II 2017 as a novel core pathomechanism (1). Generally, "neurosensory abnormalities" can be described as a disconnection between discomforts and ongoing peripheral pathology without a clear peripheral cause. In which, there are 2 types of neurosensory abnormalities in DED (11,31):

- (i) Neuropathic: "hypersensitivity to stimulation" refers to a neurosensory abnormality. In the context of DED, small changes in tear osmolarity can induce discomfort and pain in patients' eyes.
- (ii) Neurotrophic: If a patient has severe epithelial damage but no discomfort symptoms, they possibly have DED neurosensory abnormalities. The severity of the epitheliopathy is measured by the slit-lamp examination.

There are DED risk factors such as contact lens wear or corneal surgery, which can induce (i) local inflammation and (ii) nerve injuries, which afterward alter the electrophysiological properties of corneal sensory terminals, peripheral axons, and collateral branches of axons in nociception path (32). If these changes are not appropriately controlled, axon dysfunction and neurosensory abnormalities occur chronically. There are several receptor families and neurotransmitters involved with the nociception abnormalities such as the Transient receptor potential cation channel subfamily V member 1 (TRPV1), Calcitonin gene-related peptide (CGRP), and neurotransmitters such as glutamate, GABA (γ -Aminobutyric acid), and the Substance P (a neuropeptide relating to extreme stimuli).

- (i) Proinflammatory mediators can directly interact with nociceptors to cause higher excitation and sensitization. If the stimulus persists, the nociception functions will be permanently altered,

leading to neurosensory disorders such as increasing expression of TRPV1 channels (33,34), enhancing Substance P (35), glutamate release (35) (relating to neurotoxicity level), and various ionic channels (32).

(ii) Nerve injuries that were caused by surgical procedures (LASIK) or environmental stresses (toxic effects, trauma, etc.) also initiate neurotransmitter releasing. If the injury persists or the neurotransmitters are excessively and uncontrollably released, glutamate or GABA (36) or substance P and CGRP (35) pose potential risks to induce neurotoxicity or neurogenic inflammation.

In response to the neurosensorial abnormalities, the human body simultaneously releases endogenous substances that block TRPV1 sensitization and activate voltage-gated Ca^{2+} channels (9,37) to restore the homeostatic conditions. However, if neurosensory abnormalities with chronic inflammation persist, neuropathic pain may develop consecutively, further contributing to the vicious circle by exaggerating DED.

Targeting neurosensorial abnormalities as a therapy for DED:

As a component of the DED vicious circle, an approach consisting of multiple therapies is more effective and beneficiary than monotherapy to treat a single symptom. In the concept of DED, anti-neuropathic pain therapy should be indicated together with anti-inflammatory and wound-healing agents (9,37). For DED patients with pain, neuropathic pain management should be indicated, in which gabapentinoids, tricyclic antidepressants, and serotonin-norepinephrine are used as the first-line indication (38). Amitriptyline inhibits cholinergic, adrenergic, and histaminergic receptors and ionic channels, while gabapentin reduces Ca^{2+} influx to the cells (37,38). If these 1st medications fail to provide effects, the 2nd medication is opioid therapy, specific for moderate to severe pain (38). Beside pain management, opioid-based therapies also maintained corneal nerve sensitivity in different DED mice models (39,40).

As a protective mechanism, many endogenous bioactive lipid mediators are produced during injury or inflammation to modulate the initiation and progression of pain (32). Two endocannabinoids, anandamide and arachidonoyl glycerol (2-AG), are among these protective-mechanism lipids (32). These substances were released in the ocular surface, binding to cannabinoid receptors (CBRs) to counteract the neurosensory abnormalities by modulating the TRPV1 sensitization and controlling neurotransmitter and ion channels (41,42). Endocannabinoids activate Gi/o-coupled GPCRs

(protein-coupled receptors (GPCRs), which consequently inhibits TRPV1 sensitization and activates voltage-gated Ca^{2+} channels (9,37). In general, CBRs' effects are hypothesized to restrain and reverse the neuro-sensory abnormality pathways in DED.

1.3.3 Epithelial wound-healing in DED

The standard stability of the cornea epithelium is described by the X, Y, Z hypothesis (in a healthy equilibrium state, $X + Y = Z$) (43). While superficial epithelial cells are continuously shed into the water layer of the tear film (Z), they are replaced by the centripetal movement of cells from the limbus (Y), as well as the proliferation of basal cells (X) (43,44). In a pathological state, Z increases, and X and Y processes are interrupted. In DED, corneal epithelial injuries cause increasing Z, while inflammation and neurosensory abnormalities delay X and Y processes (13). As mentioned, the ocular surface system shared the same continuous epithelium. Generally, the wound-healing rate depends on multiple steps, such as enhancing the migration of adnexa and superficial cells into damaged areas, improving basal or wing cell proliferation and differentiation, and facilitating adhesion to form a new layer covering the wound area.

Targeting wound healing as a therapy for DED

As corneal epitheliopathy is an important DED milestone, effective wound-healing therapies that aim to restore the integrity of corneal epithelial layers should be considered at the first line.

Compared to other lubricant eye drops, the symptoms of severe DED patients were significantly relieved after using high molecular weight hyaluronic eye drops (45,46). *In vitro* sodium hyaluronate stimulates the migration of CD44+ expression in corneal epithelial cells, which results in rapid wound closure (45,46).

Autologous or heterologous serum or platelet-derived eye drops can be used as wound healing and tissue regeneration agents. These bio-products contain abundant growth factors and bioactive proteins, which stimulate chemotaxis, cell proliferation, and other essential steps for tissue repair (47). Also, due to the similarity to natural tears, the autologous serum including lipids, proteins, antimicrobial elements, and growth factors is more well-tolerated than artificial tears (48).

Among endogenous substances relating to the wound-healing process, the mammalian trefoil factor (TFF) is a group of trio peptides produced by goblet cells and the epithelium at the nasolacrimal ducts. Applying exogenous rTFF3 peptide as ophthalmic drops enhanced the wound-healing rate in both in-vitro and in-vivo models (49). Corneal wounds immediately induced the production and release of endogenous TFF3 (49).

1.4 The endocannabinoid system

1.4.1 Definition

The Endocannabinoid biological system (ECS) includes endogenous cannabinoids, cannabinoid receptors (CBRs), and related enzymes for synthesizing and degrading endocannabinoids (50,51). Endogenous cannabinoids are lipid-based substances that function as neurotransmitters by binding to cannabinoid receptors (CBRs) to exhibit their functions (50,51). The term “cannabinoid” originated from well-known herbal cannabis and its active ingredients. In fact, cannabis (or marijuana) was used thousands of years ago, whereas the chemical structure of THC (trans- Δ^9 -tetrahydrocannabinol) was also found long before the ECS (50,51).

1.4.2 Cannabinoid receptors (CBRs)

Following the discovery of THC in the 1960s, the identification of THC-binding targets in the human body indicated the presence of cannabinoid receptors (CBRs), a class in the G protein-coupled receptor superfamily (50,51). The two most relevant receptors for cannabinoids are Cannabinoid receptor 1 (CBR1) and Cannabinoid receptor 2 (CBR2).

CB1R is encoded by the gene “*cnr1*”. The mRNA signal of CB1R was detected and quantified in the human brain, peripheral neural systems, and several tissues responsible for sensation, digestion, and physical movement (52). CBR2 is encoded by the gene “*cnr2*” (CBR2 shares 44% sequence homology with CB1R at the protein level). In humans, CBR2 was found mainly in the tissues relating to immune processes such as spleen, thymus, tonsils, bone marrow, pancreas, mast cells, and peripheral blood leukocytes; and later, CBR2 expression was confirmed in various cultured immune cell models (50,52). However, as the complexity of ECS and CBRs, experiments with CB1^{-/-} and CB2^{-/-} receptor knockout mice also found responsiveness to different cannabinoid ligands such as THC or other synthesized cannabinoids like WIN55,212-2 (50). The cannabinoid-like effects, which were reported even when these receptors were not being expressed, indicate a group of unspecific cannabinoid receptors (53) such as TRPV1, GPR18, and GPR55 receptors (50).

1.4.3 Endogenous cannabinoids and enzymes

Endogenous cannabinoids (or endocannabinoids) are lipid-based substances produced naturally in the body. Endocannabinoids act as intra- and inter-cellular messenger molecules, released from one cell to activate CBRs in neighboring or the same cell (51,54). These endocannabinoids are only "on-demand" synthesized and released in response to pathological factors (such as neurotoxicity,

inflammation, or injuries) and then metabolized after signal processing (55–57). From a pharmacodynamic point of view, controlling the enzyme system can change the concentration of endogenous endocannabinoids at the synaptic cleft. For example, de fatty acid amide hydrolase (FAAH) is an enzyme that degrades endocannabinoids (58). Inhibiting this enzyme would increase both the concentration and duration of endocannabinoids at the target sites, resulting in stronger ECS effects similar to those produced by potent exogenous CBR agonists (50,58). N-arachidonylethanolamine (AEA) and 2-arachidonoylglycerol (2-AG) are two endocannabinoids found in the eye tissues (including in the cornea and lacrimal gland).

1.4.4 Exogenous cannabinoids:

Exogenous cannabinoids are CBRs ligands artificially introduced to the human body. Generally, exogenous cannabinoids (like THC) induce stronger effects than endocannabinoids (59,60) because endocannabinoids are metabolized too rapidly to produce THC-mimetic effects (59,60). Furthermore, recent developments in chemical engineering have synthesized exocannabinoids with various functions and targets (61,62). Exogenous CBR ligands can be categorized as:

- Origin (beside endocannabinoids mentioned above section)
 - Phyto-cannabinoids: (Δ -9- tetrahydrocannabinol (THC), cannabidiol (CBD))
 - Synthetic cannabinoids such as WIN 55,212-2, JWH-, or AM- series (63).
- Pharmacological activity (64,65):
 - Selective CB1 antagonists: SR141716A (66) (which was available commercially), AM251(67)),
 - Selective CB1 agonists: JWH-018, ACEA (62)
 - Selective CB2 antagonists: such as (SR144528 (68) and AM630(69)
 - Selective CB2 agonists (JWH-015 (70), HU308(71)
 - Non-selective agonist (or full agonist): THC (phytocannabinoid) and WIN55,212-2 (synthetic cannabinoid) are categorized as combined CBR1/CBR2 agonists (or non-selective agonists) with high efficacy and affinity to the receptors (72,73).
 - Non-selective antagonist: CBD was categorized as a partial antagonist for both CBR1 and 2 (74,75).

Generally, the abundance of synthetic cannabinoids (65) and the long history of using naturally occurring herbal phytocannabinoids (such as THC (50)) results in a variety of choices for cannabinoids for clinical applications.

1.4.5 Cannabinoid receptor (CBR) function

CB1R was mentioned as a protective mechanism for neurotoxicity and neuronal damage (53,76). In the context of DED, the effect of CB1R on neurotransmitters is presented in the following table, including GABA (77), noradrenaline (78), substance P, and other mediators (67). Due to controlling neurotransmission, CB1R-related pathways exhibited neuroprotection effects to support synaptic integrity and plasticity in the nervous system (79,80).

Table 1: CB1R effects on different neurotransmitter release

	Neurotransmitter	Effects on synaptic release	Cannabinoids	Reference
1	Acetylcholine	↓ (under 0.5mg/kg injection) ↑ (2.5 and 5 mg/kg injection)	WIN 55,212-2 (biphasic effect)	(81,82)
2	Aspartate release	↓ K ⁺ induced [³ H]D-aspartate release	Anandamide, methanandamide, and WIN 55,212-2 (agonist)	(83)
3	Ca(2+) influx	↓	HU210 (CB1R agonist)	(67)
4	Calcitonin gene-related peptide (CGRP)	↓	WIN55,212-2	(84)
5	dopamine, norepinephrine, serotonin	↓ due to the regulation of monoamine oxidase activity	THC (agonist)	(85)
6	GABA	↓	Anandamide, THC	(86)(80)
7	Glutamate and aspartate	↓ neuro-toxicity effect of aspartate	THC (agonist)	(87)
8	Substance P	↓	HU210 (CBR1 agonist)	(67)
9	Substance P	↑	SR141716A (CBR1 selective antagonist)	(88)

“↑”: increasing, “↓”: decreasing

CBR2 is found on various immune cells (89), which are listed in the following Table 2. Notably, these cells were mentioned (details in previous section 1.3) to be involved with the DED pathological mechanism (89). Generally, activating the CB2R pathway inhibits activities of immune cells such as cell migration, adhesion, and also cytokine production (such as IFN- γ , TNF- α , or IL-1 β) (89,90). Generally, the inhibition effect of CB2R agonists (like THC) on immune cells was considered anti-inflammatory effects, further details are presented in the following table:

Table 2: Activating CB2R inhibits different immune cells and cytokine releasing

	Immune cells	CB2 expression	CB2 Activation	
1	Langerhans cells or (Dendritic cells)	+	↓migration, MMP-9, cytokine responsiveness	(91) (92)
2	Macrophages	+	↓ gene expression ↓macrophage infiltration ↓leukocyte adhesion	(93)
3	Monocytic precursor	+	↓leukocyte, monocyte recruitment	(94) (95)
4	Neutrophils	+	↓TNF-a-induced MMP-9 release ↓MIP-2a-induced migration	(96,97)
5	T cell CD4+	+	↓activation of CD4+ T cells	(98)
6	T cell CD8+	+	↓SDF-1 induced ↓migration	(99)
	Inflammatory mediators			
8	COX-2, iNOS, NF- κB		↓	(100)
9	IL-1β, IL-6 TNF-α NF-κB dependently		↓	(100,101)

“+”: positive CB2R expression. “↑”: increasing, “↓”: decreasing

1.5 Cannabinoid receptor (CBR) expression at the ocular surface

1.5.1 Previous studies about CBR expression at the ocular surface

CBRs expressions have been studied directly using immunostaining and mRNA expression. Furthermore, CBRs were also characterized by detecting subsequent enzymes and descriptions of the physiological effects of CBR ligands (102–105). The expression of CB1R and CB2R in the DED-relating tissues was also reported (Table 3) (50,106).

Cornea:

CBR1 is expressed in the epithelial and endothelial layers and the stroma (104,107,108). CB1 receptors were found along cell margins in a human corneal epithelial cell model (109). CBR1 is involved in corneal nociception, and activating CBR1 (via WIN 55,212-2) decreased cornea-evoked neural activity; CBR1 has also been found to be primarily present on sensory neurons, where it is found in axon and synaptic terminals (53,76,110), via this location, CBR1 functions are involved with the neurotransmission.

CBR2 expression in the cornea is more intriguing than CBR1 expression. In several in-vitro epithelial models, CBR2 levels were low or undetected (69,111), in contrast to the fact that CBR2 signals were found by histology or PCR techniques in the ocular surface of both healthy and injured

in-vivo animal models (111,112). The reason for this is that CBR2 is primarily found on immune cells. Thus, in-vitro epithelial cell models couldn't detect CBR2 expression. In fact, *in-vivo* experiments showed that CBR2 signals are stronger in the limbus and periphery of the cornea than in the center, where resident immune cells, macrophages, and Langerhans cells are located (111,112). CBR2 signals were detected after an injury during immune cell infiltration into the wound site (111).

Conjunctiva:

In the conjunctiva, CBRs are expressed in the epithelium of the bulbar conjunctiva, the fornix, and near the lid margin (108). In goblet cells, the CBR1 signal is in the cytoplasmic rim surrounding the mucous droplet (108). Both CBR1 and CBR2 expression were both reported in the lacrimal gland (113,114). Moreover, using suitable agonists to stimulate CB1R in the extra orbital lacrimal gland regulated tear production via the neurotransmission process (114).

Table 3: Expression of CBRs in several ocular surface tissues

	Cornea			Conjunctiva			Lacrimal gland & accessory
	Epithelium	Stroma	Corneal nerves	Epithelium	Substantia l layer	Goblet cell	
CBR1	(++) Human, IHC (107)	(+) (107)	(+) Rat, CB1 function (115)	(++) Mouse, IHC & PCR (108) Human, IHC (116)	(+) Mouse, IHC (108) (+) Human, IHC (116)	(++) Mouse, IHC (108) Human, IHC (116)	(++) Porcine, enzyme activity (117) (++) Mouse, IHC, Western blotting, and PCR(114) (++) Axons of cholinergic neurons (114) (+)myo-epithelial and acinar cells(114)
CBR2	(++) Mouse, IHC (69),	(+) Mouse, IHC (69),		(++) Mouse, IHC (108) Human tissue, IHC (116)	(+) Mouse, IHC (108) Human tissue, IHC (116)	(++) Mouse, IHC (108) Human tissue, IHC (116)	Porcine, enzyme activity (117)

“++”: decent signal, “+”: less or scattering signal, “IHC”: Immunohistochemistry

1.5.2 DED model to study the role of the ECS

The data mentioned above implied the expression and function of ECS on the ocular surface. Therefore, this study has a hypothesis if ECS and CBRs functions can improve DED. Additionally, CBRs have not been investigated experimentally in the context of DED. To better understand the functional role of the ocular ECS relating to DED, *in-vivo* animal models were applied to identify novel targets for the DED cannabinoid-based therapy.

The desiccating stress (DS) mouse model was first described by Dursun et al. (118), which combines a constant airflow (at least 15 to 20h), a low relative humidity (not more than 30%), and cholinergic blockade by scopolamine administration (by subcutaneous injection or osmotic pump implantation) to inhibit lacrimal gland secretion (118). Due to its similarity with human DED conditions, this model is the most popular way to study DED pathogenesis and potential therapies (13,118,119). The DS induces mice to recapitulate different DED aspects including corneal epitheliopathy, immune-cell infiltration, cytokines modification, and epithelium apoptosis (13,118). Therefore, this study selected the desiccating stress model to characterize DED phenotypes together with:

- CBR expression in naïve mice and DED-induced mice
- Effects of CBR ligands (as an eyedrop) on the DED readouts of induced mice

1.6 Cannabinoids and eye drop formulation

1.6.1 General information about cannabinoid eyedrop formulation

Using eye drops is a convenient and often patient-compliant route of drug administration, particularly for treating ocular surface diseases. Eye drops resemble a local drug delivery system that avoids systemic cannabinoid side effects and other issues associated with invasive systemic administration such as oral intake or inhalation. However, as lipophilic substances, cannabinoids pose challenges in stability and permeability. In fact, cannabinoid eyedrops have been reported to be failed to reach adequate concentrations at the target organs because the ocular surface acts as a "barrier" to prevent drugs from permeating (73,120). Thus, a drug formulation study for cannabinoids is also demanded. This drug formulation study was conducted for THC, the most recognized biologically active ingredient of cannabis. Because cannabinoids, especially phytocannabinoids, share a similar lipophilic property and other chemo-physical properties, results from this study can be transferred to future potential CBRs ligands.

1.6.2 The ocular surface as a barrier for drug-delivery

Generally, because of the precorneal loss and the cornea barrier, less than 5% of the initial dose permeated through the cornea (121). A topical drop instillation to the eye is followed by a rapid "washing out" with the tear. The volumes of commercial eye drops are between 25 and 70 μL (122). However, only about 10 μL of the instilled dose remains in the precorneal pocket, while a significant remaining part gets lost due to reflex blinking (122,123).

In addition to this, the cornea has three physical barrier layers: epithelial, stromal, and endothelial. The epithelial layers, tight junction non-keratinized cells, hinder the permeation of large and hydrophilic drugs, while the stroma is a thick hydrophilic layer containing highly hydrated collagen, limiting the permeation of lipophilic drugs (121). Notably, small and lipophilic molecules (like cannabinoids) are absorbed through the cornea, whereas large hydrophilic molecules such as proteins or gene-based medicines are absorbed via the conjunctiva and sclera (124,125). Thus, the ocular absorption of ophthalmic eye drops depends on the transcellular transport across the corneal epithelium and stroma (124,125). Besides, the conjunctival-scleral pathway is a non-efficient path with poor bioavailability (124). Due to the hydrophobic nature of THC or CBR ligands, the hydrophilic stroma would prevent these lipophilic drugs from permeating further. As a result, cannabinoids will concentrate primarily on the cornea's epithelial layers.

1.6.3 Further requirements for cannabinoid eye drops

1.6.3.1 To formulate THC eyedrops with high concentration and stability:

Firstly, due to the lipophilic property of THC ($\log P = 5.648$), different surfactants, known to include lipophilic compounds in micellar structures in aqueous media, and other oily solvents (126) were used to get an eye drop with adequate concentration (such as, e.g., 0.5% or 1% of THC) (127). In addition, when THC is formulated as an emulsion or a micellar aqueous solution, the physical stability of the formulation should be considered and carefully evaluated (e.g., by measuring the constant size and size distribution or the absence of phase separation over time upon storage) (126). Secondly, due to the time-dependent instability of THC, a reduction of the THC content during storage should also be assessed. Also, glass or low-binding containers should be used to prevent THC adsorption to plastic containers (15).

1.6.3.2 Permeability of the eye drops:

The corneal epithelium easily absorbs THC (a small hydrophobic molecule), but the underlying hydrophilic stroma then constrains them. As mentioned in glaucoma trials, cannabinoid-eyedrop treatments were ineffective due to poor ocular bioavailability rather than pharmacological activity at the target site (128). Because THC should be able to reach CBR1 and CBR2 in the ocular surface, permeation enhancers (such as surfactants or co-solvents) should be used. Meanwhile, due to the side effect of THC, systemic absorption should be controlled. Therefore, the corneal permeability property study should be evaluated.

1.6.4 Recent drug formulations for THC and other cannabinoids

1.6.4.1 Aqueous vehicle

While aqueous vehicles (with a small amount of excipients) are very popular for eye drop formulations, challenges for the lipophilic THC as an eye drop formulation are expected. However, recent drug formulation studies suggested some vehicles for THC formulations and other cannabinoids. THC stability was improved in the presence of cyclodextrins (CD) at 5% w/v (129,130). In an aqueous formulation, CD's structure has a central cavity that forms inclusion complexes with lipophilic drug molecules (131). After dropping onto the eye, complexes of drug/CD are aggregating at the epithelial surface at high concentrations, facilitating drug release from the complex to penetrate the eye (131). Thus, in vitro corneal permeability data of Δ^9 -THC suggests that the complexation with HP β CD, RM β CD, and S β CD significantly improves its trans-

corneal diffusion. Among aqueous vehicles, the permeability enhancement order is α -cyclodextrin > HMPC (80-120 centipoises) > PVA > HPMC (3500-5600 centipoises) > PVP (29-32 centipoises) > PVP (12-18 centipoises) (132).

1.6.4.2 Oil vehicle and water-free vehicles:

Oily or lipid vehicles used in ocular delivery preparations can be mineral oils (paraffin) or phyto-oils such as sesame, castor, and olive oil. Due to their solubilization properties for lipophilic compounds, mentioned oil vehicles were used to dissolve THC (127,133). A formulation using mineral oils (0.1% THC) showed the highest THC permeability into the cornea, better than formulations containing 10% polysorbate 80 in saline or sesame oil(127,133).

However, oily vehicles were mainly responsible for breaking down the corneal epithelial integrity (134,135). Also, other side effects such as blurred vision, burning sensation, and tearing were related to such a vehicle's topical toxicity (136). These findings somehow explain why purely oily carriers were not used in commercial topical products. Instead, the oily contents (required for drug solubilization) are emulsified by surfactants in the outer aqueous phase of the drug delivery system to form an emulsion or microemulsion (14,137). Notably, these formulations prevent direct contact of oils with the ocular surface (137). Tocrisolve™ is an example of an emulsion vehicle for cannabinoids, which contains soya oil and water (at a 1:4 ratio) and Pluronic F68 as a surfactant. This vehicle can be used to dissolve cannabinoids and related substances in the laboratory (138,139). However, while it has been successfully used in preclinical animal trials and is exciting, it is currently unavailable for human use and is no longer manufactured by the originator.

Previously, several studies from both academic and industrial agents about the solubility of THC in different solvents were reported. Details can be found in Table 4:

Table 4: List of pharmaceutical excipients suitable for THC eye drop formulations

	Excipients	THC solubility	Dosage forms	Ref.	FDA conc.*
1	Polysorbate 80	280 mg/mL	Emulsion	(140)	4% w/w
2	DMSO (Dimethyl sulfoxide)	540 mg/mL	Solution	(140)	Up to 50%
3	Transcutol P (or HP)	434 mg/mL	Emulsion	(120,140,141)	Up to 10%
4	Ethanol	1000 g/mL	Solution	(142)	0.5% w/v
5	Glycerol	390 mg/mL	Emulsion	(140)	2.25 w/v
6	Soybean oil	300-400 mg/mL	Emulsion	(140)	up to 25%
7	Mineral oil	up to 100mg/mL	Emulsion	(138,140)	36.95% w/v
8	Paraffin	up to 100mg/mL	Emulsion, ointment	(127)	69 %

FDA conc.: Excipient concentrations in approved drug products according to the US FDA database (143)*

Although THC solubility in EtOH is relatively high, the range of Ethanol concentrations in ophthalmic use is only 0.5% (**Table 4**), which is too low to prepare a THC aqueous formulation. Therefore, instead of using it as a solvent, Ethanol was used as a co-solvent combined with high-viscous solvents such as polysorbate and glycerol for THC eyedrops.

1.6.4.3 Water-free delivery of semi-fluorinated alkanes

Semi-fluorinated alkanes (SFAs), such as F6H8 or F4H5, are non-aqueous amphiphilic liquids (144,145). In the context of dry eye disease, NovaTears® (Novaliq GmbH), consisting of F6H8, was marketed in the European market to improve DED symptoms under a CE certificate (complies with European health, safety, and environmental protection requirements) and marketed as non-prescription drug product (146). Especially, SFAs can dissolve lipophilic drugs, like THC or other cannabinoids. In fact, a phase III clinical trial of 0.1% cyclosporine (water-insoluble substance) in the SFA platform (Eyesol) is currently being conducted, aiming for DED (147,148). In addition, as non-aqueous and inert solvents, SFAs prevent unstable substances from potential hydrolytic degradation. Due to mentioned properties, these solvents are possible and feasible choices for THC or cannabinoid formulations indicated for DED patients (149).

1.7 Aim of study and project overview

Dry Eye Disease (DED), one of the high-prevalent eye diseases worldwide, is a multifactorial disease characterized by abnormalities in any ocular surface component. Previous studies about the Endocannabinoid system (ECS) and its receptors (CBRs) showed that activation and inhibition of CBRs produce anti-inflammatory, pain, and wound-healing (re-epithelialization) responses. As a result, using CBRs ligands (such as THC or other cannabinoids) is proposed as a potential therapy for DED. This research on drug development for dry eye disease has the main hypothesis: CBR ligand eyedrops have therapeutic effects on the DED mouse model.

To formulate cannabinoids as eyedrops for in-vivo experiments, DMSO was chosen to dissolve cannabinoids as a stock solution (120,140,141). Furthermore, the DMSO stock solution is readily miscible with cell culture media or aqueous liquids for further biomedical studies. Despite the popularity and advantages of DMSO in scientific research (150,151), there are still no commercial eyedrops containing DMSO as an excipient. Therefore, a drug formulation study was conducted to propose potential formulations or pharmaceutical excipients for future industrial applications.

In this thesis, three objectives were investigated in this context:

- (i) Desiccating stress model and cannabinoid receptor (CBRs)
 - CBR expression and DED-induction in an *in-vivo* model
 - Effects of CBR ligands on (i) DED phenotype, (ii) neurosensory abnormalities, (iii) inflammation
- (ii) *Ex-vivo* wound-healing model
 - Cannabinoid effects on the wound healing process (re-epithelialization)
- (iii) Drug development study
 - Drug formulation: Excipient selection, stability test
 - Drug permeability experiments

Objectives (i) and (ii) are to answer whether CBR ligands and their effects are involved in the three core pathomechanisms of DED. Objective (iii) is to develop a formulation ready for clinical preparation and the pharmaceutical industry.

2 Material

2.1 Animals

Female C57BL/6N mice (8-12 weeks old) were purchased from Charles River Laboratories, Germany. Husbandry and all experimental procedures were carried out by the approved protocols established by the State Agency for Nature, Environment and Consumer Protection (LANUV). All in-vivo experiment protocols were harmonized with the Association for Research in Vision and Ophthalmology (ARVO, Statement for the Use of Animals in Ophthalmic and Vision Research).

2.2 Pharmaceutical active ingredients (cannabinoids)

Δ^9 -tetrahydrocannabinol (THC): Experiments with tetrahydrocannabinol were authorized by the Federal Institute for Drugs and Medical Devices (Bundesopiumstelle des Bundesinstituts für Arzneimittel und Medizinprodukte, Lincence Nr: 463 1128). THC was handled and managed according to the provider's guidance (Bionorica SE, Neumark, Germany, details in the method).

Other pharmaceutical active ingredients are mentioned following:

Pharmaceutical substances	Manufacturer	CAT num. (#)
THC (also called Dronabinol)	Bionorica SE, Neumark, Germany	02887668
CBR1 selective antagonist, SR-141716A	Sigma-Aldrich, Darmstadt, Germany	SML0800
CBR2 selective antagonist, SR144528	Sigma-Aldrich, Darmstadt, Germany	SML1899
Scopolamine hydrobromide trihydrate	Sigma-Aldrich, Darmstadt, Germany	S1875
Isoflurane (Isofluran-Piramal (250 mL)	Piramal, Drayton, UK	09714675
Rimadyl Injectable (Carprofen)	Zoetis, Berlin, Germany	10000319
D-3H-mannitol	Perkin Elmer, Walham, MA, US	NET101001MC
3H-Propranolol	Perkin Elmer, Walham, MA, US	NET515250UC

2.3 Media, buffer, and solutions

Reagents	Manufacturer	Cat. Number
Dulbecco's modified eagar medium (DMEM) /F12 (1:1)	Gibco-Thermo Fisher Sci., Darmstadt, Germany	D0697
Penicillin/Streptomycin	Gibco-Thermo Fisher Sci., Darmstadt, Germany	15140-122
Fetal Bovine Serum (FBS)	Thermo Fisher Sci., Darmstadt, Germany	A4766801
Sodium chloride , 0.9% (w/v)	Merck, Darmstadt, Germany	106400
1x PBS	Thermo Fisher Sci., Darmstadt, Germany	10010023
RIPA buffer	Thermo Fisher Sci., Darmstadt, Germany	89900
Trypsin/EDTA	Sigma-Aldrich, Darmstadt, Germany	T3924
Ethanol	Sigma-Aldrich, Darmstadt, Germany	32205-M
Isopropanol	Sigma-Aldrich, Darmstadt, Germany	34863
Hematoxylin Solution, Gill No. 1	Fisher-scientific, Darmstadt, Germany	HXGHE1LT
Fluorescein Alcon® 10%	Alcon Pharma, TX, US	01467007
Eosin G 1% (v/v)	Carl Roth, Roth, Germany	3137.2
Bovine serum albumin (BSA)	Amresco	0332
Formalin (~4 % Formaldehyde)	Sigma-Aldrich, Darmstadt, Germany	#F8775
Hydrochloric acid (37%)	Roth, Roth, Germany	X942
RNase away	Molecular Biopro,	70003
Goat Serum	Abcam, Cambridge, MA, US	AB7481
Trypan blue	Biochrome, Berlin, Germany	L6323
Methanol	Sigma-Aldrich, Darmstadt, Germany	14372511
DAKO Mounting medium	Sigma-Aldrich, Darmstadt, Germany	S302380-2
Dimethylsufoxide (bio)	Sigma Aldrich, Darmstadt, Germany	D8418
RNAlater	Sigma Aldrich, Darmstadt, Germany	R0901
Freund's Adjuvant, Complete Freund's	Alcon Pharma, Fort Worth, TX, US	F5881

2.4 Antibodies

Reagents	Manufacturer	Cat. Number
rabbit anti-mouse β 3-tubulin	Abcam, Cambridge, MA, US	ab18207
goat anti-rabbit IgG (HL, Alexa Fluor 488)	Thermo Fisher Sci., Darmstadt, <i>Germany</i>	A11034
CD4 Monoclonal Antibody	eBioscience, Cheshire, UK	GK1.5, 14-0041-85
CD8a Monoclonal Antibody	eBioscience, Cheshire, UK	14-0081-82
Goat anti-Rat IgG (HL, Alexa Fluor 555)	eBioscience, Cheshire, UK	A21434

2.5 KITs and commercial probes

Reagents	Manufacturer	Cat. Number
RNAscope Probe - Mm-Cnr1	Advanced Cell Diagnosis, CA, US	420721
RNAscope Probe - Mm-Cnr2-C2	Advanced Cell Diagnosis CA, US	407351-C2
RNAscope® 2.5 HD Duplex Reagent	Advanced Cell Diagnosis, CA, US	322430
Qiagen RNeasy Plus Mini Kit	Qiagen, Hilden, Germany	74134
RevertAid Synthesis Kit	Thermo Scientific, Darmstadt, Germany	K1622
SSoFast EvaGreen	Bio-rad, Hercules, CA, US	1725201

Target gene	Forward & Reverse primers
Cnr1 (for CB1R)	For: TTGCTCAGACATCTTCCCCTC Rev: CTGTGAGCCTTCCAGAGAATGT
Cnr2 (for CB2R)	For: GTGAAGACAAGGGACCTGTTCT Rev: AGGATGAAGCAGGAACCAGAAG
IL-1 β	For: GTCCTGTGTAATGAAAGACGGC Rev: CTGCTTGTGAGGTGCTGATGTA
IFN- γ	For: CTTTGCAGCTCTTCCTCAT Rev: GTCACCATCCTTTTGCCAGT
HPRT	For: GTTGGATACAGGCCAGACTTTGTTG Rev: GATTCAACTTGCGCTCATCTTAGGC

2.6 Devices

Devices

Autoclave, Labklav 25
Anesthesia machine,
Precision & Analytic balance
Centrifuge, Refrigerated Benchtop, 4K15C
Centrifuge, Refrigerated Benchtop, Heraeus" 16
Digital camera ColorView III
Fluorescence microscope BX51
Fridge, UK1720, 4°C
Fridge, G 521008, -20°C
Freezer, Forma 906, -86°C
Homogeniser, Precellys ® 24
Magnetic stirrer, heatable, VMS-A
Microscope Illumination, KL1500 compact
Spectrophotometer, Epoch Microplate reader
Ultrasonic processor, Vibra cell™ 72434
PCR Bio-rad
Cryostat CM3050
HybEZ Hybridization system
Imager.M2 microscope
Nanodrop 2000
Vortex-Genie
Zetasizer Malvern
Franc Diffusion cell Lauda E100
2450 Microplate Counter
Osmostat OM-6020

Manufacturer

SHP Steriltechnik, Haldensleben, Germany
UNO BV, Rijswijk, Neitherland
Sartorius, Goettingen, Germany
Sigma Lab., Darmstadt, Germany
Thermo Fisher sci., Darmstadt, Germany
Olympus Optical Co., Hamburg, Germany
Olympus Optical Co., Hamburg, Germany
Liebherr International
Liebherr International
Thermo Fisher sci., Darmstadt, Germany
Bertin Technologies, Frankfurt, Germany
VWR International, Darmstadt, Germany
Schott AG, Mainz, Germany
Bio-Tek, Bad Friedrichshall, Germany
Bioblock sci, Illkirch-Graffenstaden, France
Bio-rad, Hercules, CA, US
Leica, Wetzlar, *Germany*
Advanced Cell Diagnostics, CA, US
Zeiss, Oberkochen, Germany
Thermofisher, Darmstadt, Germany
Scientific Industries
Malvern, Malvern, UK
Harvard Apparatus, MA, USA
Perkin Elmer, Walham, MA, US
Daiichi, Kyoto, Japan

2.7 General consumables

Consumables	Manufacturer	CAT
Culture plates, 6-well	Greiner Bio-One International	833920

Cover slip	Carl Roth, Roth, Germany	P231.1
Eclipse needle 0.6x25 mm	BD and co., Franklin Lakes, NJ, US	309628
Osmotic pump	ALZET, Cupertino, CA, US	Model 1002
Disposable Scalpel, No.11	FEATHER Safety Razor	2978-11
Disposable syringe 1 ml	Dispomed, Gelnhausen, Germany	22011
PCR tube (0.1 & 0.5mL)	Eppendorf, Hamburg, Germany	0030124804 or 0030124707
Eppendorf Safe-Lock Tube	Eppendorf, Hamburg, Germany	0030121023
Superfrost Plus	ThermoFischer, Darmstadt, Germany	J1800AMNT
Sterile filter: PTFE 0.22µm, 13mm)	VWR, Darmstadt, Germany	514-1275
Clear glass vial	VWR, Darmstadt, Germany	548-8011
96-well microtiter plate	Sarstedt, Nümbrecht, Germany	83.3924
Cover glasses 18x18 mm	Th.Geyer, Renningen, Germany	7695023

2.8 Software(s) and data analysis

Software	Developer or manufacturer
Graphpad Prism 7.0	Graphpad Software, Motulsky, CA, US
MeVisLab 2.8.1.	MeVisLab, Bremen, Germany
Image J	Wayne Rasband (freeware, retired from NIH)
Matlab 8.5	MathWorks, Natick, MA, US

3 Methods

3.1 In-vivo DED-induced mouse model and effect of cannabinoids

3.1.1 Experimental DED mouse model:

Dry eye disease (DED) was induced in C57Bl/6N mice (8 to 12 weeks old) using the desiccating stress model (DS). The in-vivo experiment protocol was performed as in previous publications with minor modifications (118,120).

Pretreatment:

Mice were kept and housed in the standard conditions for two weeks before experiments. Before DED-inducing experiments, mice were screened with DED phenotypes (details are mentioned in section 3.1.2). Mice with low body weight (not more than 20g) were excluded from the experiments.

Anesthesia:

In the experiment, mice were anesthetized in the chamber (UNO Induction Box and Gas Exhaust Unit, UNO BV). Isoflurane (4.5% v/v, isoflurane) was provided at a flow rate of 0.5-0.8 $\mu\text{l}/\text{min}$. When the desired depth of anesthesia conditions was obtained, the mouse was inhaled with 3% (v/v) isoflurane at a flow rate of 0.25-0.3 $\mu\text{l}/\text{min}$.

Scopolamine implantation and desiccating chamber:

Before an experiment, a baseline check was done to exclude mice with significant DED phenotypes or other ocular surface diseases. For the DED induction, each mouse received scopolamine hydrobromide (an anticholinergic agent) at 5mg/kg/day. Each mouse was subcutaneously implanted with an Alzet osmotic pump (model 1002) containing a scopolamine solution (6.5mg/mL in PBS). After that, scopolamine-implanted mice were housed under DS conditions (humidity: 25 ± 5 %, temperature: $25 \pm 5^\circ\text{C}$, with a constant airflow for 19 hours/day). The constant air flow in each mouse cage was provided by 2 fans (80 mm fan size) at 50 CFU airflow speed.

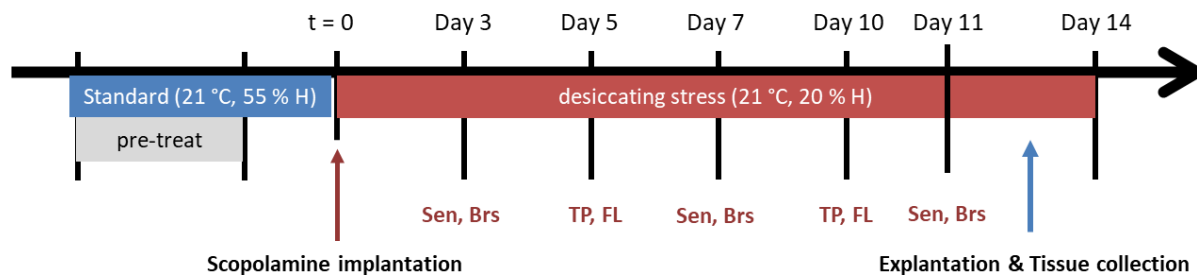


Figure 2: Desiccating stress model: schedule of the experiment

“TP”: Tear production, “FL”: Fluorescein score, “Sen”: mechanical sensitivity (von-Frey filament test), “Brs.”: brush test

3.1.2 DED phenotype evaluation

During DS (14 days), DED phenotypes were reported at different timepoints (Figure 2). Experiments were conducted as a blind study; the researcher did not know which groups received drug formulation or carrier (without drug substances). Before experimentation, naïve mice which showed significant ocular surface diseases were excluded.

DED phenotype tests were conducted to screen mice (at pretreatment) and monitor disease severity (during DED-induction). The DED readouts are (i) fluorescein score (FL, for corneal epitheliopathy), (ii) tear production (TP), (iii) mechanical sensitivity (Sen.), and (iv) brush test (Brs.). To avoid interference, the readouts were done at least 10 hours after applying eyedrops. To prevent heavy stress on the mice due to the phenotype test, TP and FL were done on day 5 and day 10 of the DS, while sensitivity and Brs. were done on Day 3, 7, and 11.

(i) *Fluorescein score (FL)*: Diluting fluorescein sodium (Alcon, TX, USA) into PBS (1% w/v). The obtained solution was applied to the mouse eye. After rinsing once with isotonic saline, the fluorescein signals remained in cornea areas where the epithelium was abrasive or injured. The corneal epitheliopathy was observed with a cobalt blue filter and a biomicroscope (Nikon Illuminator Intensilight C-HGFI). The score (FL score) was rated according to the Oxford scheme (0 to 5); the test was carried out on both eyes of each mouse (152).

(ii) *Tear production (TP)*: Cotton phenol red threads were used to measure the amount of tears produced by the experimental animals. The yellow thread was placed into the lateral canthus for 8 to 12 seconds. Then the phenol red thread absorbed tears and changed color from yellow to red due to the pH-sensitive property to the alkaline tear (pH from 7 to 8). TP values were reported as the length (mm) of the red part. Experiments were performed for both eyes of each mouse.

(iii) *Mechanical sensitivity (Sensitivity)*: The protocol is according to Bonin’s “simplified up-down” procedure (153). The experiment started with the smallest-diameter von Frey’s filament (0.008 grams force), which was applied to the center of the cornea. If a negative result occurs (without blinking), the stimulus force increases to a higher power (using thicker filaments). If a positive occurs, the test will be at a stimulus 1 step down from the previous stimulus. Each eye was tested 5 times with different filament forces (153). The fifth (5th) filament value was used to calculate the von Frey force threshold (g) for each eye. Depending on the response (positive or negative) to the 5th filament, the von Frey force (g) was calculated as:

“Von Frey filament (g) = The value of the 5th filament ± 0.5 stimulus intervals.”

- Positive “+” adjustment: if there was a negative response to the 5th filament, the response threshold should be higher than the force provided by the 5th filament.
- Negative “-“ adjustment: if there was a positive response to the 5th filament, the response threshold should be lower than the force provided by the 5th filament.

3.1.3 Cannabinoid receptor ligands treatment:

To determine the effect of cannabinoid ligands, DED-induced mice (n = 5) were topically applied drug formulations (5 µl/eye) with 3 different substances:

- (i) The non-selective agonist is Δ^9 -tetrahydrocannabinol (THC),
- (ii) The selective CB1R antagonist is SR141716A (AntaCB1),
- (iii) The selective CB2R antagonist is SR144528 (AntaCB2)

Eyedrop formulation for each substance will be presented in the next section. Each formulation was topically applied 3 times per day from day 1 (after scopolamine implantation) for 14 days continuously. To confirm the effect of the cannabinoid, each experiment was carried out with a group (n =5) of the carrier (formulation without drug) and a group of DED-induced mice without any eyedrop treatment (served as untreated DED control, n=5).

All experiments were done in a blind fashion. Two separate experiments with 3 groups (drug application, carrier, and untreated DED, n = 5/group) with observing and reporting the DED phenotype readouts were conducted, then DED-induced mice were euthanized to collect tissues for gene expression and immunohistology. Representative data was shown for 5 mice (n = 10 eyes) per group.

3.1.4 Gene expression analysis by RT-qPCR

Tissue collection: After the final phenotype test, mice were euthanized by CO₂ in a specialized chamber. Tissues of corneal, conjunctiva, and lacrimal gland were dissected to isolate and analyze the mRNA of CB1R and CB2R. Two corneas or 2 conjunctivae from each mouse were put into 1 tube (1 cornea sample or 1 conjunctiva sample, respectively). Collected tissues were kept in an Eppendorf tube (1.5mL) filled with β -mercaptoethanol and Buffer RLT Plus (1:100, v/v). The samples were then frozen with liquid nitrogen (-196°C) and later kept in the -80°C freezer conditions. The followed-up protocol and related solutions were done according to the RNA isolation Kit's manual guide (QIAGEN RNeasy Plus Mini Kit).

RNA isolation: The frozen tissues were then thawed on ice (0-4°C) for RNA isolation. The cornea and conjunctiva samples were homogenized by a sonicator (Lab Handheld Portable Ultrasonic Homogenizer Sonicator Processor) (20 secs x 3 times). To reduce RNA degradation (by heating caused by the sonicator), Eppendorf tubes (with samples) were kept in ice (4-8°C) during the sonicating time. The RNA isolation procedures followed the manual guide with minor modifications. To elute the maximal amount of RNA, 15 μ L RNase-free water was pipetted onto the silica-gel membrane and incubated for 10min at room temperature. The isolated RNA solution was put in the (-80 °C) freezer. To measure the concentration, 1 μ l of final RNA samples was placed in the NanoDrop 2000 (Thermo Fisher, DE, USA). The UV absorption wavelength for RNA is 260 nm. A sample with a 260/280 ratio (the ratio of 260 nm and 280 nm absorbance values) over 1.6 is considered a qualified-purity sample.

cDNA preparation: First-strand cDNA was synthesized with a protocol and materials from Thermo Scientific RevertAid Synthesis Kit (DE, USA). Four hundred (400) ng of total RNA was transcribed in each experiment. The synthesized cDNA was stored in a 0.1mL PCR tube at -20 °C until qPCR experiments.

RT-qPCR: Real-time PCR was performed using SsoFast EvaGreen Supermix (Biorad Laboratories). Assays were performed in triplicate in each sample in a 96-well plate. To prevent inter-day variability, each PCR run (96 wells) was designed and carried out with all groups: an untreated group, a drug-treated DED group, and a carrier-treated group (without drug substance). The qPCR primers are presented in the material session (2.1.5). The endogenous reference for each qPCR run was the HPRT gene. The CBRs expression was analyzed by the comparative CT method ($2^{-\Delta\Delta Ct}$), and the mean Ct in the control group was used as the calibrator.

3.1.5 In-situ hybridization

Tissue collection and fresh frozen cryosections: After the mouse was euthanized, the whole eyes (with both eyelids) were enucleated. Snap freezing samples were done by placing samples in liquid nitrogen and then stored in the -80°C freezer. Cryosections of 10 µm thickness were prepared with a cryostat. Sections were mounted onto a microscope glass slide and stored at -20°C until further use for in-situ hybridization or immunostaining.

Fixation process for fresh frozen tissues: After taking new frozen tissue (mounted on glass slides) from -20°C, the slides were immediately immersed in pre-chilled 4% PFA for 15min at 4°C. The slides were then immersed consecutively in ethanol (EtOH) with increasing concentrations (from EtOH 50%, EtOH 70%, to EtOH 100%), 5min for each EtOH solution. The slides in EtOH 100% can be stored for 24h for the next step.

In-situ hybridization process: This experiment was performed according to the protocol provided by Advanced Cell Diagnostic. RNA hybridization Kit (RNAscope® 2.5 HD Duplex Reagent Kit) and related probes (negative control, positive control, CB1R, and CB2R) were purchased from Advanced Cell Diagnosis (Details were mentioned in 2.1.5). After counterstaining with hematoxylin and mounted on a glass slide, tissue sections were examined under a standard bright field microscope. The KIT can detect two target RNAs independently in a dual hybridization process. Each target probe is in a different color (CB1R signal is blue/green, CB2R signal is red).

3.1.6 Corneal nerve immunohistochemistry

Tissue collection: After the mouse was euthanized, the whole mount cornea was collected in an Eppendorf tube with 500 µL PBS; the sample tubes were then stored in ice (0-4°C) during the tissue collection process and kept in a fridge (4-8°C). Depending on the number of tissues and experiment schedule, the whole-mount cornea samples should be processed in less than 24h to keep the cornea as fresh as possible.

Immunostaining process: The cornea samples were washed several times with PBS to remove blood or contaminants during surgery. Surgery knives and scissors could be used to remove sticky black pigments (which influence the immunostaining signal at the end). Then each cornea was kept in an Eppendorf tube (1 cornea/tube) during the whole staining and washing process.

The samples were fixed by soaking in paraformaldehyde 4% for 30 min with a shaking machine. Next, sections were blocked with bovine serum albumin (BSA) for 3 hours, followed by primary antibody incubation at 4°C overnight. The primary antibody is the rabbit anti-mouse β3-tubulin (at

dilution 1:1000 in PBS) (#ab18207, Abcam). On the second day, samples were washed PBS (3 times) and incubated with the secondary antibody (goat anti-rabbit IgG-HL, Alexa Fluor 488, #A11034, Thermo Fisher) for 1 hour at room temperature, again followed by three times of PBS washing. Because the secondary antibody is fluorescently labeled, the samples were kept in a dark condition. After a final wash in PBS, each cornea was embedded with Dako fluorescent mounting medium.

Imaging and data analysis: Fluorescence images from β 3-tubulin staining corneas were taken using a BX53 Olympus (Hamburg, Germany) microscope.

The tubulin signal (in green) was analyzed in a freeware imaging program, MeVisLab (version 2.8.1., Germany). Depending on image quality (brightness, contrast, sharpness, and fluorescein-staining quality), up to 10 seed points and Region growing parameters were manually set in MevisLab software. The algorithm would calculate areas covered by nerves (binary images), excluding the background (semi-automatically algorithm). The nerve density was calculated based on the area (in pixels) covered by the nerve. The axon length per area (mm/mm²) was quantified from the skeletonized images (with 1-pixel width). The data was collected from both eyes of each animal (n=10 eyes/ 5 mice).

3.1.7 Immunostaining CD4⁺ and CD8⁺ T-cell infiltration into conjunctiva

Tissue collection and fresh frozen cryosections: Tissue collection and fresh frozen process were similar to the previous section 2.2.5. However, the cryosection was set at 8 μ m thickness to optimize the immuno-staining signal.

Immunostaining process: The cryosections (8 μ m) were fixed with acetone (-20°C, 10 min). After washing, the samples were then stained with the diluted primary antibody solution in PBS (1:150) overnight at 4°C. To avoid dehydration of the sections, glass slides were kept in a humidity incubation plastic chamber.

The next day, after washing with PBS, samples were incubated with Goat anti-Rat IgG-HL, Alexa Fluor 555 (1:150 dilution). Then the cell nucleus was stained with 0.1 mg/ml DAPI for 10 minutes in the dark at room temperature. Finally, the samples were washed with PBS (3 times) and then fixed with DAKO fluorescent mounting medium.

Imaging and data analysis:

Representative cryo-sections from each eye were selected, in which the chosen section should contain an intact upper lid and lower lid. The stained samples were observed and recorded by the

Olympus BX53 microscope with different fluorescein filters (Olympus, Hamburg, Germany). Quantification of CD4⁺ conjunctival T-cells and CD8⁺ T-cells in the conjunctival epithelium was reported as numbers per 100 μm (total n = 4 for each group).

3.2 *In-vitro* wound healing model

To evaluate the cannabinoids' effects on corneal re-epithelization, the ex-vivo alkali-burned model was set up as reported previously [28,29].

3.2.1 Animals and tissue preparation:

To prevent the interference of the black pigment from B16/N mice at the final imaging process, BALB/cN mice were used at 12 weeks of age, acquired from Charles River Laboratories, Germany. Mice were anesthetized by isoflurane as mentioned conditions. The naïve mice were then sacrificed by cervical dislocation. The eyeball was quickly enucleated by cutting to disconnect the eyeball from the optic nerve and underlying tissue. Nuclei were explanted and glued into glass Petri dishes with tissue glue (3M Vetbond, 1469).

Preparing NaOH-soaked Whatman filter paper: A round piece (2 mm in diameter) of Whatman filter paper was soaked with NaOH 0.5% before the experiment.

Inducing cornea wound: The NaOH-soaked Whatman filter paper was placed onto the cornea and kept for 2 minutes. The remained epithelium was removed using a micro-scalpel. The eye nucleus was cultured in DMEM/F12 1:1, supplemented Pen-Strep 1%, with standard culture conditions (37 °C, 5 % CO₂).

3.2.2 Cannabinoid ligand treatment:

Cannabinoids were dissolved into the medium at different concentrations: THC (0.1, 0.5, 1, and 10 μM), CB1, and CB2 antagonists (0.1 μM and 1 μM). The medium with cannabinoids was replaced by the fresh one every 12 hours. The culture medium without any supplement (DMEM/F12 1:1) was used as a negative control; while a positive control medium was prepared with fetal bovine serum in DMEM/F12 at a concentration of 10%.

3.2.3 Imaging and data analysis:

The corneal wounds were visualized by fluorescein staining (Fluoreszein SE Thilo, AlconPharma). After documenting the corneal defects using a blue light source and fluorescein filter, fluorescein dye was rinsed from the bulbs, and fresh medium was filled into the Petri dishes. Between the measurements, the samples were transferred back to the incubator. Images were observed and

measured by using Image J open software. The wound area was measured at the time points: 0h (immediately after wound making), 6h, 12h, 24h, 30h, 36h, and 48h.

3.3 Drug formulation study

Cannabinoid ligands used for the in-vivo DED-induce experiment and wound healing experiment are 3 following substances:

- (i) Non-selective agonist: Δ^9 -tetrahydrocannabinol (THC),
- (ii) Selective CB1R antagonist: SR141716A (AntaCB1),
- (iii) Selective CB2R antagonist: SR144528 (AntaCB2)

The supplier (Bionorica, Germany) provided THC in a glass syringe with a gray rubber cap. At room temperature, THC is in a liquid form with high viscosity (also called a “resin” form). After removing the gray rubber cap, the THC syringe was heated at 60°C (the recommended temperature by the manufacturer), then heated THC was injected into an Eppendorf tube.

3.3.1 Excipient selection study

DMSO was used at the beginning for the cannabinoid formulation due to its availability and popularity in bio-laboratory. However, to aim for a THC eyedrop formulation, further drug development studies were carried out to select other excipients besides DMSO. The formulation process was carried out with 3 following steps:

- (i) Preparation of stock solution (Stock solution): Based on the chemical-physical properties of THC, several pharmaceutically acceptable solvents for ophthalmic use were tested to dissolve THC raw material.
- (ii) Eye-drop formulation (micellar solution): Adding the stock solution into a water phase with different surfactants to have a final concentration (5mg/mL). There are 5 water phases were selected:
- (iii) Sterile filtration: the final formulation was filtered through a 0.22 μm filtration to prevent microbial contamination during the preparation process

The trial formulations were made according to (i) and (ii). The products were filtrated as mentioned in (iii). Trial formulations were characterized with technical feasibility (absence of phase separation), physical appearance (no drug substance precipitation), and short-term stability (7 days, physical appearance & THC concentration).

3.3.2 Eyedrop permeability study with radio-labeled substances

Radio-labeled substances and formulation: Selected formulations were evaluated for the permeability profile. At first, to assess the formulation effect on the drug permeation profile, the radiolabeled substances, H3-Mannitol (PerkinElmer, Waltham, MA, US), were purchased and prepared according to the guidance of the manufacturer. The radiolabeled substances were added into the formulations right before the permeability experiment.

Tissue preparation: This experiment was done on the porcine eye model. Before the experiment, porcine (pigs) were housed at the animal quarter, University of Eastern Finland (Kuopio, Finland). After the pig was sacrificed, its eyes were explanted. The eyes were collected into a tube filled with PBS. The samples were kept on ice (0-4°C) during the transportation. The cornea was dissected from the eyeball using a surgery scissor to cut along the limbus area. BSS Plus solution (pH 7.4, Alcon Laboratory, TX, USA) was applied to the cornea during the preparation process to prevent tissue dehydration.

Permeability study:

This experiment used a Franz cell diffusion apparatus (Figure 3). The experiments were started when filling the donor chamber with 0.5mL radio-labeled formulation (t=0). At each time point, a volume of 500 µL sample was collected from the receptor chamber to quantify the drug permeating through the cornea, and the removed volume in the receptor chamber was replaced with the fresh BSS buffer. The experimental time points were 15, 30, 45, 60, 75, 90, 120, 150, 180, 210, 240, 270, 300, 330, and 360 min. Samples from the donor chamber were also collected, in which a 100 µL sample was taken at t =0 and after 360min (the experiment endpoint). Radio-labeled samples were stored at room temperature before analysis. The permeability profile was evaluated in (i) %permeated and (ii) Paap values (permeability coefficient)

% Permeability: is the percentage value denoting the quantity of drug permeated (in the receptor chamber) at different time points when compared to the original amount (in the donor chamber at t =0)

Papp (permeability coefficient)(154): The equation of the permeability coefficient (Papp, cm/s) was mentioned as: “ $P_{app, CJ} = J / (C_0 * A)$ ”

In which,

J (ng/s) is the rate of drug diffusion across the tissue, calculated based on concentration in receiver chambers at different time points.

C_0 is the drug concentration (ng/mL) in the donor chamber (at $t = 0$),

A is the area of the exposed tissue (approximately 0.64 cm^2 , equivalent to the circular aperture of the donor chamber).

Each cornea was kept in sink conditions between the donor and chamber sides during the whole experiment. The formulation with higher Paap values can deliver higher drug permeated through the cornea.

Radiolabeled quantification: The quantification process was done according to the Perkin Elmer protocol. Ultima Gold TM (#6013326) was used for sample preparation. Briefly, a $100 \mu\text{L}$ sample (in BSS buffer) was mixed with $400 \mu\text{L}$ Ultima Gold in a 6-well plate. The well plates were kept at room temperature overnight before measurement by a radio-labeled microplate counter (2450 MicroBeta, PerkinElmer).

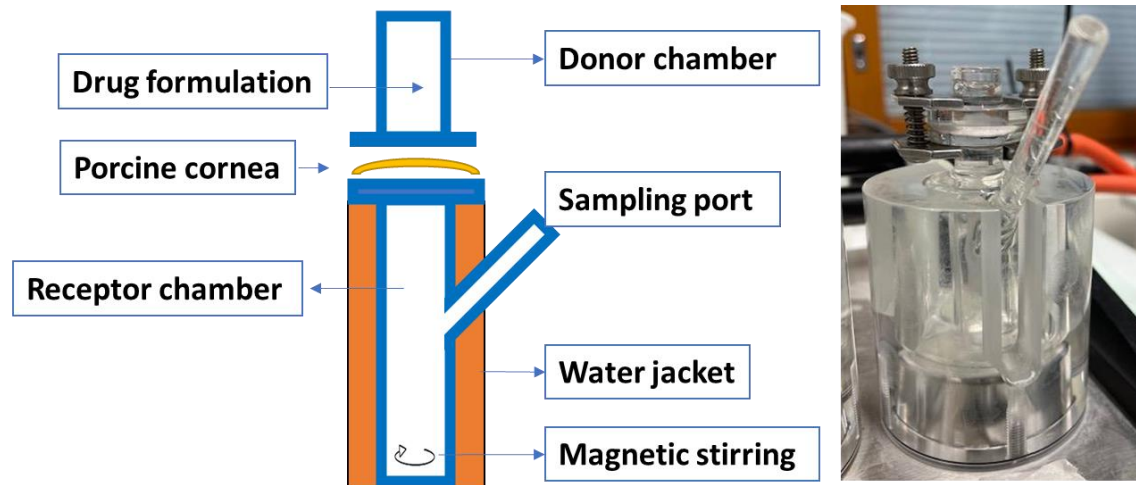


Figure 3: Illustration of drug permeability experiment: (left) Franz diffusion cell diagram, (right) Franz diffusion cell image

3.3.3 Other pharmaceutical quality criteria

3.3.3.1 THC quantification:

The analytical method for in-vitro studies was supported by the Institute of Forensics, University Hospital Cologne (Forensische Toxikologie und Alkoholologie, Institut für Rechtsmedizin, Universitätsklinikum Köln).

It was carried out on an HPLC-UV with an autosampler. The mobile phase included acetonitrile: water (0.085% H_3PO_4) at a flow rate of 1.2 mL/min . The eye drops were diluted (1:10) with mobile phase and quantified immediately after preparation. The detection was carried out at a wavelength of 226 nm .

3.3.3.2 *Particle size and particle size distribution analysis:*

Dynamic light scattering technique (DLS, Zetasizer Nano ZS90, Malvern Instruments, Malvern, UK) was used to measure particle size distribution including the average diameter (Z values, nm) and polydispersity index (PDI) of the micellar or oily droplets dispersed in the aqueous phase. About 1 mL of eyedrop formulation (without dilution) was put into the equipment and analyzed in triplicate (n = 3) ((155).

3.3.3.3 *Osmotic parameters:*

The osmolality values of the THC formulations were determined by measuring ice crystal formation temperature in 200 μ L of sample in a measurement cell. Osmotic pressure was calculated based on a calibration-based analytical curve using an osmometer with an autosampler (osmostat OM-6020, Daiichi Kagaku, Kyoto, Japan). Before sample analysis, the osmometer was calibrated with standard solutions (300 and 1000 mOsm/kg solutions).

3.4 Statistics and data analysis

The sample size in this study was selected based on pilot studies and previous reports in the same laboratory conditions by Gehlsen et al. (119). The statistical differences among naïve, DED-induced, and therapeutic effects were detected when experiments were conducted with n = 10 eyes (5 mice) in each experiment (119). The selected sample-size, experimental time points, and frequency of tests used in this desiccating model were based on mouse phenotypes and the development of the DED induction, which are similar to previous reports about this model conducted by different groups (118,156,157). After preliminary experiments, the sample size was also re-calculated by power analysis based on DED phenotypes, in which selecting 5 mice (10 eyes) matched the sample-size requirement.

The results were reported and presented as mean and standard deviation. Statistical calculation was carried out using Graph-pad Prism 7.04 (GraphPad, CA, USA). The normality of the data was assessed with D'Agostino-Pearson test (suggested by GraphPad software). If the data followed a normal distribution, two-way or one-way ANOVA (with Tukey posthoc) and the T-test were used. If the data did not follow a normal distribution, the obtained data were analyzed by non-parametric ANOVA with Tukey post hoc; the Mann-Whitney test was used to compare two groups. A p-value of less than $p < 0.05$ was considered statistically significant.

4 Results

Results presented in sections 4.1 and 4.2 have been published as (120), Tran et al., the Ocular Surface, 2022.

4.1 Expression of cannabinoid receptors on naïve mice and DED-induced mice

4.1.1 Expression of cannabinoid on naïve mice

4.1.1.1 RT-qPCR result

This experiment aimed to confirm the expression of CB1R and CB2R in the ocular surface system (cornea, conjunctiva, and lacrimal gland). The trigeminal ganglion (Gang) and spleen were used as the control samples for CB1R and CB2R, respectively. The results are presented in the following Figure 4.

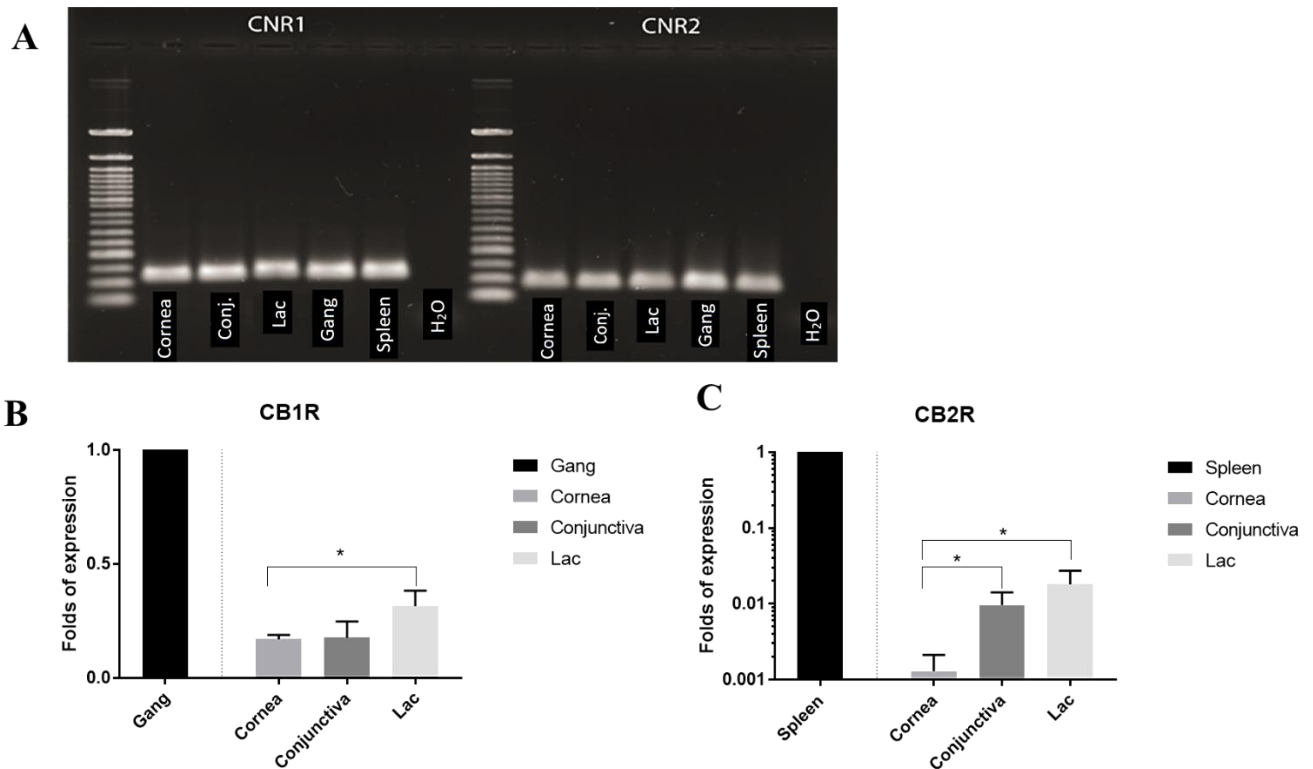


Figure 4: (A) Electrophoresis detection for PCR amplification of CB1R and CB2R mRNA transcripts in different ocular surface tissues; control tissues are trigeminal ganglion for CB1R and spleen for CB2R. (B and C) RT-qPCR analysis for CB1R and CB2R expressions among tissues: lowest in cornea, highest in lacrimal gland, “conj,”: conjunctiva, “Lac”: lacrimal gland, “Gang”: trigeminal ganglion, * $p < 0.05$, adapted from (120)

In Figure 4, CBRs signals were detected in the cornea, conjunctiva, and lacrimal gland (Figure 4A and B). As shown in Figure 4B, expressions of CB1R and CB2R were different among tissues and

lower than control tissues (trigeminal nerve for CB1R, and spleen for CB2R). The lacrimal gland was reported with a higher CB1R and CB2R expression than that of the cornea ($p < 0.05$), whereas CB2R expression(s) in the lacrimal gland and conjunctiva were not statistically different ($p > 0.05$).

4.1.1.2 *In-situ hybridization*

In addition to RT-qPCR, the in-situ hybridization technique was also used to characterize the expression of CB1R and CB2R, in which mRNA signals of CB1R and CB2R were labeled by the commercial CB1R and CB2R ACD RNAscope probes. In Figure 5, the blue arrows point to the CB1R signals, and the red arrows point to the CB2R. In detail, CB1R and CB2R were observed in the epithelial layers at a higher density than the stroma or substantial layer. The CBRs signals were low and scattering in the stroma and substantial layer of the conjunctiva. In general, the images obtained from in-situ hybridization also confirmed the expression of the two CBRs.

Figure 5 and Figure 6 present data from 2 different types of Hematoxylin (Mayer's and Gill's, respectively), in which according to the manufacturer (ACD), CB2R signals were fainter by Mayer's Hematoxylin. However, both methods showed a similar pattern regarding CBRs' signal distribution.

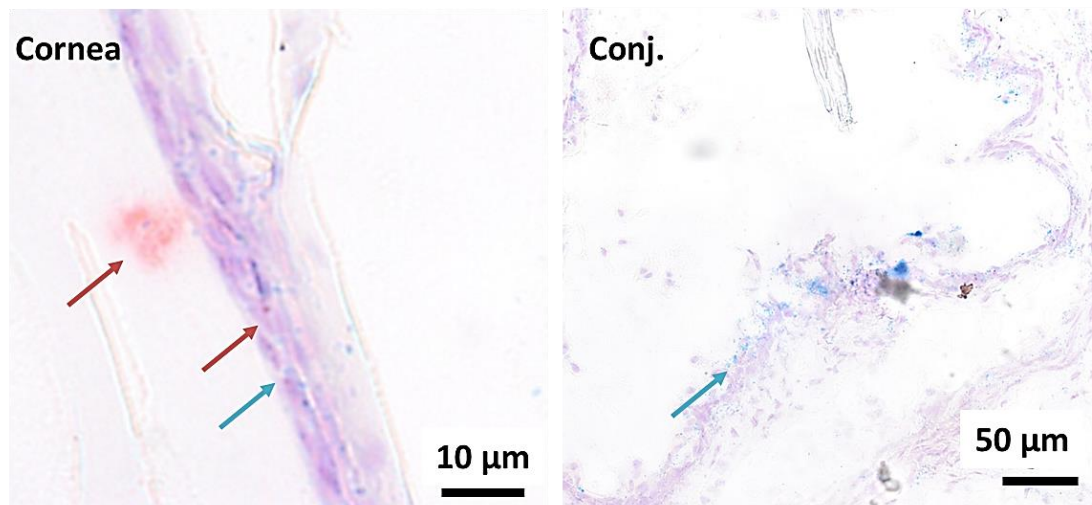


Figure 5: Representative in-situ hybridization images of CB1R and CB2R signals in the cornea and conjunctiva using Hematoxylin Mayer's (blue arrows: CB1R, red arrows: CB2R)

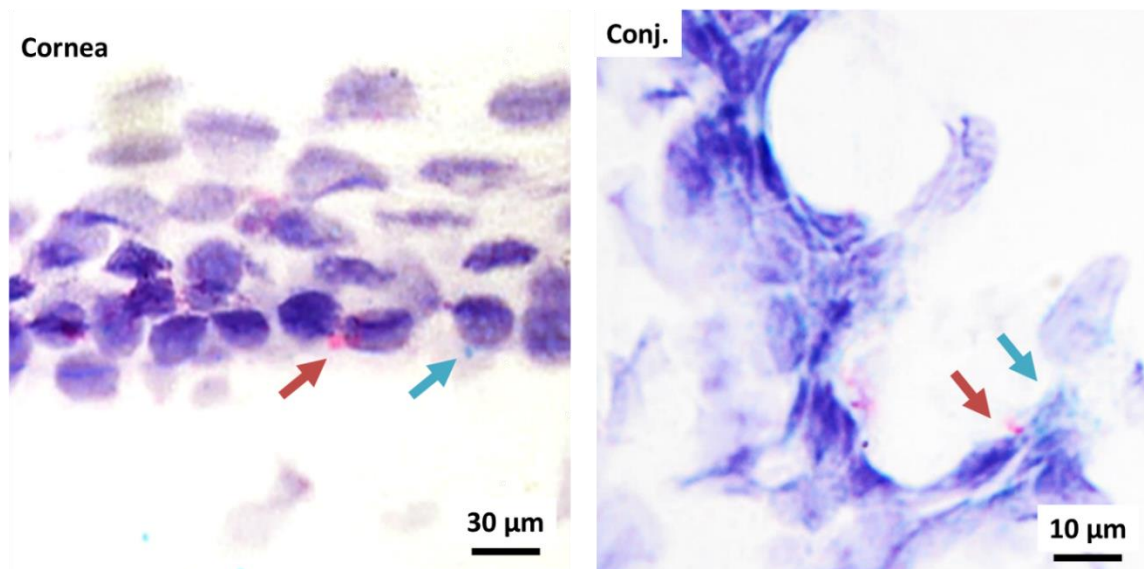


Figure 6: Representative in-situ hybridization images of CB1R and CB2R signals in the cornea and conjunctiva using Hematoxylin Gill's, blue arrows: CB1R, red arrows: CB2R, adapted from (120)

4.1.2 Desiccating stress (DS) model and DED phenotype readouts

In the *in-vivo* DED-induced experiment, DED phenotypes were observed for 10 days (Figure 7). Tear production (TP) was significantly decreased from day 3, and low TP was maintained during DS (Figure 7A). The corneal fluorescein staining score (FL score) was increased from day 3 to day 10. The higher the FL score, the more DS damaged the cornea (Figure 7B). In addition, mechanical corneal sensitivity was tested by the von Frey filaments (Figure 7C). During 10 days of DS, the von-Frey force (required to generate a mouse response) increased. This result indicated that the corneal sensitivity in DED-induced mice was lower than in naïve mice, with statistical significance from day 3 to day 10 compared to naïve mice (Figure 7C).

The brush test was also conducted by brushing the mouse's face with a small paintbrush. In the case of allodynia caused by DED, the brush touching can evoke a response from the animal. Figure 7 shows that the number of "non-response" animals was reduced during 10 days of DS. The "maybe" cases denote situations in which the animal displayed a response, but the response was insignificant or not assured to be caused by the brush. However, due to the large variations and too many inconclusive results, this test was not selected to further evaluate the cannabinoid effects.

In general, the experimental DED model successfully induced animals to display significant DED readouts that mimic DED conditions in humans. Implanted scopolamine inhibited tear secretion due to its anticholinergic effect (118). DS (low humidity and constant airflow) combined with low

tear production caused mice to significantly increase corneal epitheliopathy (higher fluorescein staining score), an essential feature of DED. Therefore, this model was selected to investigate the presence of CBRs and the effects of cannabinoids in DED.

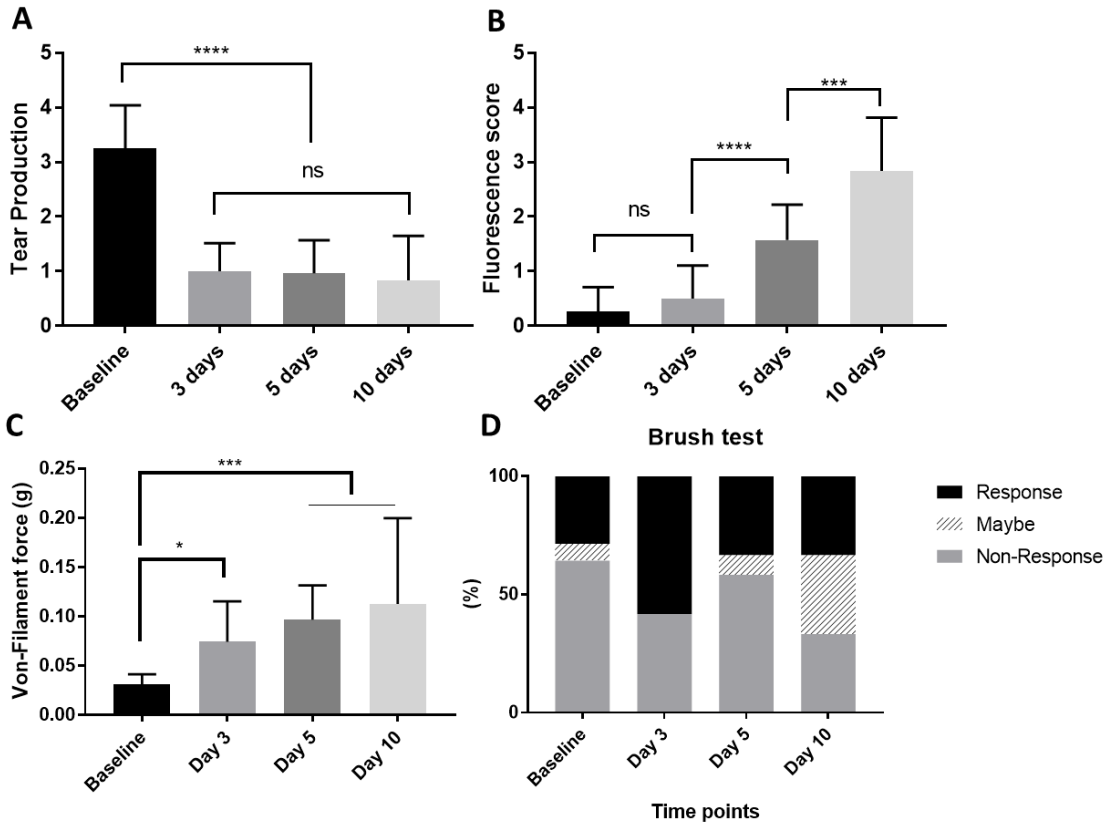


Figure 7: DED phenotype readouts during DS: (A) Tear production (TP) was reduced and maintained at 1 mm, (B) fluorescein staining (FL) score increased from day 3 until day 10, (C) Mechanical sensitivity was reduced (von-Frey forces increased) from day 3 until day 10, and (D) Brush test results showed an increasing trend of responsive animals

4.1.3 Desiccating stress model and cannabinoid receptor (CBRs) expression

Desiccating stress (DS) statistically increased the mRNA levels of CB1R and CB2R in the cornea, conjunctiva, and lacrimal gland in C57BL/6 mice (Figure 8). Compared to the baseline of the naïve corneas, 10 days of DS increased CB1R and CB2R expression by 1.84 and 12.74 folds, respectively. Data from conjunctiva and lacrimal glands also showed increased CB1R and CB2R. In general, the results implied a rise in CBRs expression correlating with DED phenotype changes during DED induction.

The ratio of CB1R/CB2R in the cornea was decreased on day 10 compared with baseline ($p < 0.05$). This data showed that while both CB1R and CB2R transcripts increased during the DED induction,

the increasing rate of CB2R was higher than that of CB1R. A similar trend was also observed in the conjunctiva. However, the ratios of CB1R/CB2R in lacrimal glands in naïve and day 10 were not significantly different.

Because CBRs' expression increased simultaneously with DED phenotype readouts (section 4.1.2), the results suggested that CB1R and CB2R were involved with the DED pathogenesis. In detail, both CB1R and CB2R expression increased during the DS.

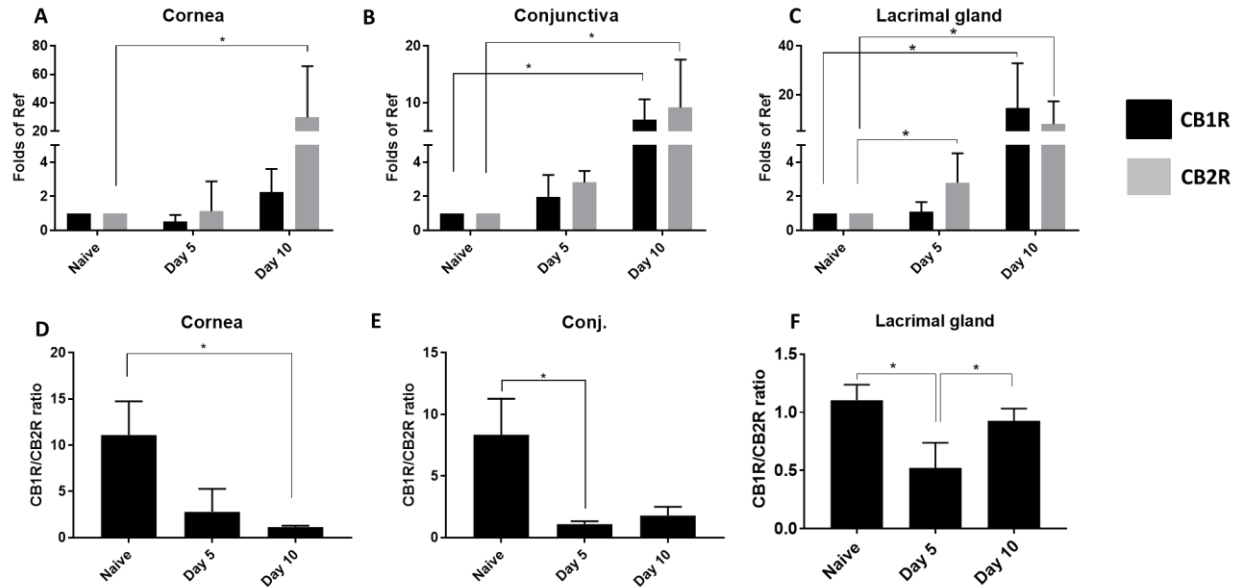


Figure 8: RT-qPCR analysis showed that CB1R and CB2R increased during 10 days of DS in the cornea (A), conjunctiva (B), and lacrimal gland (C) (upper row). In the lower row, while CB1R/CB2R ratios were reduced during 10 days of DS in the cornea (D) and conjunctiva (E), the CB1R/CB2R ratio in the lacrimal gland (F) was at the lowest value on day 5 ($n = 10$ eyes, 5 mice/group) *: $p < 0.05$, adapted from (120)

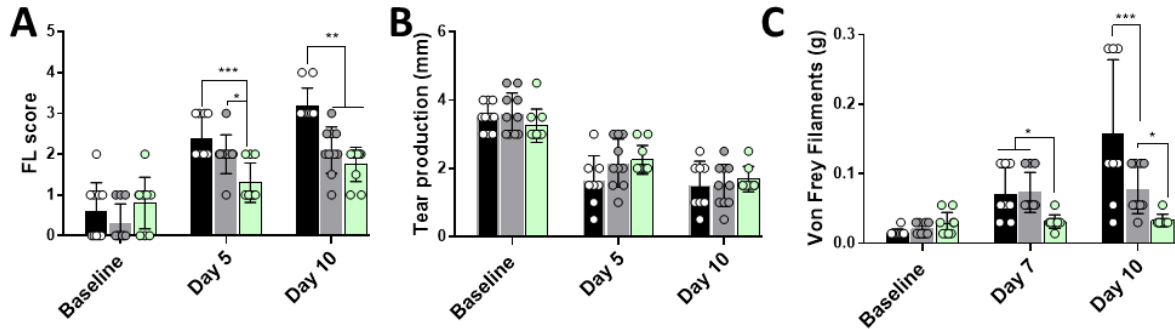
4.2 Effect of CBR ligands on DED pathogenesis

In the previous section, it was shown that CBRs are involved in DED pathogenesis. This section presents results in which 3 different CBR ligands were used in the form of eyedrops for DED-induced mice.

4.2.1 Phenotype readouts

The effects of cannabinoids during DED induction were investigated, results are in Figure 9. Similar to previous sections, the readouts are cornea damages (FL scores), tear production (TP), and mechanical sensitivity (Sen). The black columns (from A to F) present data from DED-induced mice without treatments. Again, the data confirmed the DED phenotypes (similar to 4.1.2) and the validity of the model.

THC effects



Anta CB1 & Anta CB2 effects

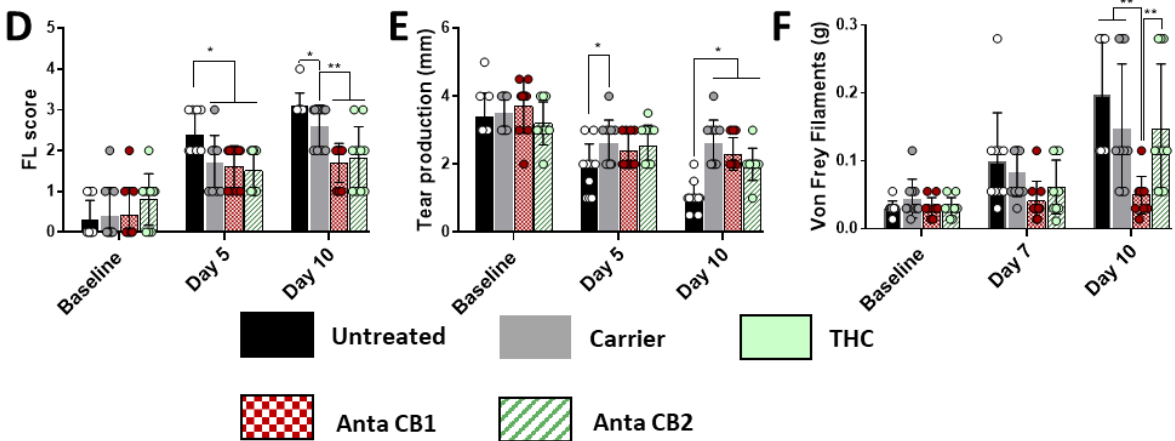


Figure 9: Effects of cannabinoids on phenotypes of DED-induced mice: THC experiment (A, B C) and antagonist experiment (D, E, F). The phenotypes, including FL score (A, D), TP (B, E), and sen (C, F), showed treatment effects compared to the corresponding carriers and untreated groups. (n=10). *: $p < 0.05$, **: $p < 0.01$, *: $p < 0.001$, adapted from (120)**

4.2.1.1 *FL scores*

The FL results for 2 sets of experiments (antagonists and THC) are depicted in Figure 9A and D. The results in Figure 9A and D showed a consistently increasing trend in the untreated group (black column). The effects of THC and the related carrier are depicted in Figure 9A. THC demonstrated therapeutic activity on day 5 when the FL results in the THC group was 1.3 ± 0.48 , which was significantly lower than the FL result in the carrier group ($p < 0.05$). This result confirmed the THC effect in reducing corneal damage. Additionally, there was no difference when comparing untreated and carrier at the same time. On day 10, even though the difference between the 2 groups was not statistically significant, the FL score in the THC group was lower than that in the carrier group. The effects of 2 selective antagonists for CB1R and CB2R (AntaCB1 and AntaCB2) are shown in Figure 9D. After 5 and 10 days, the FL scores in the AntaCB1 and AntaCB2 groups were significantly lower than those in the untreated animals ($p < 0.05$). On day 10, FL scores of the AntaCB1 and AntaCB2 formulations were 1.70 ± 0.48 and 1.80 ± 0.79 , respectively, which exhibited more significant effects on FL score reduction than Carrier (2.60 ± 0.51 , $p < 0.01$). In summary, as the FL score is an important indicator for DED conditions, cannabinoid application showed a therapeutic effect on reducing corneal epithelial damages).

4.2.1.2 *Tear production*

The TP data are summarized in Figures 9B and E. In the untreated group, TP was reduced from 3.52 ± 0.70 (naïve mice, baseline) to 1.05 ± 0.44 (DED mice, day 10 of DS). As shown in Figure 9E, TP values in THC-treated mice (1.95 ± 0.55 mm, day 10) and carrier-treated mice (1.45 ± 0.68 mm, day 10) were higher than in the untreated DED group. However, when there is no statistical difference ($p > 0.05$) in the THC experiment (Figure 9C). A similar trend was observed in Figure 9E, although AntaCB1, AntaCB2, and the carrier had higher values than the untreated. In summary, applying cannabinoids as an eyedrop did not significantly affect the tear production in this model.

4.2.1.3 *Mechanical sensitivity*

Figures 9C and F show the results of corneal sensitivity determined by von Frey filaments. During DS, the filament forces increased in the untreated group, indicating decreased mechanical sensitivity. Reversely, when a lower von-Frey filament force was required, a higher sensitivity was reported. As shown, mice treated with THC had higher sensitivity than mice treated with carrier or the untreated group. The significant effects of THC were found on days 7 ($p < 0.05$) and day 10 ($p < 0.001$).

Among the antagonist experiments shown in Figure 9F, only AntaCB1 exhibited responses at lower von Frey forces (0.004 ± 0.0030 and 0.0049 ± 0.0028 g on days 7 and 10, respectively) with statistical differences ($p < 0.05$).

In summary, only THC and AntaCB1 maintained corneal sensitivity during DS, while AntaCB2 and the carrier had no noticeable effect.

4.2.2 Corneal-nerve morphology immunostaining

4.2.2.1 Corneal nerve morphology of untreated DED-induced mice

As shown in the following images, 10 days of DS significantly influenced the β 3-tubulin staining pattern. In untreated DED mice, DS significantly reduced the number of nerves in DED mice (Figure 10B) compared with naive animals (Figure 10A). The therapeutic effect of THC was shown in Figure 10C, in which THC-treated mice showed a larger area covered by green nerve signals than DED mice, AntaCB1, and AntaCB2 groups. The images obtained from the microscopy were then analyzed by computer software to characterize the nerve density and length; the results are in Figure 11.

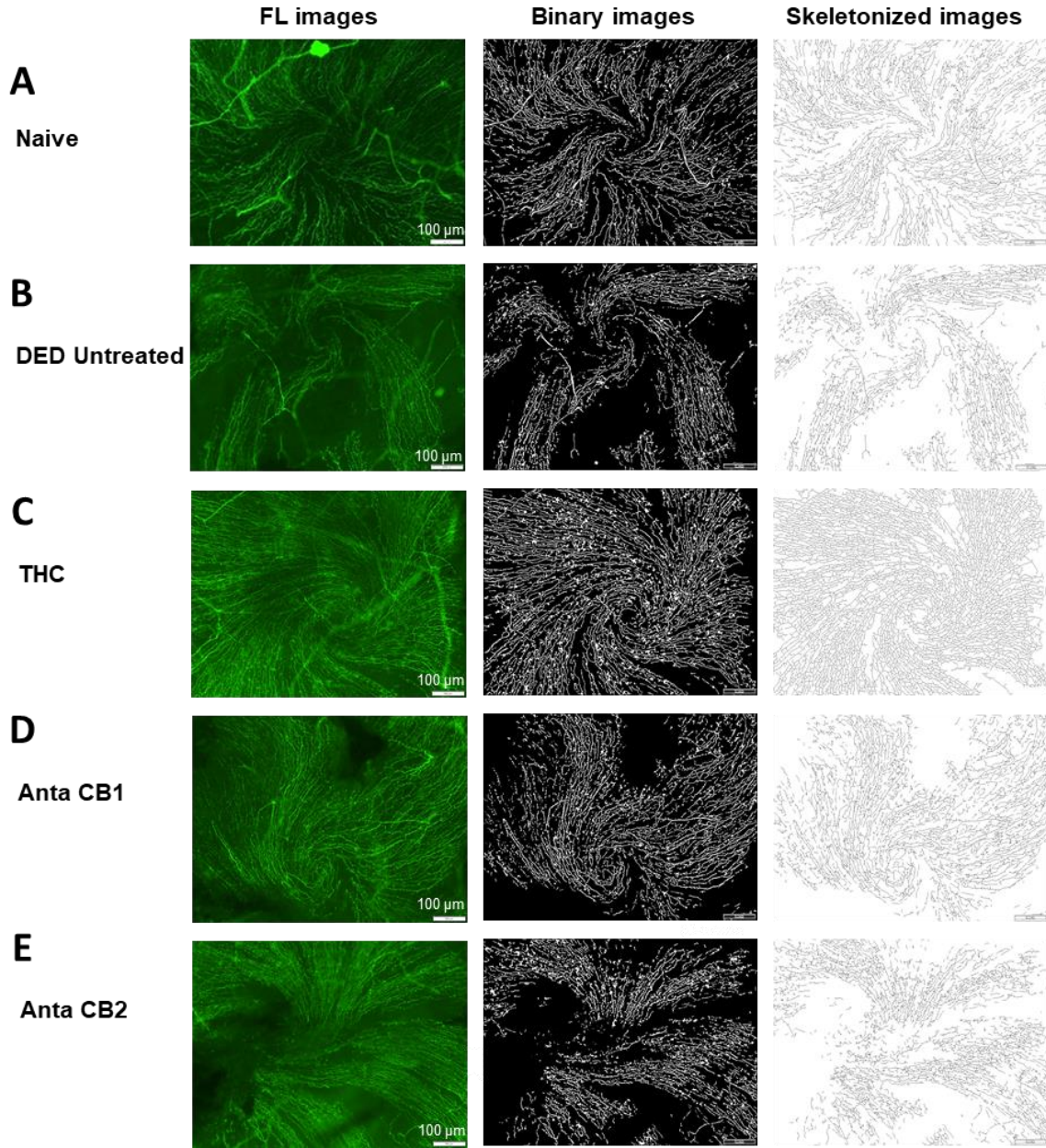


Figure 10: Representative images of center areas of the cornea (tissues were collected on day 10 of experiment): significant effects of DED-induction and cannabinoids on corneal nerve morphology. The left side $\beta 3$ -tubulin immunostaining images are shown along with the corresponding binary images (in the middle) and skeletonized images (right). (bar=100m). After 10 days, untreated DED mice showed lessened nerve morphology, whereas nerve morphology was maintained in the THC-treated group. Adapted from (120)

4.2.2.2 Image analysis to quantify corneal nerve density

Together with the representative images, corneal nerve morphology was also quantified based on corneal nerve density and corneal nerve length per area (mm/mm²). Data is shown in the following figure:

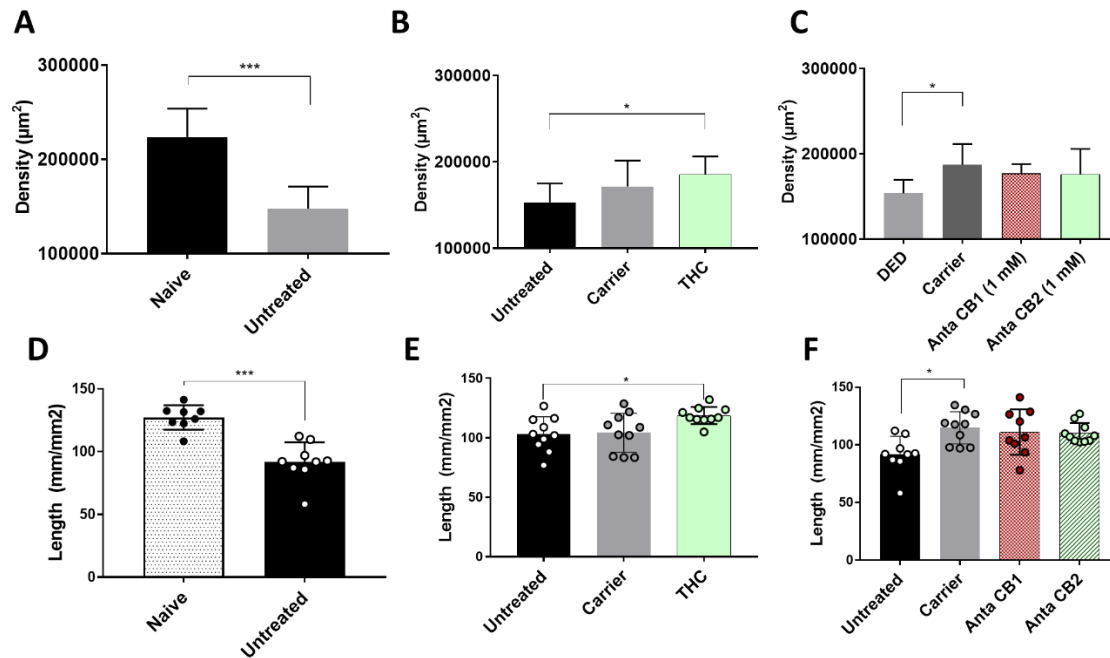


Figure 11: Semi-automatic quantification of tubulin-staining images: (A-C) Mean of corneal nerve density was quantified (calculated per cornea) and is presented, and (D-F) Mean of corneal nerve length per area (in mm/mm², D-F). Both corneal nerve density and length were reduced at day 10 compared to Naïve mice. Only THC significantly maintained corneal nerve density and length during 10 days of DS (B and E). Data are presented as mean and SD (n = 10 eyes/ per group). * p < 0.05, adapted from (120)

After 10 days, the obtained results confirmed a significantly lower nerve density and length in the untreated group (on day 10, Figure 11A and D, p < 0.001).

In Figure 11B, the density of the THC-treated mice was significantly higher than the density of untreated DED animals (Figure 10p < 0.05). On the other hand, when comparing nerve density in the central cornea of the antagonist experiment, no statistically significant difference was detected when comparing the two antagonist groups with untreated DED. There was a statistical difference between the carrier and DED group in the antagonist experiment (Figure 11C, p < 0.05)

In Figure 11 D-F, only THC treatment showed a significant effect, in which higher nerve length per area was reported in THC-treated mice than untreated DED mice (Figure 11E, p < 0.05). There was no significant difference between the carrier and untreated groups. In the antagonist

experiment (Figure 15F), while AntaCB1 and AntaCB2 did not affect the nerve length compared to the untreated group, the carrier ($114.72 \pm 13.91\text{mm/mm}^2$) displayed a statistical difference in comparison with the untreated DED mice (Figure 11C and F).

4.2.3 Inflammation cytokines following DED induction and cannabinoid treatment

As inflammation is a core pathomechanism of DED, this part is to characterize the effect of cannabinoids on inflammation cytokines after 10 days of DS. In untreated DED animals (Figure 12), DED-induction increased the IL-1 β level in the cornea (Figure 12A) and both IL-1 β and IFN- γ in the conjunctiva (Figure 12B and C). Signals of IFN- γ in the cornea were inadequate to be detected at acceptable Cq values ($Cq > 38$).

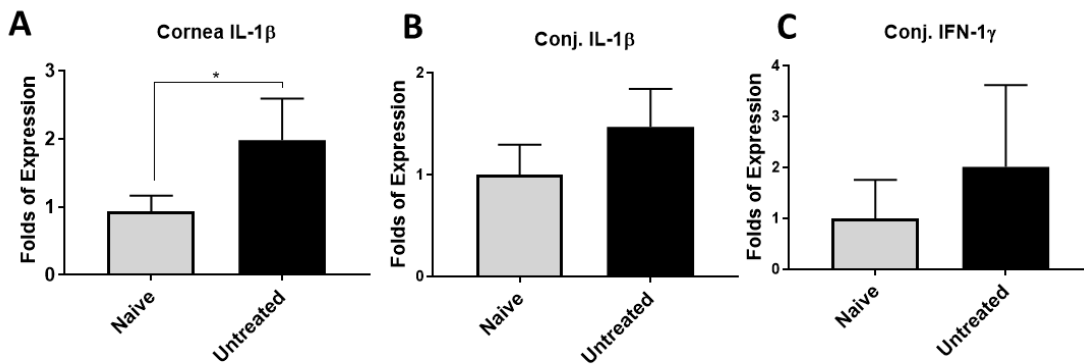


Figure 12: Effect of DS on some inflammatory cytokines in cornea and conjunctiva ($n = 5$), adapted from (120)

Based on the results presented in Figure 12, the effects of cannabinoids are shown in Figure 13A. Compared to the untreated group, THC lowered IL-1 β in the cornea (0.51 ± 0.16). However, THC did not significantly affect the 2 cytokines in the conjunctiva (Figure 13, A and B).

In the antagonist experiment (Figure 13D-F), AntaCB1 and AntaCB2 treatment exhibited a lower IL-1 β in the cornea than untreated DED mice, and there was a statistical difference in AntaCB2 compared to the carrier and untreated DED mice (Figure 13D). Interestingly, AntaCB2 administration resulted in reducing IL-1 β levels (Figure 13E) and increasing IFN- γ in the conjunctiva (Figure 13F, both $p < 0.05$). When comparing the 2 antagonists, there was a significant difference between the AntaCB1 and the AntaCB2 group regarding IL-1 β expression in the conjunctiva ($p < 0.05$).

THC effects

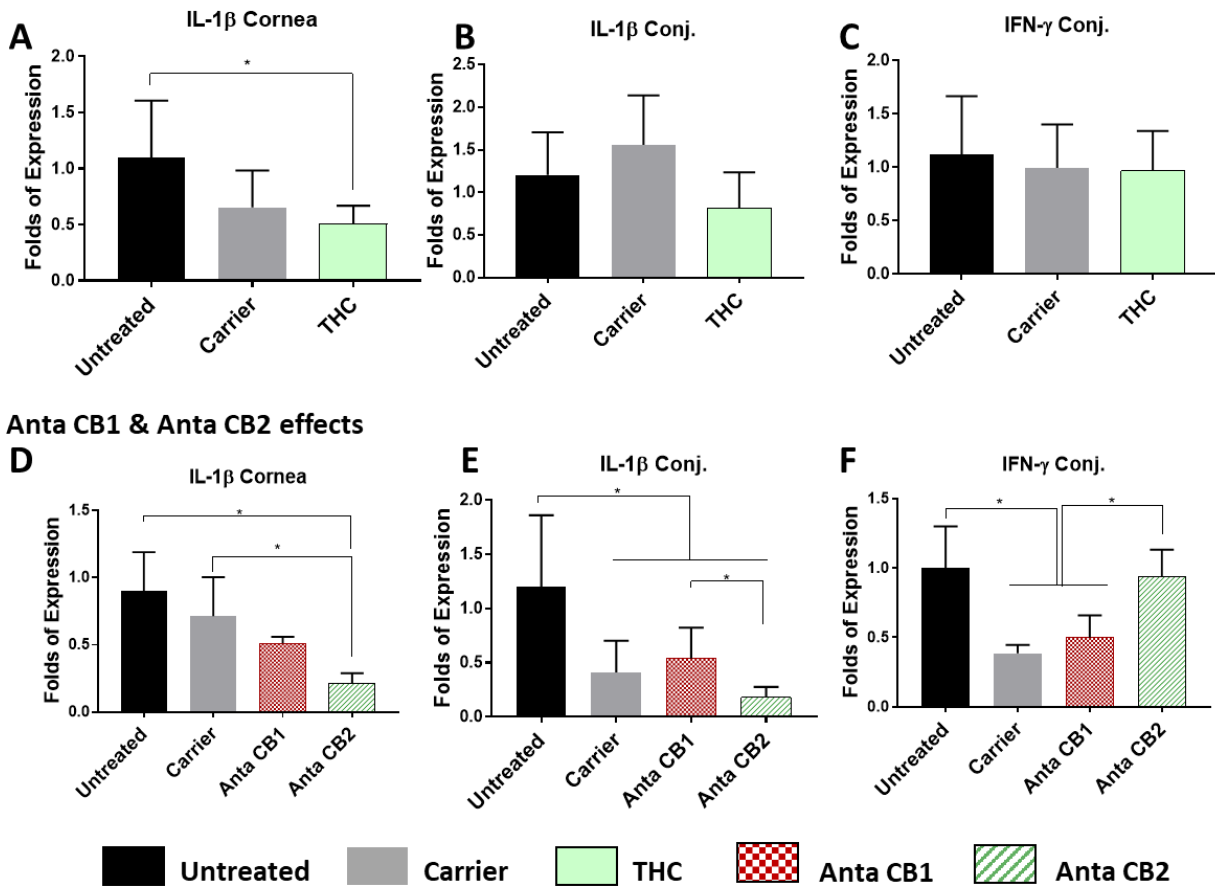


Figure 13: Cytokine levels following 10-day treatments of THC (A-C) and antagonists (D-F): In the cornea, THC, AntaCB1, and Anta CB decreased IL-1 β (A and D). In the conjunctiva, AntaCB2 administration simultaneously reduced IL-1 β and increased IFN- γ (C, E). Data are expressed as mean \pm SD (n=5 mice/group). * p < 0.05, adapted from (120)

4.2.4 The infiltration of CD4⁺ and CD8⁺ T-cell into the conjunctiva

During DED-induction, CD4⁺ T-cell density increased significantly compared to naïve mice (p < 0.05, Figure 14). In contrast, THC administration significantly decreased infiltrated CD4⁺ cells (p < 0.05, Figure 14A). Also, a reduction in CD4⁺ cells was seen in the conjunctiva after treatment with AntaCB1 (p < 0.05, Figure 14A). On the other hand, the AntaCB2 treatment did not change CD4⁺ T-cells in the conjunctiva.

On the other hand, both THC and AntaCB2 increased CD8⁺ T-cell density more than the untreated DED animals (Figure 14B). As a result, CD4: CD8 ratios were reduced in the THC and

AntaCB2 treated groups than that of the untreated group ($p < 0.05$) or AntaCB1.

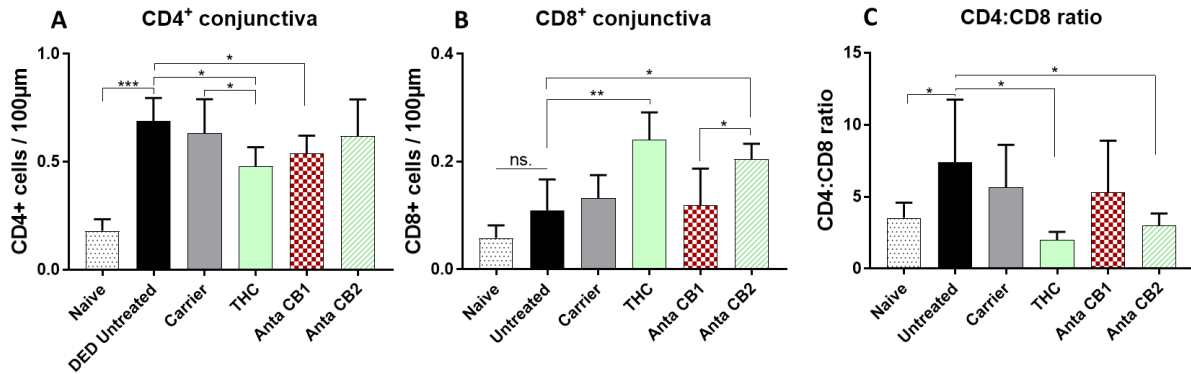


Figure 14: (A) THC and AntaCB1 reduced conjunctival CD4⁺ T-cell density compared to the untreated DED group. (B) THC and AntaCB2 increased conjunctival CD8⁺ T-cell density compared to untreated DED group. (C) THC and AntaCB2 reduced CD4:CD8 ratio compared to the untreated DED group. Data are expressed as mean \pm SD ($n=4$ eyes/group). * $p < 0.05$, ** $p < 0.01$, adapted from (120)

4.2.5 CBRs expression following cannabinoid treatment

As presented in 4.1.1 and 4.1.3, an increasing trend of both CB1R and CB2R was observed during 10 days of DED induction. Figure 15 presents CBRs' changes when the DED-induced animals were topically applied with a cannabinoid eye drop.

Applying THC (Figure 15A-D) reduced CB1R and CB2R expression compared to the untreated control. There was a statistical difference when comparing the THC group and the carrier ($p < 0.05$) in both the cornea and conjunctiva.

In Figure 15 E and F (effect of antagonists on the cornea), CB1R and CB2R expressions were reduced significantly when using AntaCB1 and AntaCB2 eyedrop. However, in Figure 15 G and H, AntaCB1 treatment significantly increased both CB1R and CB2R levels in the conjunctiva ($p < 0.01$), while the AntaCB2 effect is not significantly different from the carrier.

THC effects

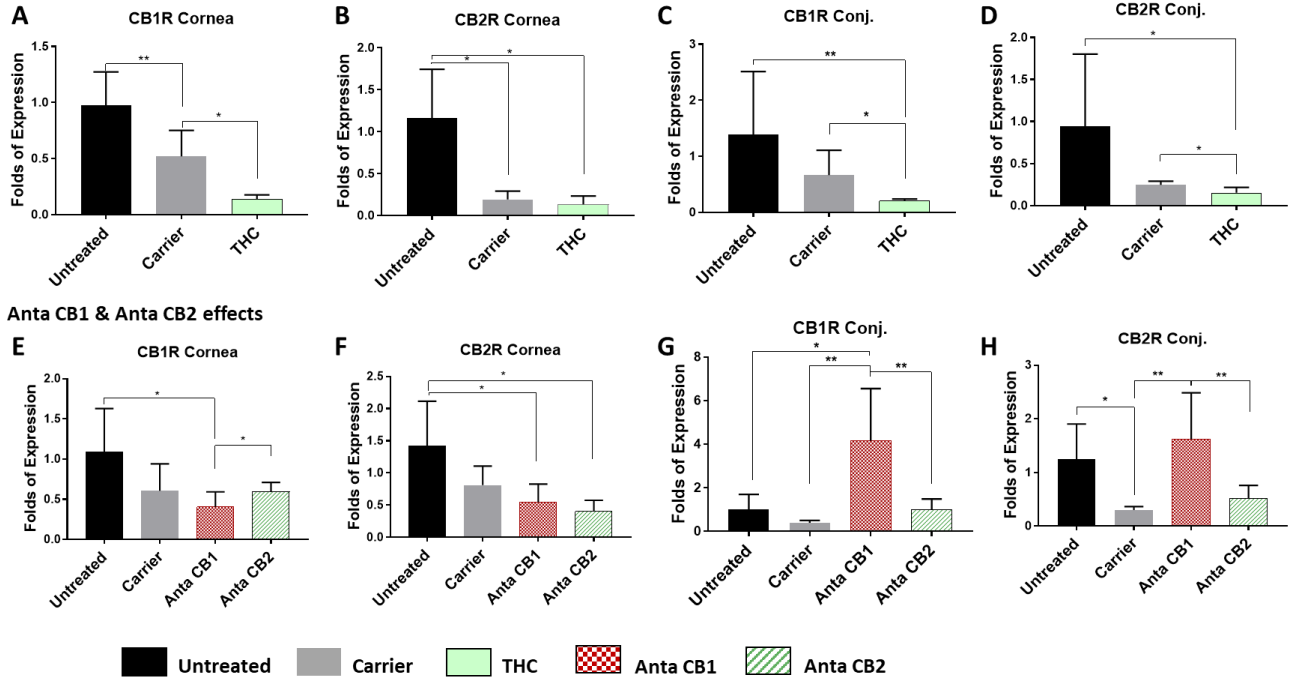


Figure 15: CBR expression after topical application of 3 different cannabinoid ligands for 10 days: A-D) THC (non-selective agonist application), E-H) two selective antagonists. (A-D) THC reduced CBRs expression. (E-F) AntaCB1 and AntaCB2 groups exhibited a lower CBRs expression in the cornea than untreated DED mice, (G-H) AntaCB1 increased both CB1R and CB2R in the conjunctiva compared to others. Data are presented as mean \pm SD (n=5/group). adapted from (120)

4.3 Effect of CBR ligands on corneal epithelial wound

4.3.1 Wound healing model

Previous sections showed functions of CB1R and CB2R ligands on (i) the inflammation process and (ii) neurosensory abnormalities in the experimental DED-induced mouse model. In this section, we used an *in-vitro* alkaline burn wound healing model to evaluate CBR ligands' effects on the re-epithelialization process (49,109).

To create a wound on the cornea, a 2-mm filter paper disk soaked in NaOH 0.5% was placed onto the center of the cornea. Due to the alkaline effect, the corneal epithelium cells were then easily removed by a micro-scalpel. The re-epithelialization process was visualized by applying a fluorescein solution to the corneas after 6, 12, 24, 30, and 36 hours. When the corneal epithelium was healed entirely, no fluorescein signal was detected. The representative images of the corneal wound-healing process are depicted in Figure 16. The corneal wound in the negative samples was not completely healed after 24 hours, while the wound was closed in the positive-control samples. The difference between negative and positive samples suggested that this model can be used to compare wound-healing effects by preparing different substances in the incubation medium.

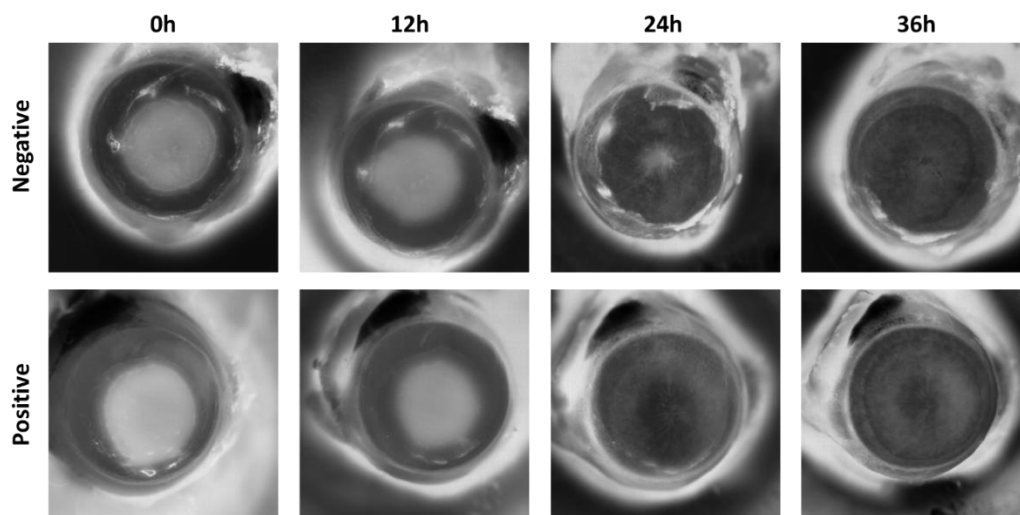


Figure 16: Representatives of corneal wound healing model: Positive and negative control samples

4.3.2 The biphasic effect of THC on the re-epithelialization process

Based on the preliminary results, THC was prepared in the incubation medium to evaluate the effect of THC on re-epithelialization. Different THC concentrations (from 0.01 up to 10 μM) were compared with untreated controls. The obtained results are demonstrated in Figure 17

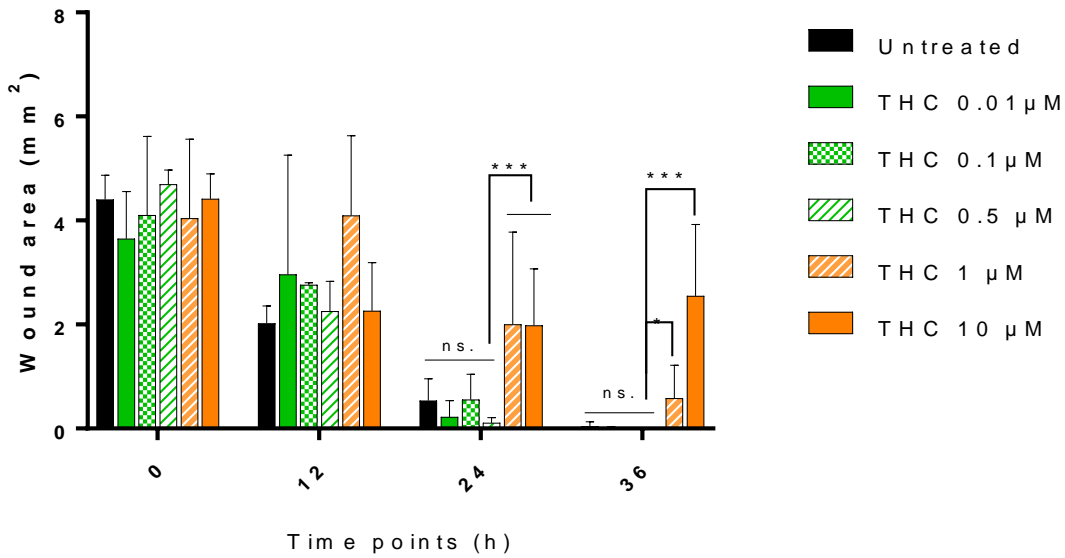


Figure 17: Wound area in mm² when samples were treated with different THC concentrations

There was no significant difference among the 3 low concentrations (0.01, 0.1, and 0.5 μM). However, among the 3 low concentrations, THC 0.5 μM showed a stronger effect (the wound area was smaller at 24h compared to the 2 remaining concentrations). After 36-hour incubation, the wounds were healed entirely in these 3 low-concentration samples. In contrast, the two high THC concentrations (1 and 10 μM) delayed the wound-healing process. When treated with high concentrations of 10 μM of THC, the wound area increased significantly from 24h to 36h. There was a statistical difference between 1 and 10 μM of THC.

To confirm the difference between low and high concentrations of THC, 2 concentrations (0.5 μM and 10 μM) were compared with the negative control sample and analyzed using Kaplan Meyer analysis (Figure 18).

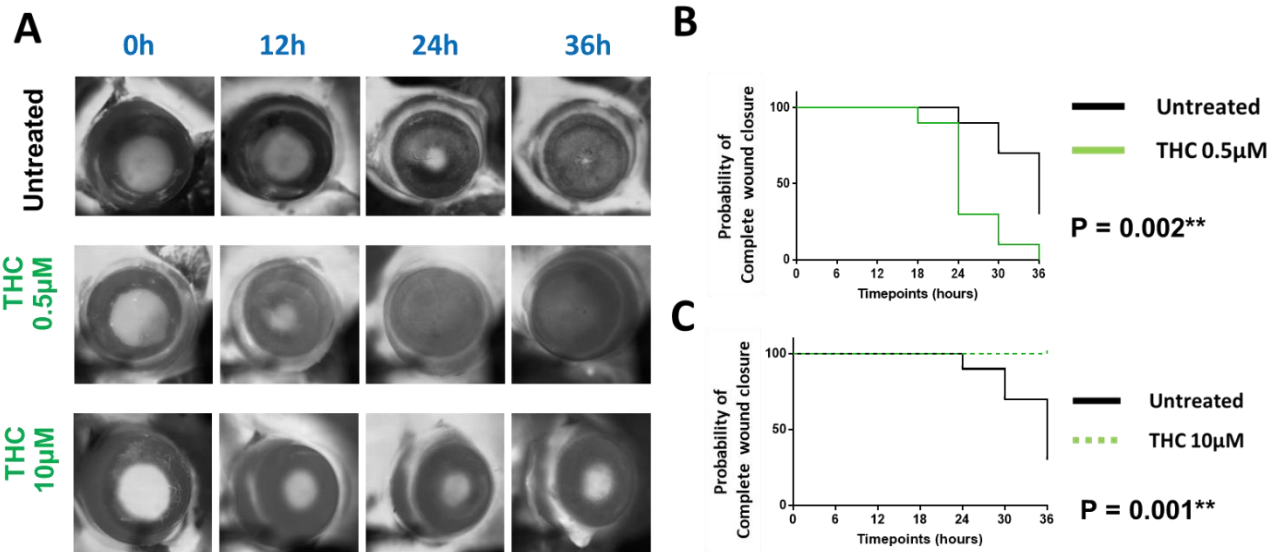


Figure 18: THC biphasic effect on wound healing process: (A) Representative images showed that THC 0.5 µM improved wound healing rate while THC 10 µM delayed wound healing; and (B, C) data analysis of wound healing process confirmed THC effects (n = 10)

Figure 18 shows representative images from the eye nuclei(s) in different treatments (left). At early time points (0 or 12h), the corresponding wound remained open. At 24h, complete wound closure was observed in the THC 0.5µM treated group. Meanwhile, at high concentrations (THC 10µM), wounds were not healed (even at 24 or 36h). Eventually, the wound was broadened from 12h to 24h (Figure 18, left) when using THC 10µM. Kaplan-Meier analysis and log-rank test were performed to compare each group with the untreated group. The test confirmed that THC 0.5µM treatment improved the wound healing process ($p = 0.002$), while the high concentration of THC (10µM) showed a significant delay effect compared to the untreated group ($p = 0.001$).

4.3.3 The effect of antagonists on the re-epithelialization process

We next assessed the potential impact of the CBR selective antagonists on the re-epithelialization in the *in-vitro* wound healing model. Each antagonist was prepared in the incubation medium at 2 different concentrations (Figure 19).

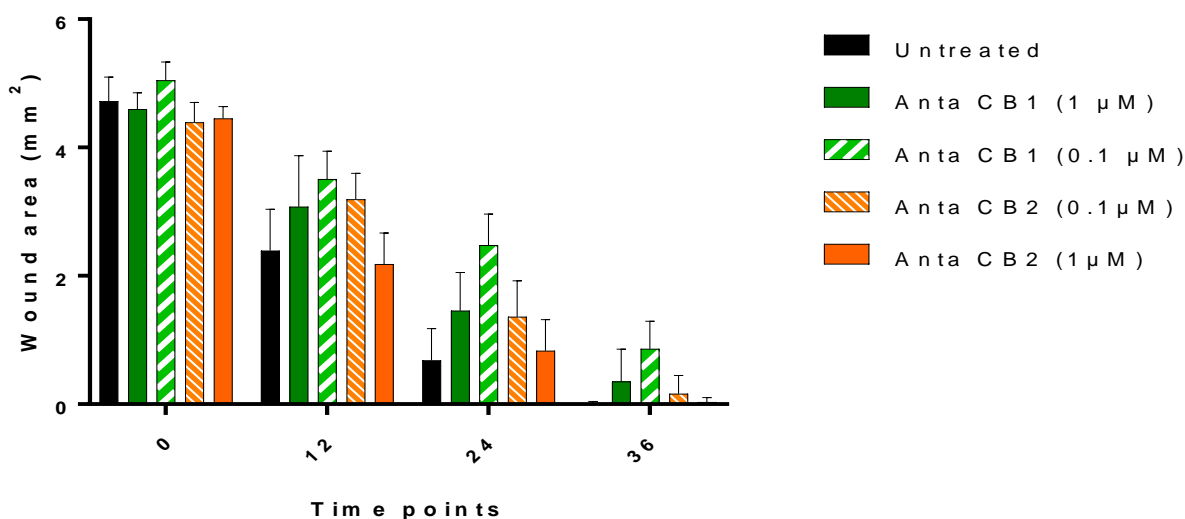


Figure 19: Wound area in mm² when samples were treated with CB1R and CB2R antagonists
 For AntaCB1, there was no significant difference between the 2 concentrations of AntaCB1 (0.1 and 1 µM). The wound area was still high (over 1 mm², at 24h), and still open at 36h. Compared to the untreated group, wound areas in AntaCB1-treated samples were higher at 24h and 36h. For AntaCB2, Figure 19 showed that the wound area in the AntaCB2 experiments was similar to the untreated at the same time points. There was no statistical difference between the 2 concentrations of AntaCB2. Representative images and Kaplan-Meier analysis will be presented in the following Figure 20.

In Figure 20, representative images were shown to compare the effect of AntaCB1 and AntaCB2 with untreated and THC. In the untreated group, the wound was still opened at 24h, but the wounds were almost closed at 36h. In contrast, AntaCB1 samples showed that the wound area was high, and the wound was still opened at 24h or 36h. Kaplan Meyer analysis confirmed that AntaCB1 delayed the re-epithelialization compared to the untreated group, while there was no difference between AntaCB2 and the untreated samples.

Together with results from THC and antagonist experiment, it can be concluded that the effect of THC on the re-epithelialization process was via the CBR1 pathway. THC, a non-selective agonist, showed a biphasic effect, while the CB1R antagonist delayed wound healing.

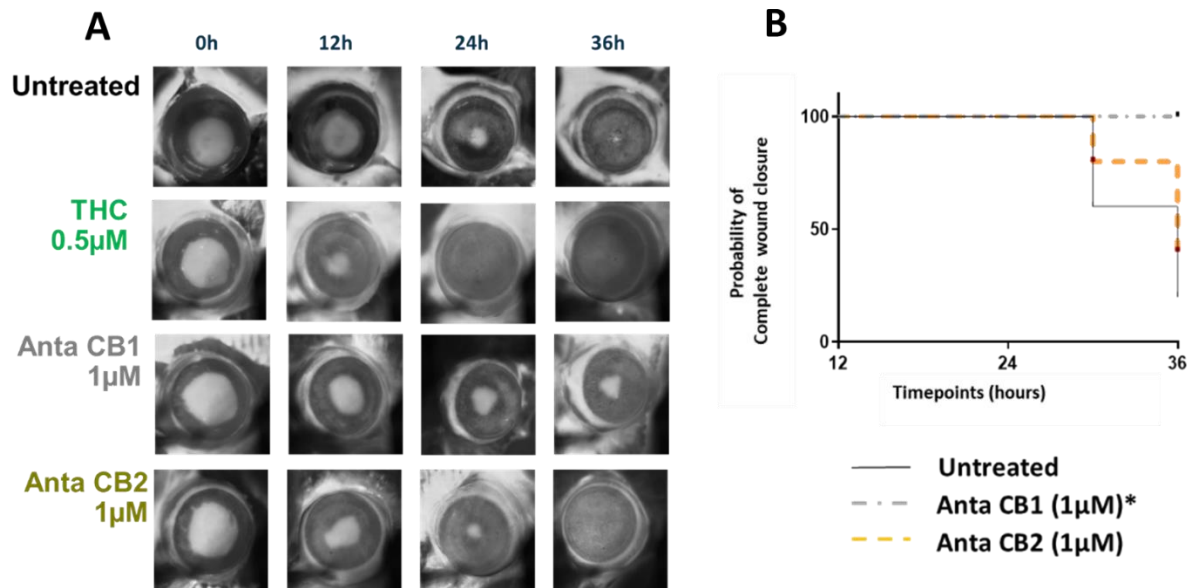


Figure 20: CBR Antagonists' effect on the wound-healing process: A) representative images showed that AntaCB1 delayed the wound healing process, and AntaCB2 did not have a significant effect (B) Kaplan-Meyer data analysis of wound healing process (n =10)

4.4 Drug formulation study

4.4.1 Excipient selection

This part of the ongoing project on developing an eye drop formulation for cannabinoid substances for potential later human use focuses on formulation screening at the laboratory scale. The experiment was conducted according to 3 main steps of formulation preparation (mentioned in Method 3.3)

- (i) Preparation of stock solution
- (ii) Eye-drop formulation (micellar solution): Adding the stock solution into a water phase with different surfactants to have a final concentration (5mg/mL). There are 5 water phases were selected:
- (iii) Sterile filtration

4.4.1.1 *Select the solvent for the stock solution*

THC is a resinous substance that adheres to the container, especially a plastic surface. According to the provider's guidance (Bionorica, Frankfurt, Germany), THC was heated to reduce the viscosity before weighing or compounding. Based on previous reviews (section 1.6.4), the following solvents were selected and tested as THC stock solutions:

Stock 0: DMSO* (this stock solution was used for the in-vivo study)

Stock 1: Polysorbate 80: EtOH (5%)

Stock 2: Transcutol HP

Stock 3: Glycerol: EtOH (1:1)

Stock 4: Glycerol

Stock 5: Soybean oil

The following Table 5 presents the feasibility of stock solutions evaluated based on physical appearance. A stock solution should be a homogenous solution in which THC is entirely dissolved (the minimum concentration of THC was 50 mg/mL). In addition, the stock solution should not be too viscous to cause difficulties for next steps (dilution or filtration).

Table 5: Select solvent as the stock solution

Stock number	Solvent	THC Con. (mg/mL)	Homogenous solution	Non-homogenous	Note
Stock 0*	DMSO*	60.00	X		
Stock 1	Polysorbate 80: EtOH, 10:3, v/v	138.00	X		
Stock 2	Transcutol HP	50.00	X		
Stock 3	Glycerol:EtOH (1:1, v/v)	121.22	X		
Stock 4	Glycerol	X		X	Too viscous
Stock 5	Soybean oil	55.55	X		

“*”: The stock solution (DMSO) was used for the in-vivo experiment, section 4.1 and 4.2

According to Table 5, five stock solutions (stock 0, stock 1, stock 2, stock 3, and stock 5) were selected for the subsequent experiments. Although polysorbate 80 and glycerol were reported to have a high THC solubility (126), these solvents have such a high viscosity that they are not suitable for dissolving THC in lab conditions (e.g. on small-scale vortexing in a small Eppendorf tube).

4.4.1.2 Select the water phase

Beside DMSO (Stock 0), obtained 4 stock solutions from the previous section were diluted into 6 different water phases to make the final eyedrop formulation with a concentration of 5mg/mL of THC. The physical appearance of these screened formulations was evaluated at $t = 0$ (immediately after preparation) and after 24h storage at room temperature (RT) and protected from light (Details are in Table 6). The selection criteria include the physical appearance, in which obtained formulations are homogenous liquid (solution or emulsion) immediately after preparation and after 24h storage at RT.

Water phase 0: NaCl 0.9% with Cremophor EL 15% (This F00 was used for the in-vivo experiment before)

Water phase 1: NaCl 0.9% without surfactant

Water phase 2: NaCl 0.9% without surfactant, but organic solvent Transcutol HP (10%)

Water phase 3: NaCl 0.9% with Cremophor EL (5%) and Polysorbate 80 (4%)

Water phase 4: NaCl 0.9% with Polysorbate 80 (4%)

Water phase 5: NaCl 0.9% with Cremophor EL (5%)

Water phase 6: NaCl 0.9% with Poloxamer 188 (10%)

Table 6: Formulation screening with different stock solutions and water phases

	Form. Code	Stock number	Water phase	T = 0		T = 24h	
				Non-homogenous	Homogenous	Non-homogenous	Homogenous
1)	F00*	0	0		X		X
2)	F11	1	1	X			
3)	F12	1	2		X		X
4)	F13	1	3	X		X	
5)	F14	1	4	<i>Not prepared, Tween 80 was used as a solvent in the stock solution</i>			
6)	F15	1	5				
7)	F16	1	6		X	X	
8)	F21	2	1	X			
9)	F22	2	2	<i>Not prepared, Transcutol was used as solvent in the stock solution</i>			
10)	F23	2	3		X		X
11)	F24	2	4		X		X
12)	F25	2	5		X	X	
13)	F26	2	6		X		X
14)	F31	3	1	X			
15)	F32	3	2		X	X	
16)	F33	3	3	X			
17)	F34	3	4	X			
18)	F35	3	5	X			
19)	F36	3	6		X	X	
20)	F51	4	1	X			
21)	F52	4	2		X	X	
22)	F53	4	3	X			
23)	F54	4	4	X			
24)	F55	4	5	X			
25)	F56	4	6		X	X	

“*”: The stock solution (DMSO) was used for the the in-vivo experiment, section 4.1 and 4.2

After preparation (t =0), 10 of the 25 trial samples were in the form of a homogeneous liquid. However, only 5 formulations (F00, F12, F23, F24, F26) were stable after 24 hours (t = 24h). The “sediment” and “precipitate” conditions were observed and shown in the following Figure 21 to illustrate “non-homogenous” samples (upper line, F13, F34, and F52). The white precipitates were observed in F13 and F34 at t = 0, in which the solid substances formed a layer (F13) or a small

dusty particle (F34). The sediment (or phase separation) was observed when using soybean oil as a stock solution.

The most important criterion for an emulsion is its ability to maintain its properties over time, so 24h duration was selected for the screening purpose to compare the stability of different trial formulations. If a formulation were not stable around 24h, it would be difficult for physio-chemical analysis and quality assurance in drug development. “Homogenous” forms are shown in Figure 3 (lower line, F23, F24, and F26). F23 or F24 were considered a colloid system, in which the appearance of these colloid dispersions was “smoky or foggy air” due to scattering light. Differently, F26 was more transparent than F23 or F24, without scattering “smoky or foggy air”, suggesting that F26 particle size was smaller (or finer) than that of F23 and F24. Based on the above table results, the formulations selected for the next step are F11, F23, F24, and 26.

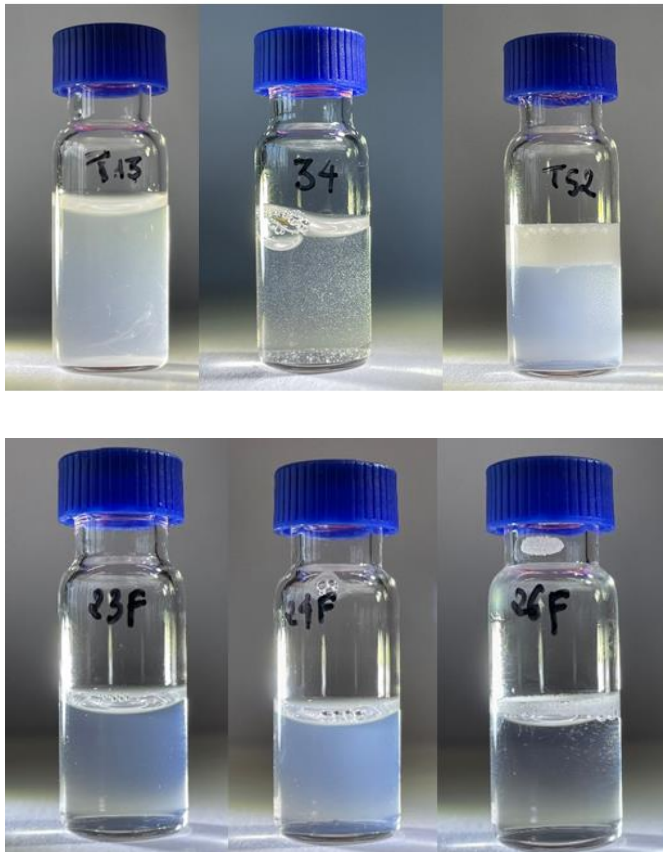


Figure 21: Representative images of THC formulations (t = 0)

4.4.2 Effect of sterile filtration and short-term stability

This experiment was conducted for 5 following formulations (Table 7):

Table 7: Final formulations selected for sterile filtration and short-term stability

Formulation	Stock solution	Diluent (NaCl 0.9%)
F00*	DMSO	Cremophore EL
F23	Transcutol HP	Polysorbate 80 Cremophore EL
F24	Transcutol HP	Cremophore EL
F26	Transcutol HP	Kolliphor P 188
F12	Polysorbate 80: ethanol	Transcutol HP

The THC content is present in Figure 22. At $t = 0$ (immediately after preparation), all 5 formulations had THC content at 5 mg/mL. The sterile filtration and 2 storage conditions did not significantly affect THC contents ($p > 0.05$). However, after 7 days of storage, the formulations F12 (purple) and F26 (green) had a lower THC concentration after 7 days of storage at RT. There were 3 final formulations, F23, F24, and F00, which maintained (i) physical appearance and (ii) THC content during the filtration process and 2 storage conditions in 7 days. Because F23 and F24 had similar formulation components (with Transcutol and Cremophor EL), F24 would be further selected to compare with F00 in drug formulations and permeability in the next part.

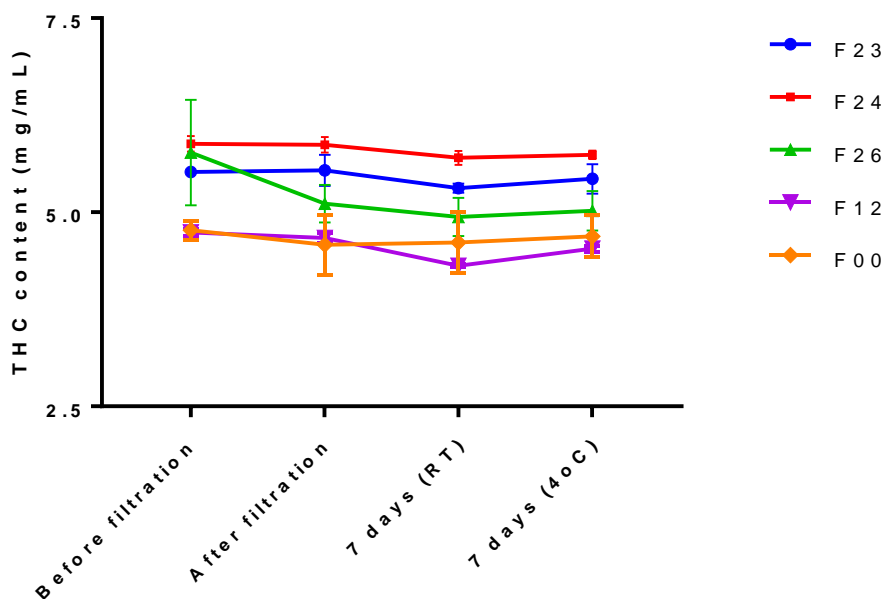


Figure 22: THC content before filtration, after filtration, and after 7-day storage at 2 conditions (RT and 4°C)

4.4.3 Other pharmaceutical criteria (particle size, pH, and osmolarity)

4.4.3.1 Particle size measurement

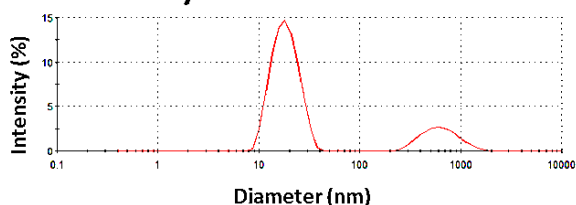
Table 8: Particle size measurement of THC formulations at day 0 and 7 days of storage

Formulation	Day 0		Day 7 (RT)		Day 7 (4°C)	
	Z* (nm)	PDI**	Z (nm)	PDI	Z (nm)	PDI
F00	25.00	0.352	18.75	0.148	18.37	0.171
F24	19.58	0.203	18.80	0.161	18.61	0.134

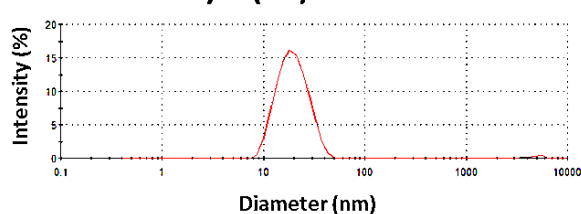
*Z (nm): particle size (reported by the equipment),

**PDI: polydispersity index (reported by the equipment)

Form. F00 Day 0: Size distribution



Day 7 (RT): Size distribution



Form. F24

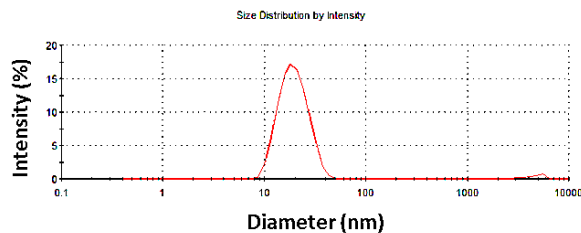
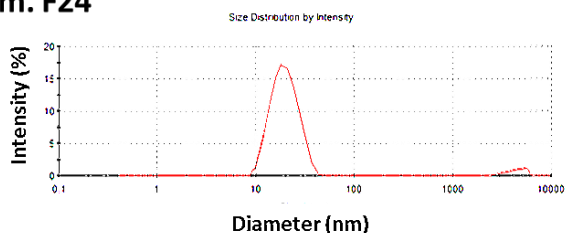


Figure 23: Intensity distribution of 2 THC formulations (via DLS technique)

Based on the physical appearance and particle size measurement, THC formulations (F00 and F24) were in the colloidal form (with around 20 nm micelles). The nonionic polymeric surfactant (Cremophor EL) played an important role in maintaining the micelle structure and THC concentration.

The particle size (Z, nm) and size distribution (polydispersity index, PDI) of the micelles formed in Cremophor EL and their mixture in an aqueous solution were evaluated from the dynamic light scattering (DLS) technique at 25°C (Figure 5 and Table 5). The polydispersity index (PDI) of these eyedrops were 0.352 and 0.203, indicating high monodispersed samples. Generally, a sample with a PDI greater than 0.7 is not suitable for DLS (ISO 13321:1996 E and ISO 22412:2008). High PDI value samples tend to aggregate more than monodisperse systems, so low PDI formulation indicated high stability (155,158).

In Figure 23, a peak (at 500nm to 1000nm) can be predicted to be a large Cremophor EL droplet dispersed in the aqueous formulation. Due to the small-scale experiment and available lab equipment (vortex), the shearing force was not high enough to diffuse Cremophor EL completely. However, because Cremophor EL can simultaneously disperse into a water phase, the large aggregates disappeared after 7 days of storage.

4.4.3.2 Osmotic parameter and pH

Three formulations (F00, F23, and F24) were selected to measure osmotic parameters and pH. For the pH values, all formulations have pH from 6.5 to 6.890, which are suitable as an eye drop. In terms of osmolarity, preparing formulations in water reduced osmotic parameters significantly than preparing formulations in NaCl 0.9% (Table 9). Additionally, the formulation F23 or F24 based on the Transcutol HP stock solution had a lower osmotic value than the DMSO stock solution (F00).

Table 9: Osmolarity and pH of the obtained THC formulations

Water phase	Prepared with NaCl 0.9%		Prepared with water	
F00 (DMSO)	High (over 3000 mOsm)	6.890	1881 mOsm	6.649
F23	1555 mOsm	6.989	1182 mOsm	6.869
F24	1476 mOsm	6.500	1011 mOsm	6.590

4.4.4 Radio-labeled mannitol permeability for carriers

Generally, the efficacies of eyedrop in drug delivery differ considerably according to their capacity to enhance the penetration of a drug through the cornea (154). To evaluate the permeability property of the 2 newly selected carriers (formulations without drug, F00 and F24), an *ex-vivo* experiment with radio-labeled mannitol was conducted to compare their permeability profiles (% permeability and Papp) with BSS plus buffer solution (Alcon Lab, TX, USA).

H3-Figure 24 Mannitol is a water-soluble substance that can be used as a “model substance” to evaluate the permeability of aqueous carriers. The permeability of the whole eyedrop formulation can imply the permeability profile of eyedrop formulations (Figure 24). The % drug permeated through porcine cornea after 6h was $(5.81 \pm 2.1\%)$ and $(4.11 \pm 1.13\%)$ for F00 and F24, respectively, which were significantly higher than that prepared in buffer $(3.25 \pm 0.7\%)$.

After calculating the amount of drug permeated via 6h, permeation coefficient (Papps) values were also calculated. “Apparent permeability (Papp)” was calculated based on the flux of H3-mannitol

across the cornea for 6h (details were mentioned in the Method section). The greater the Papp value, the greater the formulation's ability to enhance drug penetration through the cornea. Accordingly, Papp values of F00 and F24 are 1.87×10^{-6} and 1.83×10^{-6} which are higher than that of the buffer solution (0.81×10^{-6}). The result indicated that eyedrops prepared by F00 and F24 formulations efficiently permeated the cornea.

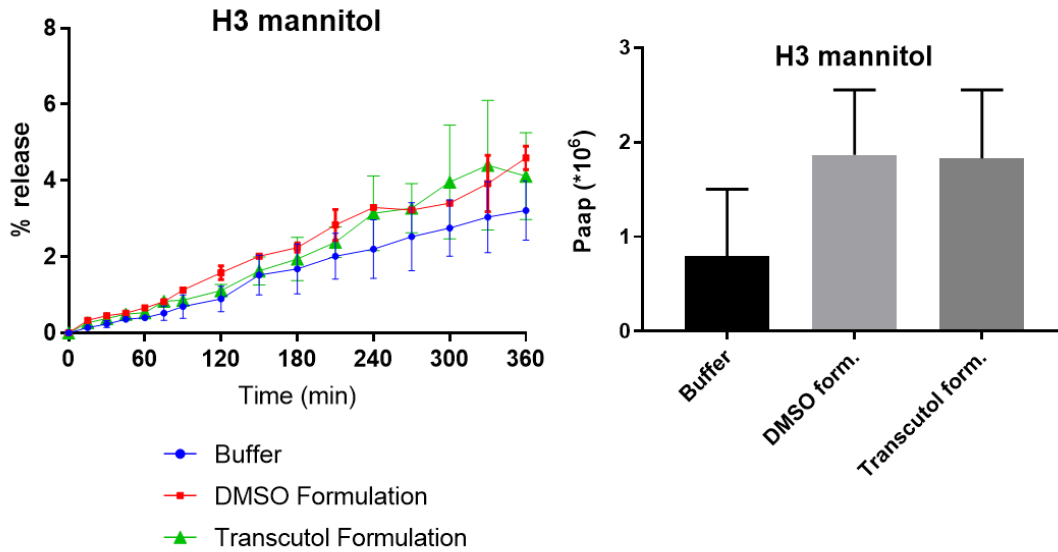


Figure 24: Permeability study of 2 formulations with H3-mannitol substances: DMSO (F00) and Transcutol (F24) significantly increased the permeability of the carriers compared to buffer.

5 DISCUSSION

5.1 ECS and DED pathology:

5.1.1 CBR expression and DED pathogenesis

In this study, cannabinoid receptors are found in the cornea, conjunctiva, and lacrimal gland. CBRs expressions are involved in DED pathology. Furthermore, various CBR ligands used in the treatment arm of the study were effective in treating DED.

Our study confirmed and expanded the previously reported CB1R and CB2R expression, in which we compared and characterized CBRs expressions in the cornea, conjunctiva, and lacrimal glands. CB1R and CB2R are distributed at a higher density in the epithelial layers, the outermost layers of the ocular surface. Due to the location of CB1R and CB2R in the epithelial layers, it is possible that DED pathology factors (such as tear film instability, hyperosmolarity, or epithelial damages) can directly influence and activate CBRs' expression and functions.

In the context of DED, this is the first time that an increase in CB1R and CB2R expression was observed during DED induction in the desiccating mouse model. The increasing trend of CB1R and CB2R was concurrent with DED phenotype readouts, including low tear amount production, high epithelial damage (high FL score), reduced cornea sensitivity, and infiltration of CD4+ cells into the conjunctiva. These findings (along with CBR ligands' activities) suggest that CB1R and CB2R play a significant role in pathology. As mentioned previously, CBR upregulation can be viewed as a protective response to pathological factors (42,86), so targeting CB1R and CB2R by using suitable CBR ligands is a potential therapy for DED.

Secondly, when CB1R and CB2R expression increased during DED-induction, CB2R increased faster than CB1R (CB1R/CB2R ratio was lower on day 10 than baseline). The main feature of DED is indicated by the movement of immune cells in the cornea and a rapid accumulation of CD4+ T-cells in the conjunctiva (118,159). These phenomena were also confirmed by the desiccating stress mouse model in this study. Because immune cells feature a high level of CB2R expression, CB2R increased concurrently with immune cell infiltration into the ocular surface and related tissues.

Therefore, it is promising to attempt to control the DED inflammation pathway by targeting CB2R. In fact, several studies suggested the potentiality of CB2R-based therapies for chronic inflammatory diseases such as rheumatoid arthritis (9), atherosclerosis (160), and inflammatory bowel disease (90,161).

Thirdly, data from von-Frey hair and corneal nerve morphology suggest cannabinoids are involved in abnormal neural sensory function. Additionally, only THC and the CB1R selective antagonist

significantly affected mechanical sensitivity (neither carriers nor CB2R selective antagonist did). This finding implied the role of CB1R and DED neurosensory abnormalities, in which CB1R expression was mentioned with sensory nerves (87,107,109). In agreement, increasing CB1R expression was reported together with discomfort symptoms in LASIK cases (162). Therefore, because CB1R and its ligands are responsible for the maintenance of the corneal neurosensory system's homeostasis, it is reasonable to use non-selective or CB1R selective ligands for DED neurosensory abnormalities. In summary, the functions of cannabinoids in inflammation and neurosensory abnormalities are discussed further in the following sections and Figure 25.

5.1.2 Cannabinoids in fluorescein score and inflammation

Previously, increasing FL scores were associated with increased expression of inflammatory mediators such as IL-1 or IFN- γ in the cornea and infiltration of immune cells (13,118,163). In our study, besides confirming DED readouts in DED-induced mice, topical cannabinoids reduced corneal damage (corneal staining), associated with lowering IL-1 β levels in the corneal epithelium. It is predicted that cannabinoids will have an anti-inflammatory effect (which will reduce the damage in the cornea during DED-induction) or stimulate the wound-healing process (which shortens the duration of wounds in the cornea epithelial layers).

As mentioned, THC and CB2R agonists were reported to have anti-inflammatory effects due to reducing cytokine releases and immune cell activities (73,89). Therefore, topical applying THC can suppress inflammation pathways in DED. In healthy human conjunctiva, CD8 $^+$ T cells are more prevalent than CD4 $^+$ T cells, but the number of CD4 $^+$ T cells outnumbers CD8 $^+$ T cells during DED, particularly in the desiccating-stress conditions (119,164). THC application significantly reduced CD4 $^+$ T cells and IL-1 in the cornea to restore CD8 $^+$ density in the conjunctiva (anti-inflammatory effect of CB2R agonist).

On the other hand, CD8 $^+$ density in conjunctiva was increased in two groups (THC and the selective CB2R-antagonist). Different from THC, the function of CB2R antagonists was more complicated. The results implied that the CB2R antagonist induced CD8 $^+$ T cells to prevent pathogenic CD4 $^+$ infiltration (163,165). Correspondingly, we also showed that the CB2R selective antagonist reduced IL-1 β in the cornea and conjunctiva, but the CB2R antagonist increased IFN- γ expression in the conjunctiva. The mouse model previously mentioned that IFN- γ upregulation decreases IL-1 β and IL-17 as an adaptive immune response to limit inflammation (166). While

activating CB2R showed an obvious anti-inflammatory function, the application of CB2R antagonists in inflammation is more complicating and involved with different cell lines (167,168). Lastly, because the Endocannabinoid system and its functions are still not fully understood, CB1R and CB2R antagonists might exhibit anti-inflammatory activities in different pathways independent of CB1R and CB2R (97). Our obtained results presented a potential role of cannabinoids in DED and suggested THC, AntaCB1, and AntaCB2 as novel strategies for treating inflammation.

5.1.3 Cannabinoids in pain and disturbed mechanical sensitivity and corneal nerve morphology in DED

Desiccating stress reduced corneal sensitivity while decreasing corneal nerve length in the in-vivo model, consistent with previous reports in DED mouse models (169,170). In DED, several environmental stresses cause a significant increase in neurotransmitters, including glutamate and substances P, which were released at such a high level that resulted in neurotoxicity (171,172).

Here, THC treatment preserved corneal nerve morphology and maintained mechanical sensitivity. The action of THC was the result of neurotransmitter suppression via the CB1R pathway (87), thereby preventing toxicity. This finding also confirms the neuroprotection properties of THC or CB1R agonists (66,173). Besides, CB1R antagonist treatment of DED maintained corneal sensitivity without changing the length of corneal nerves. Because CB1R pathways are involved in nerve transmission (66,174), our results suggest that using the CB1R antagonist increased nerve transmission (66,88), allowing corneal sensitivity to be maintained despite corneal nerve loss.

From a clinical point of view, it is well known that DED patients can exhibit both elevated and decreased corneal sensitivity. (37,175). The pharmacological effects of CB1R agonists or antagonists can be useful in treating the symptoms. In detail, CB1R agonists can potentially prevent hyperexcitability, consequently protecting the corneal nerves and maintaining sensitivity homeostasis (66,174). In contrast, CB1R antagonists can be indicated for short-term cases of decreased sensitivity, in which an enhancement of neurotransmission might reduce the symptoms. However, there is a risk that the increasing nerve transmission potentially leads to neuropathic cascades (172,176). So, depending on a particular case, CB1R pathways can relieve the symptoms, then maintain and even restore the homeostasis conditions in the ocular surface.

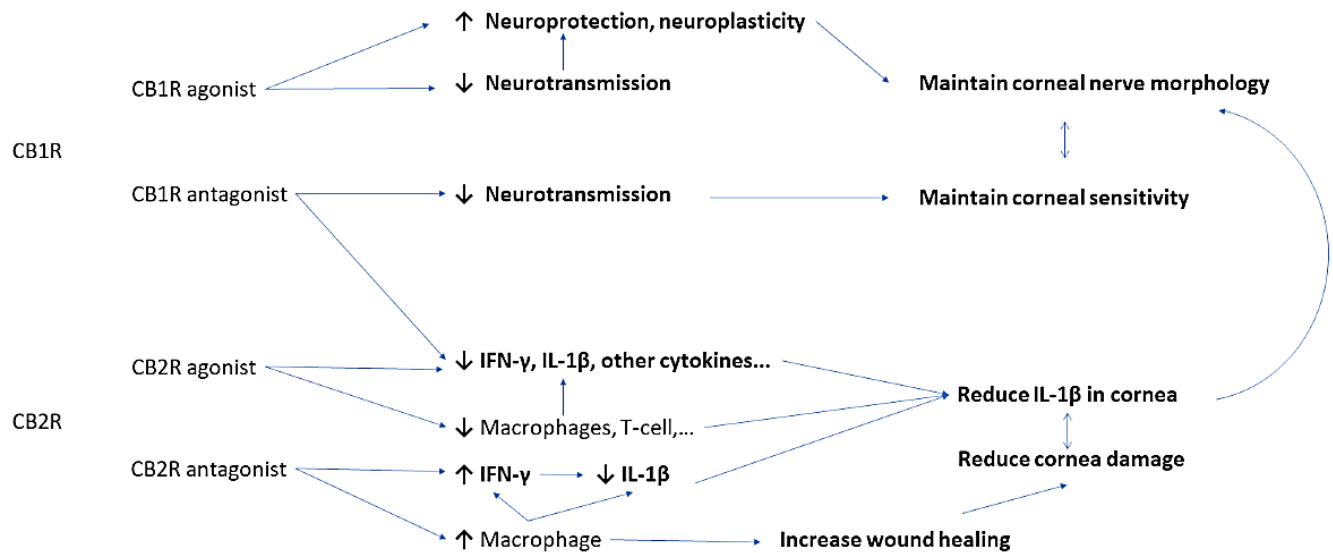


Figure 25: Summarizing the cannabinoid effects on DED phenotype with predicted involved mechanisms

5.1.4 Cannabinoids in the re-epithelialization process:

According to in-vivo DS model results, THC showed positive effects on inflammation and neurosensory of DED-induced mice. Many studies have shown that CBRs and cannabinoids affect epithelialization, epithelial cell migration, and apoptosis (177,178). Here, we showed that THC (a non-selective CBR agonist) and the CB1R selective antagonist significantly affected the re-epithelialization, while the CB2R antagonist didn't considerably affect these. It implied that the re-epithelialization depends on CB1R. This finding is relevant to other studies in which CB2R expression is low (undetectable) in the epithelial cells (178,179). In the case of the epithelial model, CB1R was detected not only at the cell margin but also intracellularly (178). Moreover, CB1R functions were reported to improve the "filopodia" process (97,180). The filopodia process is an essential migrating process in which the edge of the cells will change to "cones" or "hand-shape" forms, which is the first activity to intrude into the surrounding environment.

The connection between CB1R and re-epithelialization was also mentioned in previous studies, in which activating CB1R in bovine corneal epithelial cells improved cell migrations (177,181). Also, the healing process for corneal wounds in CB1R KO mice was slower than in wild-type mice (177). Yang et al. (177) showed evidence that CB1R pathways transactivated the epidermal growth factor receptor (EGF) receptor, significantly enhancing cell movement. Murataeva et al. (178) also suggested that the CBR ligands in the wound areas had a role in improving the rate of migration

via chemotaxis (178). The CBR ligands also served as a target that induced the movement of epithelial cells (178). Our results and previous studies also suggested that activating the CB1R pathway improves the wound healing process.

On the other hand, we found a biphasic effect of THC, which supports the well-known complexity of ECS and CBRs (82,182). In particular, THC has been tested at high concentrations (above ten micromolar) on a variety of cancer epithelial cell models, in which THC (non-selective agonist) inhibited the migration of several epithelial cancer cells and induced an apoptosis effect (183,184). This can explain why THC at high concentration delayed wound healing in the in-vitro models. There was an insignificant effect of CBR2 in an in-vitro cell-culture model, which can be explained by the fact that CBR2 is predominantly expressed in immune cells and is expressed at a low level (or undetected) in epithelial cells (19). The findings imply that CBR1 plays a beneficial role in corneal re-epithelialization, but the mechanisms are complex, and the dosing of agonists and antagonists must be thoroughly evaluated.

5.2 Cannabinoid formulation study

5.2.1 Drug formulation selection

In our study, Transcutol HP, DMSO, and Cremophor EL were used to dissolve hydrophobic cannabinoids in water-based formulations. All three mentioned excipients were mentioned as suitable for eyedrop formulation. According to US Food and Drug Administration (FDA), DMSO and Transcutol HP are categorized as less toxic and at lower risk to human or animal health (185,186). Cremophor EL (also called Kolliphor EL), a polyethoxylated castor oil, is popular in pharmaceutical products, including eye-drop (187). The application of eye drops with DMSO and Cremophor in animal models or clinical trials was reported previously (151,188,189). High concentrations of DMSO (up to 50%) (188) or Cremophore (up to 15%) were reported to be safe and well-tolerated (190). In our study, there were no abnormal reactions detected in the eye of experimental mice during experiments. Therefore, in this study, the two final carriers are suitable for cannabinoids aimed at human use.

Cremophor EL is a pharmaceutical excipient used as a surfactant to enhance the solubility of hydrophobic drugs in water and sustain the stability of liquid formulations such as emulsion or suspension (191). In an aqueous environment, the hydrophilic moiety of Cremophor EL forms hydrogen bonds with surrounding water molecules, while the hydrophobic parts of Cremophor EL molecules are sequestered inside to confine the micelle center. The micelle form can serve as a

compartment for hydrophobic drugs. Hydrophobic drugs like THC can enter the hydrophobic core of micelles, leading to increased aqueous solubility and maintaining the stability of formulations. In this study, the THC formulation is in micelle form with a 10 nm particle size diameter.

Although these formulations have osmolarity higher than tear osmolarity (approximately 289 mOsm/L), they are all in an accepted range according to US Pharmacopoeia (USP) (192). The US Pharmacopoeia implied that ophthalmic formulations with tonicity ranging from 171 mOsm/kg to 1711 mOsm/kg (equivalent to 0.5 percent to 5 percent sodium chloride) do not cause significant irritation to the eye (192). Additionally, a recent study by Dutescu et al. (193) found that the osmolarity of 51 % of the evaluated marketed products was higher than the natural tear osmolarity. The osmolarity of some eyedrops containing active pharmaceutical substances had hyperosmolarity values, up to 1955 mOsm (193).

The obtained formulation possesses certain features: non-toxic and well-tolerated components, relatively adequate THC concentration (0.5%), and the formulations were stable for 7 days. Therefore, these micelles-based formulations are ready for THC, which has prompted their use as vehicles for other cannabinoids with similar physiochemical properties.

5.2.2 Permeability

Ocular surface diseases and anterior segment diseases are commonly treated with eye drops containing drug compounds. However, delivering an optimal drug concentration at the target sites is a challenge for THC or hydrophobic substances (132,194). As mentioned, the ocular surface system is also a barrier, leading to poor bioavailability for hydrophobic drugs like cannabinoids (132,194). A small proportion of active ingredients is absorbed ocularly via eyedrop dosage form (14,121,195). Actually, eyedrops for THC were attempted previously for glaucoma, in which topical application of THC frequently fails to show a significant effect in clinical trials (136). Recently, a review from Passani et al. (136) showed that although cannabinoids (THC or WIN 55212,2) administered via injection, inhalation, or oral had a significant “lower IOP effect”, using eyedrops of THC and several cannabinoids failed to show “significant effect” when compared to placebo samples. However, THC's topical application for DED therapy has more potential than glaucoma due to the location of CBRs. This study showed that CBRs are in the outermost epithelial layers, so delivering THC into these superficial layers of the ocular surface is more feasible and practical. Moreover, because CBRs expressions are increasing at the epithelial layer during DED

pathogenesis, THC or cannabinoid molecules have a higher chance to bind to the receptors to exhibit their therapeutic effects. Future studies about pharmacokinetics, target-drug delivery, and relating therapeutic effects can be proposed to bring these products closer to commercial markets or patient use.

In the frame of this study, two formulations (F00 and F24) were proposed, in which the blank carriers significantly improved cornea permeability compared to a buffer. This finding implied that the two formulations could deliver THC across the ocular surface barrier to exhibit its effects. In summary, the findings of the drug formulation study indicate the possibility of a clinical trial in the near future.

5.2.3 Remarks and perspectives about proposed formulations

For the second part of the study, the drug formulation study proposed two formulations based on Cremophor EL and two solvents (DMSO or Transcutol HP). These results show the feasibility of an ophthalmic preparation developed in hospitals and aimed for clinical uses. Due to the available facilities, pandemic situations, and THC license requirements, there are still some limitations. THC formulations should be prepared in a pharmaceutical lab with specific equipment such as different stirring machines, particle size measurement, and THC quantification during the formulation process. Also, we couldn't present the data on THC permeability (instead, we provided the permeability with radio-label substances as a prediction model). However, the obtained results suggested a potential application.

Two final THC formulations contain 0.5% THC concentration, which is comparable to other THC eyedrops (37). Additionally, the stability when storing samples at room temperature or refrigerator (4-8°C) would facilitate its use by patients for 7 days. Because THC was formulated in 10nm micelles, we hypothesized that the permeability was significantly improved. Thus, the two formulations are expected to have low toxicity on patients and have potential therapeutic effects that were already shown in the in-vivo mouse model.

5.3 Legal discussion

In this study, THC experiments required a special license from the Bundesopiumstelle des Bundesinstituts für Arzneimittel und Medizinprodukte (BfArM), number: 463 1128). In general, the European Medical Agency (EMA) and several nations (including Germany) continue to classify cannabis products as controlled substances (196,197). In 2017, Germany's Narcotic Drugs Act was amended to allow physicians to prescribe cannabis to patients even if other therapeutic options were available (198). However, there is still a controversial debate about cannabis use (198,200), in which using cannabis as medicine is regarded as having “limited knowledge of the effectiveness and safety” (199). Therefore, the complicating rules and policies in different countries are causing challenges for pharmaceutical companies to develop these substances for pharmaceutical markets.

5.4 Perspective

The current study reveals the relationship between DED pathomechanisms and cannabinoids as an eyedrop therapy. This study has several limitations, which suggest potential follow-up studies. The complexity of both DED and ECS suggested that CB1R or CB2R knock-out (KO) mice should be tested to reveal more details about immune-regulatory mechanisms. Among three corneal nociceptors (mechanical, cold, and polymodal), also mechanical sensitivity was tested via von-Frey filaments. Thus, different DED models with varying characterizations of nociception should be conducted to have a complete overview of the CBR activities and DED (40). However, our findings support cannabinoid ligands eye drops as a DED therapy. Notably, THC, a combined CB1/CB2 agonist, displayed the most promising results. Based on current developments, THC can be used to treat other specific symptoms at the ocular surface, such as blepharitis (inflammation in the eyelids), allergic eye diseases (AED), neuropathic pain, or discomforts in the eyes, and chemical and thermal burns. The drug formulation study confirmed that THC could be formulated in eyedrops qualified for the industry. Also, results in permeability studies implied potential uses of these new formulation for intraocular pressure (196).

In summary, the results of this study suggest a novel and promising DED therapy based on cannabinoids. However, to understand in-depth the proposed modes of action, ongoing studies will need to address formulation issues, investigate the pharmacokinetics, and identify and prevent side effects before aiming for clinical trial applications.

Reference

1. Craig JP, Nichols KK, Akpek EK, Caffery B, Dua HS, Joo CK, et al. TFOS DEWS II Definition and Classification Report. Vol. 15, Ocular Surface. Elsevier Inc.; 2017. p. 276–83.
2. Craig JP, Nelson JD, Azar DT, Belmonte C, Bron AJ, Chauhan SK, et al. TFOS DEWS II Report Executive Summary. *Ocul Surf*. 2017;15(4):802–12.
3. Baudouin C, Messmer EM, Aragona P, Geerling G, Akova YA, Benítez-Del-Castillo J, et al. Revisiting the vicious circle of dry eye disease: A focus on the pathophysiology of meibomian gland dysfunction. *Br J Ophthalmol*. 2016;100(3):300–6.
4. McDonald M, Patel DA, Keith MS, Snedecor SJ. Economic and Humanistic Burden of Dry Eye Disease in Europe, North America, and Asia: A Systematic Literature Review. Vol. 14, Ocular Surface. Elsevier Inc.; 2016. p. 144–67.
5. Wlodarczyk J, Fairchild C. United States cost-effectiveness study of two dry eye ophthalmic lubricants. *Ophthalmic Epidemiol*. 2009;16(1):22–30.
6. Stapleton F, Alves M, Bunya VY, Jalbert I, Lekhanont K, Malet F, et al. TFOS DEWS II Epidemiology Report. *Ocul Surf* [Internet]. 2017;15(3):334–65. Available from: <http://dx.doi.org/10.1016/j.jtos.2017.05.003>
7. Miljanović B, Dana R, Sullivan DA, Schaumberg DA. Impact of dry eye syndrome on vision-related quality of life. *Am J Ophthalmol*. 2007;143(3):409–15.
8. DEWS Definition and Classification Subcommittee. DEWS Definition and Classification The Definition and Classification of Dry Eye Disease : 2007;5(2):75–92.
9. Russo EB. Cannabinoids in the management of difficult to treat pain. *Ther Clin Risk Manag*. 2008;4(1):245–59.
10. Farrand KF, Fridman M, Stillman IÖ, Schaumberg DA. Prevalence of Diagnosed Dry Eye Disease in the United States Among Adults Aged 18 Years and Older. *Am J Ophthalmol* [Internet]. 2017;182:90–8. Available from: <https://www.sciencedirect.com/science/article/pii/S0002939417302908>
11. Tsubota K, Pflugfelder SC, Liu Z, Baudouin C, Kim HM, Messmer EM, et al. Defining dry eye from a clinical perspective. *Int J Mol Sci*. 2020;21(23):1–24.
12. Jones L, Downie LE, Korb D, Benitez-del-castillo JM, Dana R, Deng SX, et al. The Ocular Surface TFOS DEWS II Management and Therapy Report. *Ocul Surf* [Internet]. 2017;15(3):575–628. Available from: <http://dx.doi.org/10.1016/j.jtos.2017.05.006>
13. Bron AJ, de Paiva CS, Chauhan SK, Bonini S, Gabison EE, Jain S, et al. TFOS DEWS II pathophysiology report. *Ocul Surf* [Internet]. 2017;15(3):438–510. Available from: <https://doi.org/10.1016/j.jtos.2017.05.011>
14. Agarwal P, Craig JP, Rupenthal ID. Formulation considerations for the management of dry eye disease. *Pharmaceutics*. 2021;13(2):1–19.
15. Stern ME, Gao J, Siemasko KF, Beuerman RW, Pflugfelder SC. The role of the lacrimal functional unit in the pathophysiology of dry eye. *Exp Eye Res*. 2004 Mar;78(3):409–16.
16. Stern ME, Pflugfelder SC. Inflammation in dry eye. *Ocul Surf*. 2004;2(2):124–30.
17. Gipson IK. The ocular surface: The challenge to enable and protect vision. The Friedenwald lecture. *Investig Ophthalmol Vis Sci*. 2007;48(10):4391–8.
18. Gipson IK. The ocular surface: the challenge to enable and protect vision: the Friedenwald lecture. *Invest Ophthalmol Vis Sci* [Internet]. 2007 Oct;48(10):4390–8. Available from: <https://pubmed.ncbi.nlm.nih.gov/17898256>
19. Galor A, Levitt RC, Felix ER, Martin ER, Sarantopoulos CD. Neuropathic ocular pain: An important yet underevaluated feature of dry eye. *Eye*. 2015;29(3):301–12.
20. Belmonte C, Acosta MC, Gallar J. Neural basis of sensation in intact and injured corneas. *Exp Eye Res*. 2004;78(3):513–25.
21. Belmonte C, Nichols JJ, Cox SM, Brock JA, Begley CG, Bereiter DA, et al. TFOS DEWS II pain and sensation report. *Ocul Surf* [Internet]. 2017;15(3):404–37. Available from: <http://dx.doi.org/10.1016/j.jtos.2017.05.002>
22. Corrales RM, Stern ME, De Paiva CS, Welch J, Li DQ, Pflugfelder SC. Desiccating stress stimulates expression of matrix metalloproteinases by the corneal epithelium. *Investig Ophthalmol Vis Sci*. 2006;47(8):3293–302.
23. Luo L, Li D-QQ, Doshi A, Farley W, Corrales RM, Pflugfelder SC. Experimental dry eye stimulates production of inflammatory cytokines and MMP-9 and activates MAPK signaling pathways on the ocular surface. *Investig Ophthalmol Vis Sci*. 2004;45(12):4293–301.
24. Yeh S, Song XJ, Farley W, Li D-Q, Stern ME, Pflugfelder SC. Apoptosis of ocular surface cells in

- experimentally induced dry eye. *Invest Ophthalmol Vis Sci*. 2003;44(1):124–9.
25. Perez VL, Stern ME, Pflugfelder SC. Inflammatory basis for dry eye disease flares. *Exp Eye Res*. 2020;201:108294.
 26. Stern ME, Schaumburg CS, Pflugfelder SC. Dry eye as a mucosal autoimmune disease. *Int Rev Immunol*. 2013;32(1):19–41.
 27. Petroustos G, Guimaraes R, Giraud J, Pouliquen Y. Corticosteroids and corneal epithelial wound healing. *Arch Ophthalmol*. 1983;101(11):1775–8.
 28. Holland EJ, Luchs J, Karpecki PM, Nichols KK, Jackson MA, Sall K, et al. Lifitegrast for the Treatment of Dry Eye Disease: Results of a Phase III, Randomized, Double-Masked, Placebo-Controlled Trial (OPUS-3). *Ophthalmology*. 2017;124(1):53–60.
 29. Esquenazi S, He J, Bazan HEP, Bazan NG. Use of autologous serum in corneal epithelial defects post-lamellar surgery. *Cornea*. 2005;24(8):992–7.
 30. Alio JL, Rodriguez AE, Ferreira-Oliveira R, Wróbel-Dudzińska D, Abdelghany AA. Treatment of Dry Eye Disease with Autologous Platelet-Rich Plasma: A Prospective, Interventional, Non-Randomized Study. *Ophthalmol Ther*. 2017;6(2):285–93.
 31. Craig JP, Nichols KK, Akpek EK, Caffery B, Dua HS, Joo C, et al. The Ocular Surface TFOS DEWS II Definition and Classification Report. 2017;15:276–83.
 32. Belmonte C, Nichols JJ, Cox SM, Brock JA, Begley CG, Bereiter DA, et al. TFOS DEWS II pain and sensation report. *Ocul Surf* [Internet]. 2017;15(3):404–37. Available from: <http://dx.doi.org/10.1016/j.jtos.2017.05.002>
 33. Belmonte C, Acosta MC, Merayo-Llodes J, Gallar J. What Causes Eye Pain? *Curr Ophthalmol Rep*. 2015 Jun;3(2):111–21.
 34. Sanderson J, Dartt DA, Trinkaus-Randall V, Pintor J, Civan MM, Delamere NA, et al. Purines in the eye: Recent evidence for the physiological and pathological role of purines in the RPE, retinal neurons, astrocytes, Müller cells, lens, trabecular meshwork, cornea and lacrimal gland. *Exp Eye Res* [Internet]. 2014;127:270–9. Available from: <http://dx.doi.org/10.1016/j.exer.2014.08.009>
 35. López-de la Rosa A, García-Vázquez C, Fernández I, Arroyo-del Arroyo C, Enríquez-de-Salamanca A, González-García MJ. Substance P Level in Tears as a Potential Biomarker for Contact Lens Discomfort. *Ocul Immunol Inflamm* [Internet]. 2021 Jan 2;29(1):43–56. Available from: <https://doi.org/10.1080/09273948.2019.1668024>
 36. López-de la Rosa A, Fernández I, García-Vázquez C, Arroyo-del Arroyo C, González-García MJ, Enríquez-de-Salamanca A. Conjunctival Neuropathic and Inflammatory Pain-Related Gene Expression with Contact Lens Wear and Discomfort. *Ocul Immunol Inflamm* [Internet]. 2021 Apr 3;29(3):587–606. Available from: <https://doi.org/10.1080/09273948.2019.1690005>
 37. Dieckmann G, Goyal S, Hamrah P. Neuropathic Corneal Pain: Approaches for Management. *Ophthalmology*. 2017 Nov 1;124(11):S34–47.
 38. Goyal S, Hamrah P. Understanding neuropathic corneal pain - Gaps and current therapeutic approaches. *Semin Ophthalmol*. 2016;31(1–2):59–70.
 39. Reaux-Le Goazigo A, Poras H, Ben-Dhaou C, Ouimet T, Baudouin C, Wurm M, et al. Dual enkephalinase inhibitor PL265: a novel topical treatment to alleviate corneal pain and inflammation. *Pain*. 2019;160(2):307–21.
 40. Joubert F, Guerrero-Moreno A, Fakhri D, Reboussin E, Gaveriaux-Ruff C, Acosta MC, et al. Topical treatment with a mu opioid receptor agonist alleviates corneal allodynia and corneal nerve sensitization in mice. *Biomed Pharmacother* [Internet]. 2020;132:110794. Available from: <https://www.sciencedirect.com/science/article/pii/S0753332220309872>
 41. Hohmann AG, Suplita RL, Bolton NM, Neely MH, Fegley D, Mangieri R, et al. An endocannabinoid mechanism for stress-induced analgesia. *Nature*. 2005;435(7045):1108–12.
 42. Piomelli D, Sasso O. Peripheral gating of pain signals by endogenous lipid mediators. *Nat Neurosci* [Internet]. 2014/01/28. 2014 Feb;17(2):164–74. Available from: <https://pubmed.ncbi.nlm.nih.gov/24473264>
 43. Thoft RA. The X, Y, Z hypothesis of corneal epithelial maintenance. *Invest Ophthalmol Vis Sci*. 1983;24:1442–3.
 44. Wilson SE, Mohan RRR, Mohan RRR, Ambrósio R, Hong J, Lee J. The Corneal Wound Healing Response: *Prog Retin Eye Res* [Internet]. 2001;20(5):625–37. Available from: <http://www.sciencedirect.com/science/article/pii/S1350946201000088>
 45. Choi JH, Kim JH, Li Z, Oh HJ, Ahn KY, Yoon KC. Efficacy of the mineral oil and hyaluronic acid mixture eye drops in murine dry eye. *Korean J Ophthalmol*. 2015;29(2):131–7.
 46. Gomes JAP, Amankwah R, Powell-Richards A, Dua HS. Sodium hyaluronate (hyaluronic acid) promotes

- migration of human corneal epithelial cells in vitro. *Br J Ophthalmol* [Internet]. 2004 Jun;88(6):821–5. Available from: <https://pubmed.ncbi.nlm.nih.gov/15148219>
47. L. Alio J, Arnalich-Montiel F, E. Rodriguez A. The Role of “Eye Platelet Rich Plasma” (E-Prp) for Wound Healing in Ophthalmology. *Curr Pharm Biotechnol*. 2012;13(7):1257–65.
 48. Erin C. O’Neil M, Matthew Henderson B, Mina Massaro-Giordano, MD, Vatinee Y. Bunya M. *Advances in Dry Eye Disease Treatment. Physiol Behav*. 2017;176(10):139–48.
 49. Paulsen FP, Woon CW, Varoga D, Jansen A, Garreis F, Jäger K, et al. Intestinal trefoil factor/TFF3 promotes re-epithelialization of corneal wounds. *J Biol Chem*. 2008;283(19):13418–27.
 50. Maccarrone M, Bab I, Bíró T, Cabral GA, Dey SK, Di Marzo V, et al. Endocannabinoid signaling at the periphery: 50 years after THC. *Trends Pharmacol Sci*. 2015;36(5):277–96.
 51. Howlett AC. The cannabinoid receptors. *Prostaglandins Other Lipid Mediat* [Internet]. 2002;68–69:619–31. Available from: <https://www.sciencedirect.com/science/article/pii/S0090698002000606>
 52. Zou S, Kumar U. Cannabinoid receptors and the endocannabinoid system: Signaling and function in the central nervous system. *Int J Mol Sci*. 2018;19(3).
 53. Castillo PE, Younts TJ, Chávez AE, Hashimoto Y. Endocannabinoid signaling and synaptic function. *Neuron* [Internet]. 2012;76(1):70–81. Available from: doi: 10.1016/j.neuron.2012.09.020
 54. Sugiura T, Kodaka T, Nakane S, Kishimoto S, Kondo S, Waku K. Detection of an endogenous cannabimimetic molecule, 2-arachidonoylglycerol, and cannabinoid CBI receptor mRNA in human vascular cells: Is 2-arachidonoylglycerol a possible vasomodulator? *Biochem Biophys Res Commun*. 1998;243(3):838–43.
 55. Concannon RM, Okine BN, Finn DP, Dowd E. Differential upregulation of the cannabinoid CB2 receptor in neurotoxic and inflammation-driven rat models of Parkinson’s disease. *Exp Neurol* [Internet]. 2015;269:133–41. Available from: <https://www.sciencedirect.com/science/article/pii/S0014488615001211>
 56. L. DP, D. M, T. B, V. DM, De Petrocellis L, Melck D, et al. Endocannabinoids and fatty acid amides in cancer, inflammation and related disorders. *Chem Phys Lipids* [Internet]. 2000;108(1–2):191–209. Available from: [http://www.embase.com/search/results?subaction=viewrecord&from=export&id=L30979258%0Ahttp://dx.doi.org/10.1016/S0009-3084\(00\)00196-1](http://www.embase.com/search/results?subaction=viewrecord&from=export&id=L30979258%0Ahttp://dx.doi.org/10.1016/S0009-3084(00)00196-1)
 57. Wallace MJ, Martin BR, DeLorenzo RJ. Evidence for a physiological role of endocannabinoids in the modulation of seizure threshold and severity. *Eur J Pharmacol*. 2002;452(3):295–301.
 58. Roche M, Kelly JP, O’Driscoll M, Finn DP. Augmentation of endogenous cannabinoid tone modulates lipopolysaccharide-induced alterations in circulating cytokine levels in rats. *Immunology* [Internet]. 2008;125(2):263–71. Available from: 10.1111/j.1365-2567.2008.02838.x
 59. Burkey RT, Nation JR. (R)-methanandamide, but not anandamide, substitutes for Δ-9-THC in a drug-discrimination procedure. *Exp Clin Psychopharmacol*. 1997;5(3):195.
 60. Wiley JL, Ryan WJ, Razdan RK, Martin BR. Evaluation of cannabimimetic effects of structural analogs of anandamide in rats. *Eur J Pharmacol*. 1998;355(2–3):113–8.
 61. European Monitoring Centre for Drugs and Drug Addiction (EMCDDA). Synthetic cannabinoids in Europe - update 2017. *Perspect Drugs* [Internet]. 2017;9. Available from: http://www.emcdda.europa.eu/topics/pods/synthetic-cannabinoids%0Ahttp://www.emcdda.europa.eu/publications/pods/synthetic-cannabinoids_en
 62. Hillard CJ, Manna S, Greenberg MJ, DiCamelli R, Ross RA, Stevenson LA, et al. Synthesis and characterization of potent and selective agonists of the neuronal cannabinoid receptor (CB1). *J Pharmacol Exp Ther*. 1999;289(3):1427–33.
 63. Mills B, Yepes A, Nugent K. Synthetic cannabinoids. *Am J Med Sci*. 2015;350(1):59–62.
 64. Ebrahimzadeh M, Haghparast A. Analgesic effects of cannabinoid receptor agonist WIN55,212-2 in the nucleus cuneiformis in animal models of acute and inflammatory pain in rats. *Brain Res* [Internet]. 2011;1420:19–28. Available from: <http://dx.doi.org/10.1016/j.brainres.2011.08.028>
 65. Gurney SMR, Scott KS, Kacinko SL, Presley BC, Logan BK. Pharmacology, toxicology, and adverse effects of synthetic cannabinoid drugs. *Forensic Sci Rev*. 2014;26(1):54–76.
 66. Chhatwal JP, Davis M, Maguschak KA, Ressler KJ. Enhancing cannabinoid neurotransmission augments the extinction of conditioned fear. *Neuropsychopharmacology*. 2005;30(3):516–24.
 67. Oshita K, Inoue A, Tang H-B, Nakata Y, Kawamoto M, Yuge O. CB(1) cannabinoid receptor stimulation modulates transient receptor potential vanilloid receptor 1 activities in calcium influx and substance P Release in cultured rat dorsal root ganglion cells. *J Pharmacol Sci* [Internet]. 2005;97(3):377–85. Available from: <http://www.ncbi.nlm.nih.gov/pubmed/15750287>
 68. Lou ZY, Chen C, He Q, Zhao CB, Xiao BG. Targeting CB 2 receptor as a neuroinflammatory modulator in

- experimental autoimmune encephalomyelitis. *Mol Immunol* [Internet]. 2011;49(3):453–61. Available from: <http://dx.doi.org/10.1016/j.molimm.2011.09.016>
69. Borowska-Fielding J, Murataeva N, Smith B, Szczesniak AM, Leishman E, Daily L, et al. Revisiting cannabinoid receptor 2 expression and function in murine retina. *Neuropharmacology*. 2018;141.
 70. Zhang HY, Bi GH, Li X, Li J, Qu H, Zhang SJ, et al. Species differences in cannabinoid receptor 2 and receptor responses to cocaine self-administration in mice and rats. *Neuropsychopharmacology* [Internet]. 2015;40(4):1037–51. Available from: <http://dx.doi.org/10.1038/npp.2014.297>
 71. Hanus L, Breuer A, Tchilibon S, Shiloah S, Goldenberg D, Horowitz M, et al. HU-308: A specific agonist for CB2, a peripheral cannabinoid receptor. *Proc Natl Acad Sci* [Internet]. 1999;96(25):14228–33. Available from: <http://www.pnas.org/cgi/doi/10.1073/pnas.96.25.14228>
 72. Uhelski ML, Cain DM, Harding-Rose C, Simone DA. The non-selective cannabinoid receptor agonist WIN 55,212-2 attenuates responses of C-fiber nociceptors in a murine model of cancer pain. *Neuroscience*. 2013;247:84–94.
 73. Thapa D, Cairns EA, Szczesniak A-M, Toguri JT, Caldwell MD, Kelly MEM. The Cannabinoids Δ^8 THC, CBD, and HU-308 Act via Distinct Receptors to Reduce Corneal Pain and Inflammation. *Cannabis cannabinoid Res* [Internet]. 2018;3(1):11–20. Available from: 10.1089/can.2017.0041
 74. Mechoulam R, Peters M, Murillo-Rodriguez E, Hanuš LO. Cannabidiol—recent advances. *Chem Biodivers*. 2007;4(8):1678–92.
 75. Miller S, Daily L, Leishman E, Bradshaw H, Straiker A. Δ^9 -Tetrahydrocannabinol and Cannabidiol Differentially Regulate Intraocular Pressure. *Investig Ophthalmol Vis Sci*. 2018;59(15):5904–11.
 76. Kim D, Thayer SA. Cannabinoids inhibit the formation of new synapses between hippocampal neurons in culture. *J Neurosci* [Internet]. 2001;21(10):RC146–RC146. Available from: doi: 10.1523/jneurosci.21-10-j0004.2001
 77. Katona I, Sperlág B, Sík A, Káfalvi A, Vizi ES, Mackie K, et al. Presynaptically located CB1 cannabinoid receptors regulate GABA release from axon terminals of specific hippocampal interneurons. *J Neurosci* [Internet]. 1999;19(11):4544–58. Available from: 10.1523/JNEUROSCI.19-11-04544.1999
 78. Ishac EJN, Jiang L, Lake KD, Varga K, Abood ME, Kunos G. Inhibition of exocytotic noradrenaline release by presynaptic cannabinoid CB1 receptors on peripheral sympathetic nerves. *Br J Pharmacol*. 1996;118(8):2023–8.
 79. Schwitzer T, Schwan R, Angioi-duprez K, Giersch A, Laprevote V. The Endocannabinoid System in the Retina: From Physiology to Practical and Therapeutic Applications. *Neural Plast*. 2016;2016.
 80. Marsicano G, Goodenough S, Monory K, Hermann H, Eder M, Cannich A, et al. CB1 cannabinoid receptors and on-demand defense against excitotoxicity. *Science* (80-) [Internet]. 2003;302(5642):84–8. Available from: 10.1126/science.1088208
 81. Gifford AN, Bruneus M, Gatley SJ, Volkow ND. Cannabinoid receptor-mediated inhibition of acetylcholine release from hippocampal and cortical synaptosomes. *Br J Pharmacol* [Internet]. 2000 Oct;131(3):645–50. Available from: <https://www.ncbi.nlm.nih.gov/pubmed/11015319>
 82. Tzavara ET, Wade M, Nomikos GG. Biphasic effects of cannabinoids on acetylcholine release in the hippocampus: site and mechanism of action. *J Neurosci*. 2003;23(28):9374–84.
 83. Opere CA, Zheng WD, Zhao M, Lee JS, Kulkarni KH, Ohia SE. Inhibition of potassium-and ischemia-evoked [3H] D-aspartate release from isolated bovine retina by cannabinoids. *Curr Eye Res*. 2006;31(7–8):645–53.
 84. Brooks JW, Thompson SWN, Rice ASC, Malcangio M. (S)-AMPA inhibits electrically evoked calcitonin gene-related peptide (CGRP) release from the rat dorsal horn: reversal by cannabinoid receptor antagonist SR141716A. *Neurosci Lett*. 2004;372(1–2):85–8.
 85. Fišar Z. Inhibition of monoamine oxidase activity by cannabinoids. *Naunyn Schmiedeberg's Arch Pharmacol*. 2010;381(6):563–72.
 86. Marsicano G, Moosmann B, Hermann H, Lutz B, Behl C. Neuroprotective properties of cannabinoids against oxidative stress: Role of the cannabinoid receptor CB1. *J Neurochem*. 2002;80(3):448–56.
 87. El-Remessy AB, Khalil IE, Matragoon S, Abou-Mohamed G, Tsai NJ, Roon P, et al. Neuroprotective Effect of (-) Δ^9 -Tetrahydrocannabinol and Cannabidiol in N-Methyl-D-Aspartate-Induced Retinal Neurotoxicity: Involvement of Peroxynitrite. *Am J Pathol* [Internet]. 2003;163(5):1997–2008. Available from: [http://dx.doi.org/10.1016/S0002-9440\(10\)63558-4](http://dx.doi.org/10.1016/S0002-9440(10)63558-4)
 88. Lever IJ, Malcangio M. CB1 receptor antagonist SR141716A increases capsaicin-evoked release of Substance P from the adult mouse spinal cord. *Br J Pharmacol*. 2002;135(1):21–4.
 89. Toguri JT, Caldwell M, Kelly MEM. Turning down the thermostat: Modulating the endocannabinoid system in ocular inflammation and pain. *Front Pharmacol*. 2016;7(SEP):1–9.

90. Turcotte C, Blanchet MR, Laviolette M, Flamand N. The CB2receptor and its role as a regulator of inflammation. *Cell Mol Life Sci*. 2016;73(23):4449–70.
91. Adhikary S, Kocieda VP, Yen J-H, Tuma RF, Ganea D. Signaling through cannabinoid receptor 2 suppresses murine dendritic cell migration by inhibiting matrix metalloproteinase 9 expression. *Blood, J Am Soc Hematol*. 2012;120(18):3741–9.
92. Chiurchiù V, Cencioni MT, Bisicchia E, De Bardi M, Gasperini C, Borsellino G, et al. Distinct modulation of human myeloid and plasmacytoid dendritic cells by anandamide in multiple sclerosis. *Ann Neurol*. 2013;73(5):626–36.
93. Du Y, Ren P, Wang Q, Jiang S-K, Zhang M, Li J-Y, et al. Cannabinoid 2 receptor attenuates inflammation during skin wound healing by inhibiting M1 macrophages rather than activating M2 macrophages. *J Inflamm*. 2018;15(1):1–12.
94. Ni X, Geller EB, Eppihimer MJ, Eisenstein TK, Adler MW, Tuma RF. Win 55212-2, a cannabinoid receptor agonist, attenuates leukocyte/endothelial interactions in an experimental autoimmune encephalomyelitis model. *Mult Scler J [Internet]*. 2004;10(2):158–64. Available from: 10.1191/1352458504ms1009oa
95. Lunn CA, Fine JS, Rojas-Triana A, Jackson J V, Fan X, Kung TT, et al. A novel cannabinoid peripheral cannabinoid receptor-selective inverse agonist blocks leukocyte recruitment in vivo. *J Pharmacol Exp Ther*. 2006;316(2):780–8.
96. Montecucco F, Di Marzo V, da Silva RF, Vuilleumier N, Capettini L, Lenglet S, et al. The activation of the cannabinoid receptor type 2 reduces neutrophilic protease-mediated vulnerability in atherosclerotic plaques. *Eur Heart J*. 2012;33(7):846–56.
97. Smith SR, Denhardt G, Terminelli C. The anti-inflammatory activities of cannabinoid receptor ligands in mouse peritonitis models. *Eur J Pharmacol*. 2001;432(1):107–19.
98. Cencioni MT, Chiurchiù V, Catanzaro G, Borsellino G, Bernardi G, Battistini L, et al. Anandamide suppresses proliferation and cytokine release from primary human T-lymphocytes mainly via CB 2 receptors. *PLoS One*. 2010;5(1):e8688.
99. Ghosh S, Preet A, Groopman JE, Ganju RK. Cannabinoid receptor CB2 modulates the CXCL12/CXCR4-mediated chemotaxis of T lymphocytes. *Mol Immunol*. 2006;43(14):2169–79.
100. De Filippis D, Russo A, De Stefano D, Maiuri MC, Esposito G, Cinelli MP, et al. Local administration of WIN 55,212-2 reduces chronic granuloma-associated angiogenesis in rat by inhibiting NF-κB activation. *J Mol Med*. 2007;85(6):635–45.
101. Toguri JT, Lehmann C, Laprairie RB, Szczesniak AM, Zhou J, Denovan-Wright EM, et al. Anti-inflammatory effects of cannabinoid CB2 receptor activation in endotoxin-induced uveitis. *Br J Pharmacol*. 2014;171(6):1448–61.
102. Lu QQ, Straiker A, Lu QQ, Maguire G. Expression of CB2 cannabinoid receptor mRNA in adult rat retina. *Vis Neurosci*. 2000;17(1):91–5.
103. Chen DJ, Gao M, Gao FF, Su QX, Wu J. Brain cannabinoid receptor 2: Expression, function and modulation. *Acta Pharmacol Sin [Internet]*. 2017;38(3):312–6. Available from: <http://dx.doi.org/10.1038/aps.2016.149>
104. Buckley NE, Hansson S, Harta G, Mezey E, Mezey É. Expression of the CB1 and CB2 receptor messenger RNAs during embryonic development in the rat. *Neuroscience*. 1997;82(4):1131–49.
105. Straiker A, Stella N, Piomelli D, Mackie K, Karten HJ, Maguire G. Cannabinoid CB1 receptors and ligands in vertebrate retina: Localization and function of an endogenous signaling system. *Proc Natl Acad Sci [Internet]*. 1999;96(25):14565–70. Available from: <http://www.pnas.org/cgi/doi/10.1073/pnas.96.25.14565>
106. Aiello F, Gallo Afflitto G, Li J-PO, Martucci A, Cesareo M, Nucci C. CannabinEYEds: The Endocannabinoid System as a Regulator of the Ocular Surface Nociception, Inflammatory Response, Neovascularization and Wound Healing. *J Clin Med*. 2020;9(12):4036.
107. Straiker AJ, Maguire G, Mackie K, Lindsey J. Localization of cannabinoid CB1 receptors in the human anterior eye and retina. *Invest Ophthalmol Vis Sci*. 1999;40(10):2442–8.
108. Iribarne MM, Torbidoni V, Julián K, Prestifilippo JP, Sinha D, Rettori V, et al. Cannabinoid receptors in conjunctival epithelium: Identification and functional properties. *Investig Ophthalmol Vis Sci [Internet]*. 2008;49(10):4535–44. Available from: <http://dx.doi.org/10.1167/iovs.07-1319>
109. Yang Y, Yang H, Wang Z, Varadaraj K, Kumari SS, Mergler S, et al. Cannabinoid receptor 1 suppresses transient receptor potential vanilloid 1-induced inflammatory responses to corneal injury. *Cell Signal [Internet]*. 2013;25(2):501–11. Available from: <http://dx.doi.org/10.1016/j.cellsig.2012.10.015>
110. Bridges D, Rice ASC, Egertová M, Elphick MR, Winter J, Michael GJ. Localisation of cannabinoid receptor 1 in rat dorsal root ganglion using in situ hybridisation and immunohistochemistry. *Neuroscience*. 2003;119(3):803–12.
111. Murataeva N, Miller S, Dhopeswarkar A, Leishman E, Daily L, Taylor X, et al. Cannabinoid CB2R

- receptors are upregulated with corneal injury and regulate the course of corneal wound healing. *Exp Eye Res* [Internet]. 2019;182:74–84. Available from: <https://doi.org/10.1016/j.exer.2019.03.011>
112. Suburo AM, Sgroi M, Cubilla MA, Iribarne M, Berra A. Cannabinoid Receptors and Corneal Epithelium Repair. *Invest Ophthalmol Vis Sci*. 2009;50(13):6297.
 113. Porter IV R. Cannabinoid 2 receptor signalling in endotoxin-induced uveitis. 2017.
 114. Thayer A, Murataeva N, Delcroix V, Wager-Miller J, Makarenkova HP, Straiker A. THC Regulates Tearing via Cannabinoid CB1 Receptors. *Invest Ophthalmol Vis Sci*. 2020;61(10):48.
 115. Bereiter DA, Bereiter DF, Hirata H. Topical cannabinoid agonist, WIN55, 212-2, reduces cornea-evoked trigeminal brainstem activity in the rat. *Pain*. 2002;99(3):547–56.
 116. Assimakopoulou M, Pagoulatos D, Nterma P, Pharmakakis N. Immunolocalization of cannabinoid receptor type 1 and CB2 cannabinoid receptors, and transient receptor potential vanilloid channels in pterygium. *Mol Med Rep*. 2017;16(4):5285–93.
 117. MATSUDA S, KANEMITSU N, NAKAMURA A, MIMURA Y, UEDA N, KURAHASHI Y, et al. Metabolism of anandamide, an endogenous cannabinoid receptor ligand, in porcine ocular tissues. *Exp Eye Res* [Internet]. 1997;64(5):707–11. Available from: <https://doi.org/10.1006/exer.1996.0265>
 118. Dursun D, Wang M, Monroy D, Li D-QQ, Lokeshwar BL, Stern ME, et al. A mouse model of keratoconjunctivitis sicca. *Investig Ophthalmol Vis Sci*. 2002;43(3):632–8.
 119. Gehlsen U, Braun T, Notara M, Krösser S, Steven P. A semifluorinated alkane (F4H5) as novel carrier for cyclosporine A: a promising therapeutic and prophylactic option for topical treatment of dry eye. *Graefe's Arch Clin Exp Ophthalmol* [Internet]. 2017;255(4):767–75. Available from: [10.1007/s00417-016-3572-y](https://doi.org/10.1007/s00417-016-3572-y)
 120. Tran BN, Maass M, Musial G, Stern ME, Gehlsen U, Steven P. Topical application of cannabinoid-ligands ameliorates experimental dry-eye disease. *Ocul Surf*. 2021;
 121. Ramsay E, del Amo EM, Toropainen E, Tengvall-Unadike U, Ranta VP, Urtti A, et al. Corneal and conjunctival drug permeability: Systematic comparison and pharmacokinetic impact in the eye. *Eur J Pharm Sci* [Internet]. 2018;119(2017):83–9. Available from: <https://doi.org/10.1016/j.ejps.2018.03.034>
 122. Van Santvliet L, Ludwig A. Determinants of eye drop size. *Surv Ophthalmol*. 2004;49(2):197–213.
 123. Schoenwald RD. Ocular Drug Delivery. *Clin Pharmacokinet* [Internet]. 1990;18(4):255–69. Available from: <https://doi.org/10.2165/00003088-199018040-00001>
 124. Barar J, Asadi M, Mortazavi-Tabatabaei SA, Omidi Y. Ocular drug delivery; Impact of in vitro cell culture models. *J Ophthalmic Vis Res*. 2014;4(4):238–52.
 125. Macha S, Mitra AK, Hughes PM. Overview of ocular drug delivery. In: *Ophthalmic drug delivery systems*. Routledge; 2021. p. 1–12.
 126. Rosenkrantz H, Thompson GR, Braude MC. Oral and parenteral formulations of marijuana constituents. *J Pharm Sci*. 1972;61(7):1106–12.
 127. Green K, Bigger JF, Kim K, Bowman K. Cannabinoid penetration and chronic effects in the eye. *Exp Eye Res*. 1977;24(2):197–205.
 128. Novack GD. Cannabinoids for treatment of glaucoma. *Curr Opin Ophthalmol*. 2016;27(2):146–50.
 129. Adelli GR, Bhagav P, Taskar P, Hingorani T, Pettaway S, Gul W, et al. Development of a $\Delta 9$ -tetrahydrocannabinol amino acid-dicarboxylate prodrug with improved ocular bioavailability. *Investig Ophthalmol Vis Sci*. 2017;58(4).
 130. Hingorani T, Gul W, Elshohly M, Repka MA, Majumdar S. Effect of Ion Pairing on In Vitro Transcorneal Permeability of a $\Delta 9$ -Tetrahydrocannabinol Prodrug: Potential in Glaucoma Therapy. *J Pharm Sci*. 2012;101(2):616–26.
 131. Loftsson T, Masson M. Cyclodextrins in topical drug formulations: Theory and practice. *Int J Pharm*. 2001;225(1–2):15–30.
 132. Kearse EC, Green K. Effect of vehicle upon in vitro transcorneal permeability and intracorneal content of $\Delta 9$ -tetrahydrocannabinol. *Curr Eye Res*. 2000;20(6):496–501.
 133. Jay WM, Green K. Multiple-drop study of topically applied 1% $\delta 9$ -tetrahydrocannabinol in human eyes. *Arch Ophthalmol*. 1983;101(4):591–3.
 134. del Castillo Benítez JM, Duran S, Hernandez J, García JS. Influence of topically applied cyclosporine A in olive oil on corneal epithelium permeability. *Cornea*. 1994;13(2):136–40.
 135. Del Castillo JMB, Castillo A, Toledano N, Durán S, Del Aguila C, Otero M, et al. Influence of topical cyclosporine A and dissolvent on corneal epithelium permeability of fluorescein. *Doc Ophthalmol*. 1995;91(1):49–55.
 136. Passani A, Posarelli C, Sframeli AT, Perciballi L, Pellegrini M, Guidi G, et al. Cannabinoids in glaucoma patients: The never-ending story. *J Clin Med*. 2020;9(12):1–20.
 137. Mandal A, Gote V, Pal D, Ogundele A, Mitra AK. Ocular Pharmacokinetics of a Topical Ophthalmic

- Nanomicellar Solution of Cyclosporine (Cequa®) for Dry Eye Disease. Vol. 36, Pharmaceutical Research. 2019.
138. Hosseini A, Lattanzio FA, Williams PB, Tibbs D, Samudre SS, Allen RC. Chronic topical administration of WIN-55-212-2 maintains a reduction in IOP in a rat glaucoma model without adverse effects. *Exp Eye Res.* 2006;82(5):753–9.
 139. Samudre SS, Schneider JL, Oltmanns MH, Hosseini A, Pratap K, Loose-Thurman P, et al. Comparison of topical and intravenous administration of WIN 55-212-2 in normotensive rabbits. *Curr Eye Res.* 2008;33(10):857–63.
 140. Rosenkrantz H, Thompson GR, Braude MC. Oral and parenteral formulations of marijuana constituents. *J Pharm Sci.* 1972;61(7):1106–12.
 141. Jacob SW, Wood DC. Dimethyl sulfoxide (DMSO) toxicology, pharmacology, and clinical experience. *Am J Surg.* 1967;114(3):414–26.
 142. Gattefosse. Formulating cannabinoids with lipid excipients. 2020;1–14.
 143. FDA. Inactive Ingredient Search for Approved Drug Products [Internet]. US FDA website. FDA; 2022. Available from: <https://www.accessdata.fda.gov/scripts/cder/iig/index.cfm>
 144. Gunther B, Theisinger B, Theisinger S, Scherer D. Topical pharmaceutical composition based on semifluorinated alkanes. Google Patents; 2014.
 145. Agarwal P, Scherer D, Günther B, Rupenthal ID. Semifluorinated alkane based systems for enhanced corneal penetration of poorly soluble drugs. *Int J Pharm [Internet].* 2018;538(1–2):119–29. Available from: <https://doi.org/10.1016/j.ijpharm.2018.01.019>
 146. Steven P, Scherer D, Krösser S, Beckert M, Cursiefen C, Kaercher T. Semifluorinated Alkane Eye Drops for Treatment of Dry Eye Disease—A Prospective, Multicenter Noninterventional Study. *J Ocul Pharmacol Ther [Internet].* 2015;31(8):498–503. Available from: <http://online.liebertpub.com/doi/10.1089/jop.2015.0048>
 147. Novaliq. Novaliq Announces Positive Topline Results for Second Phase 3 Trial (Essence-2) of CyclASol® in Dry Eye Disease [Internet]. Vol. 1, Novaliq Press release. Available from: <https://www.novaliq.com/press-releases/2021/12/21/novaliq-announces-positive-topline-results-for-second-phase-3-trial-essence-2-of-cyclasol-in-dry-eye-disease/>
 148. ClinicalTrials.gov. National Library of Medicine (U.S.). NCT04523129.
 149. Netzhauterkrankungen S, International DOG, Neuro-ophthalmologie M, Erkenntnisse N, Kataraktchirurgie M, Bildgebung I. Abstractband DOG 2019. *Der Ophthalmol Zeitschrift der Dtsch Ophthalmol Gesellschaft, PDo01-07, Expr Funct role endocannabinoid Recept dry eye Dis.* 2019;116(Suppl 2):25–218.
 150. Hoang C, Nguyen AK, Nguyen TQ, Fang W, Han B, Hoang BX, et al. Application of Dimethyl Sulfoxide as a Therapeutic Agent and Drug Vehicle for Eye Diseases. *J Ocul Pharmacol Ther.* 2021;37(8):441–51.
 151. Van Der Bijl P, Engelbrecht AH, Van Eyk AD, Meyer D. Comparative Permeability of Human and Rabbit Corneas to Cyclosporin and Tritiated Water. *J Ocul Pharmacol Ther.* 2002;18(5):419–27.
 152. Bron AJ, Evans VE, Smith JA. Grading of corneal and conjunctival staining in the context of other dry eye tests. *Cornea [Internet].* 2003;22(7):640–50. Available from: 10.1097/00003226-200310000-00008
 153. Bonin RP, Bories C, De Koninck Y. A simplified up-down method (SUDO) for measuring mechanical nociception in rodents using von Frey filaments. *Mol Pain [Internet].* 2014;10(1):1–10. Available from: Molecular Pain
 154. Ramsay E, del Amo EM, Toropainen E, Tengvall-Unadike U, Ranta VP, Urtili A, et al. Corneal and conjunctival drug permeability: Systematic comparison and pharmacokinetic impact in the eye. *Eur J Pharm Sci [Internet].* 2018;119(April):83–9. Available from: <https://doi.org/10.1016/j.ejps.2018.03.034>
 155. Stetefeld J, McKenna SA, Patel TR. Dynamic light scattering: a practical guide and applications in biomedical sciences. *Biophys Rev.* 2016;8(4):409–27.
 156. Niederkorn JY, Stern ME, Pflugfelder SC, De Paiva CS, Corrales RM, Gao J, et al. Desiccating stress induces T cell-mediated Sjögren’s syndrome-like lacrimal keratoconjunctivitis. *J Immunol.* 2006;176(7):3950–7.
 157. De Paiva CS, Chotikavanich S, Pangelinan SB, Pitcher JD 3rd, Fang B, Zheng X, et al. IL-17 disrupts corneal barrier following desiccating stress. *Mucosal Immunol.* 2009;2(3):243–53.
 158. Polakowski C, Sochan A, Bieganski A, Ryzak M, Foldenyi R, Toth J. Influence of the sand particle shape on particle size distribution measured by laser diffraction method. *Int Agrophysics.* 2014;28(2).
 159. Stern ME, Pflugfelder SC. What We Have Learned From Animal Models of Dry Eye. *Int Ophthalmol Clin [Internet].* 2017;57(2):109–18. Available from: <http://insights.ovid.com/crossref?an=00004397-201705720-00009>
 160. Whiting PF, Wolff RF, Deshpande S, Di Nisio M, Duffy S, Hernandez A V., et al. Cannabinoids for medical use: A systematic review and meta-analysis. *JAMA - J Am Med Assoc.* 2015;313(24):2456–73.

161. Wright K, Rooney N, Feeney M, Tate J, Robertson D, Welham M, et al. Differential expression of cannabinoid receptors in the human colon: Cannabinoids promote epithelial wound healing. *Gastroenterology*. 2005;129(2):437–53.
162. Benítez-Del-Castillo JM, Acosta MC, Wassfi MA, Díaz-Valle D, Gegúndez JA, Fernandez C, et al. Relation between corneal innervation with confocal microscopy and corneal sensitivity with noncontact esthesiometry in patients with dry eye. *Investig Ophthalmol Vis Sci*. 2007 Jan;48(1):173–81.
163. De Paiva CS, Villarreal AL, Corrales RM, Rahman HT, Chang VY, Farley WJ, et al. Dry eye-induced conjunctival epithelial squamous metaplasia is modulated by interferon- γ . *Investig Ophthalmol Vis Sci*. 2007;48(6):2553–60.
164. Niederkorn JY, Stern ME, Pflugfelder SC, De Paiva CS, Corrales RM, Gao J, et al. Desiccating Stress Induces T Cell-Mediated Sjogren’s Syndrome-Like Lacrimal Keratoconjunctivitis. *J Immunol [Internet]*. 2006;176(7):3950–7. Available from: <http://www.jimmunol.org/cgi/doi/10.4049/jimmunol.176.7.3950>
165. Hu D, Ikizawa K, Lu L, Sanchirico ME, Shinohara ML, Cantor H. Analysis of regulatory CD8 T cells in Qa-1-deficient mice. *Nat Immunol*. 2004 May;5(5):516–23.
166. Masters SL, Mielke LA, Cornish AL, Sutton CE, O’Donnell J, Cengia LH, et al. Regulation of interleukin-1 β by interferon- γ is species specific, limited by suppressor of cytokine signalling 1 and influences interleukin-17 production. *EMBO Rep*. 2010;11(8):640–6.
167. Duff G, Argaw A, Cecyre B, Cherif H, Tea N, Zabouri N, et al. Cannabinoid Receptor CB2 Modulates Axon Guidance. *PLoS One*. 2013;8(8).
168. Benito C, Tolón RM, Pazos MR, Núñez E, Castillo AI, Romero J. Cannabinoid CB 2 receptors in human brain inflammation. *Br J Pharmacol*. 2008;153(2):277–85.
169. Stepp MA, Pal-Ghosh S, Tadvalkar G, Williams A, Pflugfelder SC, de Paiva CS. Reduced intraepithelial corneal nerve density and sensitivity accompany desiccating stress and aging in C57BL/6 mice. *Exp Eye Res*. 2018;169(January):91–8.
170. Schaumburg C, Held K, Oh E, Ugarte S, Wheeler L, Calonge M, et al. Mice with desiccating stress-induced dry eye develop trigeminal neuralgia, despite decreased corneal sensitivity and nerve fiber degeneration. *Invest Ophthalmol Vis Sci*. 2013;54(15):2194.
171. Galve-Roperh I, Aguado T, Palazuelos J, Guzman M. Mechanisms of Control of Neuron Survival by the Endocannabinoid System. *Curr Pharm Des*. 2008;14(23):2279–88.
172. Launay PS, Reboussin E, Liang H, Kessal K, Godefroy D, Rostene W, et al. Ocular inflammation induces trigeminal pain, peripheral and central neuroinflammatory mechanisms. *Neurobiol Dis*. 2016;88:16–28.
173. Hill MN, Patel S, Carrier EJ, Rademacher DJ, Ormerod BK, Hillard CJ, et al. Downregulation of endocannabinoid signaling in the hippocampus following chronic unpredictable stress. *Neuropsychopharmacology*. 2005;30(3):508.
174. López-Moreno JA, González-Cuevas G, Moreno G, Navarro M. The pharmacology of the endocannabinoid system: Functional and structural interactions with other neurotransmitter systems and their repercussions in behavioral addiction. *Addict Biol*. 2008;13(2):160–87.
175. Spierer O, Felix ER, McClellan AL, Parel JM, Gonzalez A, Feuer WJ, et al. Corneal mechanical thresholds negatively associate with dry eye and ocular pain symptoms. *Investig Ophthalmol Vis Sci*. 2016 Feb 1;57(2):617–25.
176. Rosenthal P, Borsook D. Ocular neuropathic pain. 2016;128–34.
177. Yang H, Wang Z, Capó-Aponte JE, Zhang F, Pan Z, Reinach PS. Epidermal growth factor receptor transactivation by the cannabinoid receptor (CB1) and transient receptor potential vanilloid 1 (TRPV1) induces differential responses in corneal epithelial cells. *Exp Eye Res [Internet]*. 2010;91(3):462–71. Available from: <http://dx.doi.org/10.1016/j.exer.2010.06.022>
178. Murataeva N, Li S, Oehler O, Miller S, Dhopeswarkar A, Hu SSJ, et al. Cannabinoid-induced chemotaxis in bovine corneal epithelial cells. *Investig Ophthalmol Vis Sci*. 2015;56(5):3304–13.
179. Yang H, Wang Z, Capó-aponte JE, Zhang F, Pan Z, Reinach PS. Epidermal growth factor receptor transactivation by the cannabinoid receptor (CB1) and transient receptor potential vanilloid 1 (TRPV1) induces differential responses in corneal epithelial cells. *Exp Eye Res [Internet]*. 2010;91(3):462–71. Available from: <http://dx.doi.org/10.1016/j.exer.2010.06.022>
180. Soderstrom K, Zhang Y, Wilson AR. Altered patterns of filopodia production in CHO cells heterologously expressing zebra finch CB1 cannabinoid receptors. *Cell Adh Migr*. 2012;6(2):91–9.
181. Murataeva N, Li S, Oehler O, Miller S, Dhopeswarkar A, Hu SS-JJ, et al. Cannabinoid-induced chemotaxis in bovine corneal epithelial cells. *Investig Ophthalmol Vis Sci [Internet]*. 2015;56(5):3304–13. Available from: <http://dx.doi.org/10.1038/npp.2014.297>
182. Wu J. Cannabis, cannabinoid receptors, and endocannabinoid system: yesterday, today, and tomorrow. Vol.

- 40, *Acta Pharmacologica Sinica*. Nature Publishing Group; 2019. p. 297–9.
183. Santoro A, Pisanti S, Grimaldi C, Izzo AA, Borrelli F, Proto MC, et al. Rimonabant inhibits human colon cancer cell growth and reduces the formation of precancerous lesions in the mouse colon. *Int J cancer*. 2009;125(5):996–1003.
184. Caffarel MM, Sarrió D, Palacios J, Guzmán M, Sánchez C. Δ 9-tetrahydrocannabinol inhibits cell cycle progression in human breast cancer cells through Cdc2 regulation. *Cancer Res*. 2006;66(13):6615–21.
185. FDA. Q3C — Tables and List Guidance for Industry Q3C — Tables and List Guidance for Industry Q3C — Tables and List Guidance for Industry. Microsoft Word [Internet]. 2017;9765(February):1–8. Available from: <http://www.fda.gov/Drugs/GuidanceComplianceRegulatoryInformation/Guidances/default.htm>
186. U.S. Food and Drug Administration. Guidance for Industry IMPURITIES: RESIDUAL SOLVENTS VICH GL18 DRAFT GUIDANCE. 1999;(147):1–19. Available from: <https://www.fda.gov/ohrms/dockets/98fr/994071gd.pdf>
187. BASF. Kolliphor EL Safety data sheet [Internet]. Vol. 1173, BASF. 2017. Available from: <https://documents.basf.com/82664b0e4078ed0377a8552fd7a3c08054142cb6?response-content-disposition=inline>
188. Balicki I. Clinical study on the application of tacrolimus and DMSO in the treatment of chronic superficial keratitis in dogs. *Pol J Vet Sci*. 2012;15(4):667–76.
189. Gordon DM, Kleberger KE. The Effect of Dimethyl Sulfoxide (DMSO) on Animal and Human Eyes. *Arch Ophthalmol*. 1968;79(4):423–7.
190. Knagenhjelm SKH, Froyland K, Ringvold A, Bjerkas E, Kjonniksen I. Toxicological evaluation of cyclosporine eyedrops. *Acta Ophthalmol Scand*. 1999;77(2):200–3.
191. Gelderblom H, Verweij J, Nooter K, Sparreboom A. <Gelderblom 2001 Eu J Cancer.pdf>. 2001;37:1590–8.
192. Aldrich DS, Bach CM, Brown W, Chambers W, Fleitman J, Hunt D, et al. Ophthalmic preparations. *US Pharmacop*. 2013;39(5):1–21.
193. Dutescu RM, Panfil C, Schrage N. Osmolarity of prevalent eye drops, side effects, and therapeutic approaches. *Cornea*. 2015;34(5):560–6.
194. Prausnitz MR. Permeability of cornea, sciera, and conjunctiva: A literature analysis for drug delivery to the eye. *J Pharm Sci*. 1998;87(12):1479–88.
195. Deng F, Ranta VP, Kidron H, Urtti A. General Pharmacokinetic Model for Topically Administered Ocular Drug Dosage Forms. *Pharm Res*. 2016;33(11):2680–90.
196. Katz J, Costarides AP. Facts vs Fiction: the Role of Cannabinoids in the Treatment of Glaucoma. *Curr Ophthalmol Rep* [Internet]. 2019;7(3):177–81. Available from: <https://doi.org/10.1007/s40135-019-00214-z>

LIST OF FIGURES

- Figure 1: DED vicious circle, adapted from DEW II (2,3): Tear film instability and tear hyperosmolarity initiate inflammation, neuro-sensory abnormalities, and directly damage ocular surface epithelia. The vicious cycle happens when tear hyperosmolarity causes these three pathogenic processes to cascade and exacerbates hyperosmolarity. Combining different therapy approaches (yellow arrows) is required for DED patients. Cannabinoid receptors (CB1R and CB2R, green) are hypothesized to impact these 3 pathways as a potential DED therapy.9
- Figure 2: Desiccating stress model: schedule of the experiment.....35
- Figure 3: Illustration of drug permeability experiment: (left) Franz diffusion cell diagram, (right) Franz diffusion cell image.....43
- Figure 4: (A) Electrophoresis detection for PCR amplification of CB1R and CB2R mRNA transcripts in different ocular surface tissues; control tissues are trigeminal ganglion for CB1R and spleen for CB2R. (B and C) RT-qPCR analysis for CB1R and CB2R expressions among tissues: lowest in cornea, highest in lacrimal gland, “conj,”: conjunctiva, “Lac”: lacrimal gland, “Gang”: trigeminal ganglion, * $p < 0.05$, adapted from (120).....45
- Figure 5: Representative in-situ hybridization images of CB1R and CB2R signals in the cornea and conjunctiva using Hematoxylin Mayer’s (blue arrows: CB1R, red arrows: CB2R).....46
- Figure 6: Representative in-situ hybridization images of CB1R and CB2R signals in the cornea and conjunctiva using Hematoxylin Gill’s, blue arrows: CB1R, red arrows: CB2R, adapted from (120)47
- Figure 7: DED phenotype readouts during DS: (A) Tear production (TP) was reduced and maintained at 1 mm, (B) fluorescein staining (FL) score increased from day 3 until day 10, (C) Mechanical sensitivity was reduced (von-Frey forces increased) from day 3 until day 10, and (D) Brush test results showed an increasing trend of responsive animals48
- Figure 8: RT-qPCR analysis showed that CB1R and CB2R increased during 10 days of DS in the cornea (A), conjunctiva (B), and lacrimal gland (C) (upper row). In the lower row, while CB1R/CB2R ratios were reduced during 10 days of DS in the cornea (D) and conjunctiva (E), the CB1R/CB2R ratio in the lacrimal gland (F) was at the lowest value on day 5 ($n = 10$ eyes, 5 mice/group) *: $p < 0.05$, adapted from (120)49
- Figure 9: Effects of cannabinoids on phenotypes of DED-induced mice: THC experiment (A, B C) and antagonist experiment (D, E, F). The phenotypes, including FL score (A, D), TP (B, E), and sen (C, F), showed treatment effects compared to the corresponding carriers and untreated groups. ($n=10$). *: $p < 0.05$, **: $p < 0.01$, ***: $p < 0.001$, adapted from (120)50
- Figure 10: Representative images of center areas of the cornea (tissues were collected on day 10 of experiment): significant effects of DED-induction and cannabinoids on corneal nerve morphology. The left side β 3-tubulin immunostaining images are shown along with the corresponding binary images (in the middle) and skeletonized images (right). (bar=100m). After 10 days, untreated DED mice showed lessened nerve morphology, whereas nerve morphology was maintained in the THC-treated group. Adapted from (120)53
- Figure 11: Semi-automatic quantification of tubulin-staining images: (A-C) Mean of corneal nerve density was quantified (calculated per cornea) and is presented, and (D-F) Mean of corneal nerve length per area (in mm/mm^2 , D-F). Both corneal nerve density and length were reduced at day 10 compared to Naïve mice. Only THC significantly maintained corneal nerve

density and length during 10 days of DS (B and E). Data are presented as mean and SD (n = 10 eyes/ per group). * p < 0.05, adapted from (120).....54

Figure 12: Effect of DS on some inflammatory cytokines in cornea and conjunctiva (n =5), adapted from (120).....55

Figure 13: Cytokine levels following 10-day treatments of THC (A-C) and antagonists (D-F): In the cornea, THC, AntaCB1, and Anta CB decreased IL-1 β (A and D). In the conjunctiva, AntaCB2 administration simultaneously reduced IL-1 β and increased IFN- γ (C, E). Data are expressed as mean \pm SD (n=5 mice/group). * p < 0.05, adapted from (120)56

Figure 14: (A) THC and AntaCB1 reduced conjunctival CD4⁺ T-cell density compared to the untreated DED group. (B) THC and AntaCB2 increased conjunctival CD8⁺ T-cell density compared to untreated DED group. (C) THC and AntaCB2 reduced CD4:CD8 ratio compared to the untreated DED group. Data are expressed as mean \pm SD (n=4 eyes/group). * p < 0.05, ** p < 0.01, adapted from (120).....57

Figure 15: CBR expression after topical application of 3 different cannabinoid ligands for 10 days: A-D) THC (non-selective agonist application), E-H) two selective antagonists. (A-D) THC reduced CBRs expression. (E-F) AntaCB1 and AntaCB2 groups exhibited a lower CBRs expression in the cornea than untreated DED mice, (G-H) AntaCB1 increased both CB1R and CB2R in the conjunctiva compared to others. Data are presented as mean \pm SD (n=5/group). adapted from (120).....58

Figure 16: Representatives of corneal wound healing model: Positive and negative control samples59

Figure 17: Wound area in mm² when samples were treated with different THC concentrations .60

Figure 18: THC biphasic effect on wound healing process: (A) Representative images showed that THC 0.5 μ M improved wound healing rate while THC 10 μ M delayed wound healing; and (B, C) data analysis of wound healing process confirmed THC effects (n = 10)61

Figure 19: Wound area in mm² when samples were treated with CB1R and CB2R antagonists..62

Figure 20: CBR Antagonists' effect on the wound-healing process: A) representative images showed that AntaCB1 delayed the wound healing process, and AntaCB2 did not have a significant effect (B) Kaplan-Meyer data analysis of wound healing process (n =10)63

Figure 21: Representative images of THC formulations (t = 0).....67

Figure 22: THC content before filtration, after filtration, and after 7-day storage at 2 conditions (RT and 4^oC).....68

Figure 23: Intensity distribution of 2 THC formulations (via DLS technique).....69

Figure 24: Permeability study of 2 formulations with H3-mannitol substances: DMSO (F00) and Transcutol (F24) significantly increased the permeability of the carriers compared to buffer. ...71

Figure 25: Summarizing the cannabinoid effects on DED phenotype with predicted involved mechanisms75

LIST OF TABLES

<i>Table 1: CB1R effects on different neurotransmitter release.....</i>	<i>20</i>
<i>Table 2: Activating CB2R inhibits different immune cells and cytokine releasing.....</i>	<i>21</i>
<i>Table 3: Expression of CBRs in several ocular surface tissues.....</i>	<i>22</i>
Table 4: List of pharmaceutical excipients suitable for THC eye drop formulations	27
<i>Table 5: Select solvent as the stock solution</i>	<i>65</i>
<i>Table 6: Formulation screening with different stock solutions and water phases.....</i>	<i>66</i>
<i>Table 7: Final formulations selected for sterile filtration and short-term stability.....</i>	<i>68</i>
<i>Table 8: Particle size measurement of THC formulations at day 0 and 7 days of storage.....</i>	<i>69</i>
<i>Table 9: Osmolarity and pH of the obtained THC formulations</i>	<i>70</i>

Acknowledgments

This endeavor would not have been possible without the assistance of numerous individuals. In addition to scientific and industrial issues, we've dealt with pandemic restrictions and their devastating effects since March 2020.

First of all, I would like to thank Prof. Dr. med. Philipp Steven, who has supervised me from the beginning days in Germany until numerous revisions of my thesis in 2022. It was a privilege to work with our team, the Division of Ocular Surface and GvHD, to complete my PhD project and have valuable experience in Cologne, Germany.

To my supervisor board in Cologne, I would like to thank Dr. Uta Gehlsen for her extensive professional guidance and support. Together, we conducted experiments and obtained valuable results, which contributed significantly to the progression of my project. Besides, I would like to thank Dr. Michale M. Stern, who visited us in Germany and followed our project. Dr. Stern inspired us, Early-stage researchers of IT-DED³, with various DED research aspects. I want to mention Dr. Gwen Musial and Dr. Martina Mass, who supported me with their excellent expertise as supervisors and colleagues. Lastly, big thanks to my colleagues (formal and current) in the Division of Ocular Surface & GvHD, Asif Khan Setu (ESR11), Daniella Hess, Timur Birgin, Anna-Lena Zachert, Sabina Manz, and Jens Horstmann.

My project is funded by the EU Horizon 2020 Research & Innovation program, Marie Skłodowska-Curie Action (765608), a consortium of IT-DED³ Integrated Training in Dry Eye Disease Drug Development. The project provided me with the financial means to complete this PhD project.

In the frame of the project, I was supervised by Senior Scientist Christian Bucher, M.Sc, pCMC Drug Delivery and Preformulation Sciences, TMO department at the Roche Innovation Center in Basel. Many thanks for his support and professionalism in this field.

I also want to acknowledge my secondment at the University of Eastern Finland. I want to thank Prof. Dr. Arto Urtili and Dr. Marika Ruponen for giving me the opportunity to work in the lab and supervising me with pharmaceutical investigations. It is grateful to have support from Anusha Balla (ESR6) to finish my experiments, and thanks to other colleagues and friends at the University of Eastern Finland for the memory in Kuopio.

In the frame of the consortium of IT-DED³, I would like to thank the entire external advisory board for their questions during the annual meetings. A big thank you to Paz Yanez and Mayer Berg for the excellent management of the IT-DED³ project. Especially, I am grateful to mention Paz for her kindness and support from the interview day in Antwerp (May 2018) until now. I am thankful for

my ESR team, we were in Antwerp, Valladolid, Nice, and a bunch of virtual meetings together to study, discuss, and share ideas about DED, science, as well as plenty of interdisciplinary topics.

The University of Cologne provided me with an opportunity to pursue a PhD in the IPHS program. I want to thank Dr. Christoph Aszyk and Dr. Daniela Mutschler, the scientific coordinators of the Graduate Schools, for their support in related issues. In the frame of the IPHS program, I would like to thank my tutors, Prof. Dr. Uwe Fuhr and Prof. Dr. Helmar Lemann, who spent time for my projects, they worked actively and supported me in completing this project.

In Cologne, I would like to thank everyone from the Department of Ophthalmology (Augenheilkunde der Uniklinik Köln). I learned from all the professors, PI researchers, PhD students, and technicians in the laboratories of Prof. Cursifer and Prof. Langmann; we worked together and shared laboratories and animal quarters.

Last but not least, I would like to express my gratitude to my family, my wife, and my dear daughter, the greatest acknowledgments for their support and unconditional love. I want to mention my big family (my parents and my brother) for their unconditional support. Though we didn't see each other during lockdown time, they all encourage me to finish this project.

BAO TRAN's CURRICULUM VITAE

Full name: TRẦN NGỌC BẢO (or BAO TRAN)

Birthday: 26/11/1988

Nationality: Vietnam

Current address: Hanoi, Vietnam

Email: baotn@hup.edu.vn

Education:

2014 – 2015: MSc. Pharmaceutical Quality Assurance and Biotechnology,
Dublin Institute of Technology (DIT), Rep. Ireland

2006- 2011: Pharmacist degree, Hanoi University of Pharmacy, Vietnam

Work research experience:

2018-2021: University Hospital Cologne, Germany

EU researcher / PhD student at Department of Ophthalmology
Drug development for Dry eye diseases (IT-DED3)

2016-2018: Hanoi University of Pharmacy, Vietnam

2016 Yeungnam University, South Korea

Main publications:

BN. Tran et al. (2021), The Ocular Surface, <https://doi.org/10.1016/j.jtos.2021.12.008>

BN Tran et al. (2017), Arch. Pharm. Res., <https://doi.org/10.1007/s12272-017-0968-0>

Conference and award:

05/2021 Poster presentation and ARVO Travel grant award, Association for Research in Vision and Ophthalmology (ARVO)

09/2019 Poster presentation, (PDo01-07), Deutsche Ophthalmologische Gesellschaft, Berlin, Germany

Other awards:

05/2018 First & Excellent prize in Vietnam National Sci.&Tech. conference for Medical & Pharmaceutical young colleges, Vietnam.

09/2014 Irish Aid Scholarship, Ireland's Department of Foreign Affairs and Trade, Dublin, Republic of Ireland.

Erklärung

Hiermit versichere ich an Eides statt, dass ich die vorliegende Dissertationsschrift selbstständig und ohne die Benutzung anderer als der angegebenen Hilfsmittel angefertigt habe. Alle Stellen - einschließlich Tabellen, Karten und Abbildungen -, die wörtlich oder sinngemäß aus veröffentlichten und nicht veröffentlichten anderen Werken im Wortlaut oder dem Sinn nach entnommen sind, sind in jedem Einzelfall als Entlehnung kenntlich gemacht. Ich versichere an Eides statt, dass diese Dissertationsschrift noch keiner anderen Fakultät oder Universität zur Prüfung vorgelegen hat; dass sie - abgesehen von unten angegebenen Teilpublikationen - noch nicht veröffentlicht worden ist sowie, dass ich eine solche Veröffentlichung vor Abschluss der Promotion nicht ohne Genehmigung der / des Vorsitzenden des IPHS-Promotionsausschusses vornehmen werde. Die Bestimmungen dieser Ordnung sind mir bekannt. Die von mir vorgelegte Dissertation ist von Prof. Dr. Philipp Steven betreut worden.

Darüber hinaus erkläre ich hiermit, dass ich die Ordnung zur Sicherung guter wissenschaftlicher Praxis und zum Umgang mit wissenschaftlichem Fehlverhalten der Universität zu Köln gelesen und sie bei der Durchführung der Dissertation beachtet habe und verpflichte mich hiermit, die dort genannten Vorgaben bei allen wissenschaftlichen Tätigkeiten zu beachten und umzusetzen.

Übersicht der Publikationen:

Topical application of cannabinoid-ligands ameliorates experimental dry-eye disease, The Ocular Surface, Vol. 23, Jan 2022, pp. 131-139, <https://doi.org/10.1016/j.jtos.2021.12.008>

Ich versichere, dass ich alle Angaben wahrheitsgemäß nach bestem Wissen und Gewissen gemacht habe und verpflichte mich, jedmögliche, die obigen Angaben betreffenden Veränderungen, dem IPHS-Promotionsausschuss unverzüglich mitzuteilen.

...12/01/2023.....

Datum



.....
Unterschrift